Structural optimization of modular high-rise buildings

MSc Thesis

T.T.P. To

Delft University of Technology

Structural optimization of modular high-rise buildings

MSc Thesis

by

T.T.P. To

to obtain the degree of Master of Science
at the Delft University of Technology,
to be defended publicly on Thursday April 23, 2020 at 4:00 PM.

Student number:	4297156	
Project duration:	June 10, 2019 – April 23, 2020	
Thesis committee:	Dr. ir. M.A.N. Hendriks,	TU Delft, chair
	Ir. R. Crielaard,	TU Delft & Heijmans
	Ir. L.P.L. van der Linden,	TU Delft
	Mrs. dr. ir. M. Luković	TU Delft

An electronic version of this thesis is available at http://repository.tudelft.nl/.

TU Delft

Abstract

The demand for high-rise building has been increasing over the past decades which has induced new developments such as modular construction. Modular construction has advantages in terms increased speed, safer construction and less construction waste. Applying modular construction in high-rise however brings about great complexities for the structural design of the building. Therefore, a design aid is created which generates a structural model from any arbitrary shape and uses structural optimization techniques to explore a range of designs for the early design stage.

Existing optimization techniques have been studied, including Cross-Section (CS-) optimization (size) and BESO (topology). CS-optimization adapts the size of each member, considering utilization and displacement conditions whereas BESO removes or adds elements from the model based on stress level and Target Ratio (TR). Performing the methods successively further decreases the structural weight at certain TR. Generally, weight increases as more elements are removed.

By developing the two-way coupled ESO<>CS-optimization method, elements are removed by lowest strain energy density, while the cross-sections of the remaining members are updated in each iteration, thus coupling ESO (topology) and CS-optimization (size). This results in a logical load path and additional weight reduction especially in the braced frame structures loaded by lateral loads when displacement is governing. In multiple load case design, the removal of elements is somewhat hard to interpret, however the method consistently results in the lowest structural weight for the considered cases.

In order to create a modular structural design, boundary conditions are assumed by standardizing column and beam dimensions and considering multiple realistic load cases (wind+vertical load). By transforming arbitrary shapes into structural models and optimizing these, a range of solutions for the structural design is presented in which the number of elements and the structural weight are generally negatively related. For the considered rectangular buildings, the results are more efficient than core or outrigger structures and almost as efficient as mega frame structures, with the added benefit that it can be applied to any shape. Exploration of these solutions is a useful contribution to the early design stage of modular high-rise buildings, while the coupled ESO<>CS-optimization method could also be useful in other optimization problems.

Preface

During my master's study in Building Engineering, several subjects have caught my interest, including structural optimization, high-rise buildings, parametric design and modular construction. In this master's thesis, I have combined these topics to focus my final research upon. This report is the final product to obtain the degree in Building Engineering at Delft University of Technology.

Contact information

T.T.P. To, BSc

e-mail:	tonyto.tp@gmail.com
student number:	4297156
programme:	MSc Civil Engineering Building Engineering - Structural Design

The MSc graduation commmitee consists of the following members:

Dr. ir. M.A.N. Hendriks (Chair)

e-mail:	M.A.N.Hendriks@tudelft.nl
affiliation:	Delft University of Technology Applied Mechanics - Structural Mechanics

Ir. R. Crielaard

e-mail:	R.Crielaard@tudelft.nl
affiliation:	Delft University of Technology Applied Mechanics - Structural Design / Building Engineering Heijmans Utiliteit Ontwerp & Engineering

Ir. L.P.L. van der Linden

e-mail:	L.P.L.vanderLinden@tudelft.nl
affiliation:	Delft University of Technology Applied Mechanics - Structural Design / Building Engineering

Mrs. dr. ir. M. Luković

e-mail:	M.Lukovic@tudelft.nl
affiliation:	Delft University of Technology Engineering Structures - Concrete Structures

Acknowledgements

Writing this master's thesis could not have been done without support and feedback from many people around me.

First of all, I would like to thank my graduation committee, consisting of dr. ir. M.A.N. Hendriks, ir. R. Crielaard, ir. L.P.L. van der Linden and Mrs. dr. ir. M. Luković. Their guidance, support and constructive feedback throughout the entire project has been invaluable for me. Especially taking the time to read through my reports and scheduling multiple meetings besides their busy agendas was very well appreciated.

Also, I would like to pay special regards to my colleagues at Heijmans for providing the opportunity for me to graduate at their company. Having a professional work environment and helpful colleagues greatly boosted my productivity and gave me noticeable inspiration for this project.

Finally, my deepest gratitude go to my family and friends for always being supportive, exchanging ideas and motivating me not only during this thesis project but throughout my entire study.

T.T.P. To
April 2020

Contents

1

Introduction

This chapter addresses the motivation, relevance and scope of this Master thesis project. Some background information about high-rise buildings, modular construction and structural (topology) optimization is provided after which the research definition is formulated as well as research questions to guide this study. Lastly, the chapter concludes with a reading guide.

1.1. Background information and relevance

1.1.1. High-rise buildings

Currently, there is a high demand for residential buildings in the Netherlands. More and more people are moving to the larger cities and urban areas, which is not only the case in the Netherlands but in most parts of the world as a matter of fact. By today, already 55 percent of the world population lives in urban areas, which is expected to increase to 68 percent by 2050 [1]. In the Netherlands, this has created a sort of bubble on the housing market as the demand for housing continually increases, while the supply lacks behind.

To encounter this problem, more and more houses are being built in and nearby urban areas. As the space is limited (and therefore expensive) in urban areas, there is an increasing demand for high-rise residential towers. Examples of such towers that have been built during the last decade are 'De Rotterdam', 'Amstel Tower' and 'New Orleans'. Before the 1990's, there were no residential towers taller than 100 meters in the Netherlands while the tallest building currently in construction, the 'Zalmhaventoren', reaches a height of 215 meters.

Despite the fact that residential buildings are continually being constructed, a study has found that by 2030 there will still be a shortage of housing, especially in the larger cities [2]. The same study also reports that more and more accidents are happening on the construction site, presumably due to a higher workload and time pressure. This shows that even with higher workload, contractors and developers are unable to deliver sufficient housing to meet the people's needs by 2030.

Therefore, from an engineer's point of view, the question that arises is how to approach the design and construction of a high-rise residential tower in an efficient way in order to save time and money, especially in complex projects such as high-rise buildings. Often in complex projects, the design phase as well as the construction phase take a large amount of time. It should be strived for to reduce this amount of time by optimizing the structural design process, while reducing the use of building materials.

1.1.2. Modular building concepts

In recent building projects, more and more elements are being prefabricated and subsequently installed on site. Some great advantages of this construction method in comparison with in-situ casting of concrete are the increased speed of erection and reduced nuisance at the building site. There are also examples of demountable steel-concrete composite structures, which mainly rely on demountable shear connections [3]. This can be taken a step

further in the sense that not just 1D or 2D construction elements (such as columns, beams, walls and floors), but also 3D elements of the building, specifically volumetric modules, can be prefabricated and (de)installed on site. In some cases, not only the structural members but also Mechanical, Electrical and Plumbing (MEP) facilities and interior finishing can be accommodated. An example of this is the Prefabricated Prefinished Volumetric Construction (PPVC) method, which has been practised in a number of buildings in Singapore [4]. This method of construction is illustrated in figure 1.1.

Figure 1.1: PPVC construction in Singapore [5]

The modular concept of building blocks can be used in high-rise construction, thus stacking blocks on top of each other, reaching the desired building height. In high-rise buildings, generally speaking horizontal loads are governing. The main challenge therefore is to design a structural system that easy to assemble but at the same time ensures structural integrity. An external structure which carries the lateral load, in which modular units are placed, may also be an option.

One of the first modular high-rise buildings, 461 Dean St, New York City, seems like a great accomplishment, however there were many reported issues during construction and completion of the project was delayed [6]. The volumetric blocks used in this project were made of steel.

As stated by Generalova et al. [7], the fable of high-rise apartments only being for the wealthy is getting denied. In other words, high-rise buildings and urban apartments are becoming more and more affordable and modular construction is a promising development to support this trend.

At the moment, most of the modules that are used in modular construction projects are rectangular. Main reasons for this are because of the limited freedom of shape due to transportation requirements and to maximize usability of the space. However, within a rectangular module, the stiffness can be changed by for example adapting column dimensions, wall thickness and lateral stability elements. This is where structural optimization becomes relevant.

1.1.3. Structural (topology) optimization methods

Structural optimization generally aims to increase structural efficiency by for example reducing the weight or cost of a structure. Popular forms of structural optimization are size and topology optimization. Examples of size optimization are changing beam and column dimensions, whereas topology optimization adapts the topology of the structure within given constraints.

An example of a high-rise building where topology optimization has been applied is the conceptual Bionic Tower, shown in figure 1.2a. This example shows the outer structure of the building which has a very irregular shape. Aesthetically, this may look amazing, however such kinds of buildings seem very challenging if not impossible to construct. Despite the fact that this kind of building topology does not seem to be very practical, it does give a good insight in the methodology of topology optimization, which only applies material at locations where needed. Practicality can be dealt with by adding additional constraints.

Another more practical example is the Northwest Corner Building in New York (figure 1.2b). Topology optimization has been applied by removing unnecessary bracing, which results in a rather odd structure. However, by using the optimization technique, various solutions can be explored which normally would not have been designed. For each application, a different optimization technique may be more beneficial, while this also depends on the objective of the optimization. Bi-directional Evolutionary Structural Optimization (BESO) and Solid Isotropic Material Penalization (SIMP) are well-known topology optimization methods.

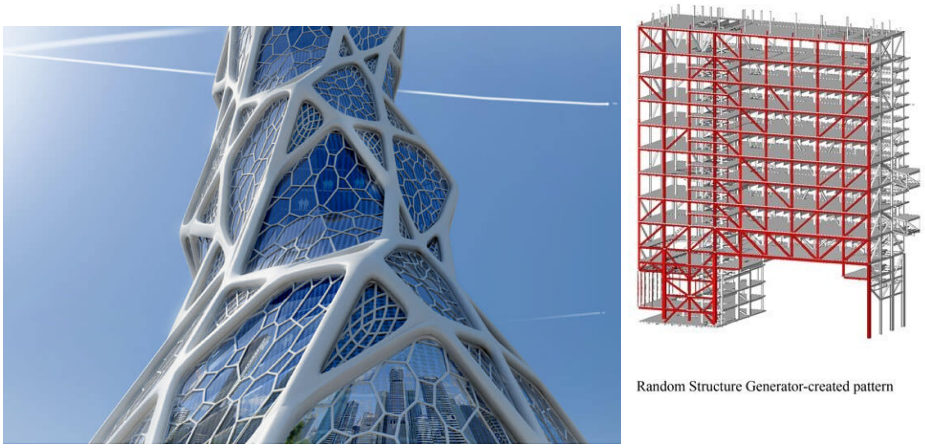

(a) (b)

Figure 1.2: (Conceptual) Bionic Tower (a) and Columbia University Northwest Corner Building (b)

For each optimization method however, there are numerous assumptions and boundary conditions. This entails that a large number of solutions are possible within each optimization method. It is important to specify the optimization method, assumptions and constraints, as well as the optimization objective clearly.

The increasing number of tools and methods that become available for structural optimization enables a better understanding of the general idea behind structural optimization. Each optimization method has its own objective and constraints, which make it interesting to see which method is most suitable in optimizing a structural design of a modular high-rise building.

1.2. Research description

1.2.1. Problem statement

The increasing demand for high-rise buildings in urban areas, as well as the relatively new developments in modular construction and structural optimization techniques calls for a study on structural optimization of high-rise modular structures. As modular construction is fairly new, especially in high-rise building, the opportunities and drawbacks are not yet fully understood. By using structural optimization techniques in modular high-rise buildings, it is strived for to come up with an optimization procedure for modular high-rise structures so that future high-rise buildings can be built more efficiently.

While topology optimization can result in abstract forms such as the Bionic Tower, it is more interesting to explore designs that are feasible and could be constructed modularly. To stay within the concept of modular construction, the idea is to create a structure with repetitive modules, or an external frame structure in which repetitive modules can be placed. Therefore rectangular modules are considered and the optimization mainly focuses on the size and topology of the structural members in each module.

In order to support the early design stage, the method is tested in various case studies in which any arbitrary shape is translated to a structural model and design space for the optimization. This way, feasibility of a design can quickly be verified.

Scope
In short, the scope of the project is defined as follows:

In scope

- Exploring existing as well as new methods for size and topology optimization
- Finding an optimization procedure applicable for modular high-rise structure
- Rectangular, corner-supported steel modules with diagonal (X-) bracing are considered
- Linear elastic analysis are performed for faster iterations
- 2D and 3D cases are considered. 3D cases include diaphragm action
- Testing the procedure for arbitrary shapes by translating these shapes in structural models with the click of a button
- Include important parameters such as module dimensions and loading conditions
- Creating a user interface to adjust parameters and view results

Out of scope

- Foundation and substructure of the building
- Building physics and services
- Different shape/topology modules (e.g. triangular, circular etc.)
- Different building materials (e.g. concrete, timber)
- Building planning, logistics and construction management
- Aesthetics and urban context

1.2.2. Research objective and approach

Research objective and expected outcome
The main goal of this research is to come up with a design aid which can generally predict the outline of any modular high-rise structure by generating the design space and optimizing the structure. This way, efficiency in the early design process is gained.

The expected outcome for this research is to develop a parametric script which generates a modular construction system from any given shape and subsequently optimizes the structure for shape and/or topology. This way an early structural design for any building can be generated by only adjusting boundary conditions such as module size and building dimensions.

Research approach
The thesis involves three parts. Firstly, the literature review will be carried out in order to gain knowledge and insight in the current state of development, future perspective and potential fields of research. Assessment criteria will be described in order to have a starting point for the optimization studies. Also the literature review aims to gain knowledge about the available tools and methods in order to pick the most suitable ones to accommodate the research.

Secondly, a study on various optimization methods and tools for the application of modular high-rise buildings is carried out. The main idea is to find appropriate optimization methods and boundary conditions.

Next, an optimization method is proposed and verified. The optimization procedure is implemented such that any shape can be analysed and optimized with given boundary conditions. The thesis concludes with answers to the research questions and a discussion of the limitations and opportunities for future studies.

Tools
The tools that are used to support this research are:

- Rhinoceros
- Grasshopper
- Various plugins for Grasshopper
  - Anemone
  - GHPython
  - Karamba3D
- Topology Optimization tools
  - Grasshopper: Ameba, Millipede, Karamba 2D TO
  - BESO2D
- Python

The motivation for using these tools relies in the integration between the various tools, familiarity with and personal interest in the software.

1.2.3. Research questions

The main research question which will be investigated is the following:

How can the optimal structural design of any high-rise building with standardized corner-supported modules be generated and optimized?

This research question is supported by the sub-questions listed below in the general report layout. Each sub-question is listed with the corresponding chapter.

1. Introduction
2. Literature review
   (a) What are the current and future developments in high-rise buildings?
   (b) How is structural stability ensured in high-rise buildings?
   (c) What are the advantages and limitations in modular construction (in high-rise buildings)?
   (d) What are the main design considerations for modular high-rise buildings?
   (e) How does a typical volumetric unit look like?
   (f) What is the objective of structural optimization?
   (g) What are types of structural optimization methods and their advantages/limitations?
3. Comparison of existing optimization methods
   (a) Which optimization tools are available?
   (b) How do various optimization tools perform?
   (c) Which existing method is most suitable for optimization of high-rise modular structures?
4. Proposed optimization method
   (a) How can the existing optimization methods be improved for modular high-rise structures?
   (b) Which boundary conditions must be taken into account?

5. Case study
   (a) Which parameters are important for an early stage structural design?
   (b) How can any geometry be translated into a structural design?
6. Conclusion and recommendations

1.3. Reading guide

As mentioned in this chapter, background information is given about the current state of the technology, the boundary conditions and limitations in structural design of high-rise buildings, modular construction and topology optimization. The main focus is to show the relevance and to see what potential research topics can be. Research questions and the general outline and aim of the project are presented.

Chapter 2 gives an overview of the relevant literature found on these topics. The literature review provides background information on the three topics and gives insight in potential fields of research.

Chapter 3 presents an overview of the structural optimization study on existing methods, specifically applied in frame structures. This will give an insight in the currently available methods and implementations. Multiple case studies are worked out and the results are used for a further study for new optimization methods and implementations.

Chapter 4 continues on the topic of structural optimization and presents a new optimization method. The method is applied in similar frame structures and the results are compared to the results of existing optimization tools.

Chapter 5 discusses the case studies which include an implementation of a design aid which proposes rough structural designs for arbitrary shapes. The proposed optimization method from chapter 4 is used in this design aid.

Lastly, chapter 6 concludes with a discussion on the results, limitation and answers to the research questions.

2

Literature review

This chapter includes the literature review and will present the relevant literature regarding high-rise buildings, modular construction and topology optimization. First, the development of high-rise buildings in the past is discussed, as well as the future vision and developments. Also the main structural systems of high-rise buildings are reviewed, as well as advancements and opportunities in modular high-rise buildings. Lastly, currently available structural optimization principles, methods and tools are discussed which will be used for the structural optimization in chapters 3 and 4.

2.1. High-rise buildings

2.1.1. General background information

Definition

Over the years, high-rise buildings have changed a lot. Firstly, lets introduce the definition of a high-rise building. A high-rise building is generally perceived as a tall building, however the exact definition may differ depending on location and regulations by municipalities, states or other instances. In this thesis a distinction is made buildings and structures. High-rise structures also include non-buildings such as the Eiffel Tower are neglected. Only high-rise buildings will be considered, however the main focus will nevertheless be on the building *structure*. The definition of a building stated by Craighead [8] is stated as follows:

> "A building is an enclosed structure that has walls, floors, a roof, and usually windows."

For a tall building, this definition is extended to a building with multiple stories which require a lift to reach these stories [8]. Subsequently, for high-rise buildings this definition is even more specific. Multiple definitions can be distinguished, including [9]:

- A lift is required to reach the destination
- Height of the building exceeds reachable fire-fighting equipment height
- Height has serious impact on evacuation

In general, this means a building with a height of larger than about 23 to 30 meters is considered a high-rise building [8] [9]. However, there are other defintions such as a building taller than X meters or a building with more than Y number of stories.

The definition of a high-rise buildings differs from the definition of a skyscraper. Generally, a building is classified as a skyscraper stands out in a city's skyline and is at least 150 meters tall (in the United States) or 80 meters tall (elsewhere) [10]. This would mean that a skyscraper always is a high-rise building but a high-rise building is not necessarily a skyscraper. The Council on Tall Buildings and Urban Habitat (CTBUH) classifies three categories of tall buildings according to their height [11]:

- Tall Buildings (<300 meters)

- Supertall Buildings (300 to 600 meters)
- Megatall Buildings (>600 meters)

Given these definitions, this means that all high-rise buildings in the Netherlands currently would be classified as 'Tall Buildings' as there is no building taller than 300 meters at the moment. Some of the tallest buildings in the Netherlands may be classified as skyscrapers since they are taller than 150 meters and define or seriously impact the skyline. Supertall buildings only started to pop up in the 20th century whereas the first megatall buildings were built in the 21st century. As seen in figure 2.1, there are currently only three buildings that match this description for megatall buildings.

For the matter of this project, the exact definition of high-rise building, (super- or mega-) tall building or skyscraper is not of utmost importance. Generally, it can be said that the idea is to investigate the structure for every building where the wind load is governing or plays a dominant role in the definition of the structural system. Usually the building height and slenderness ratio are determining factors.

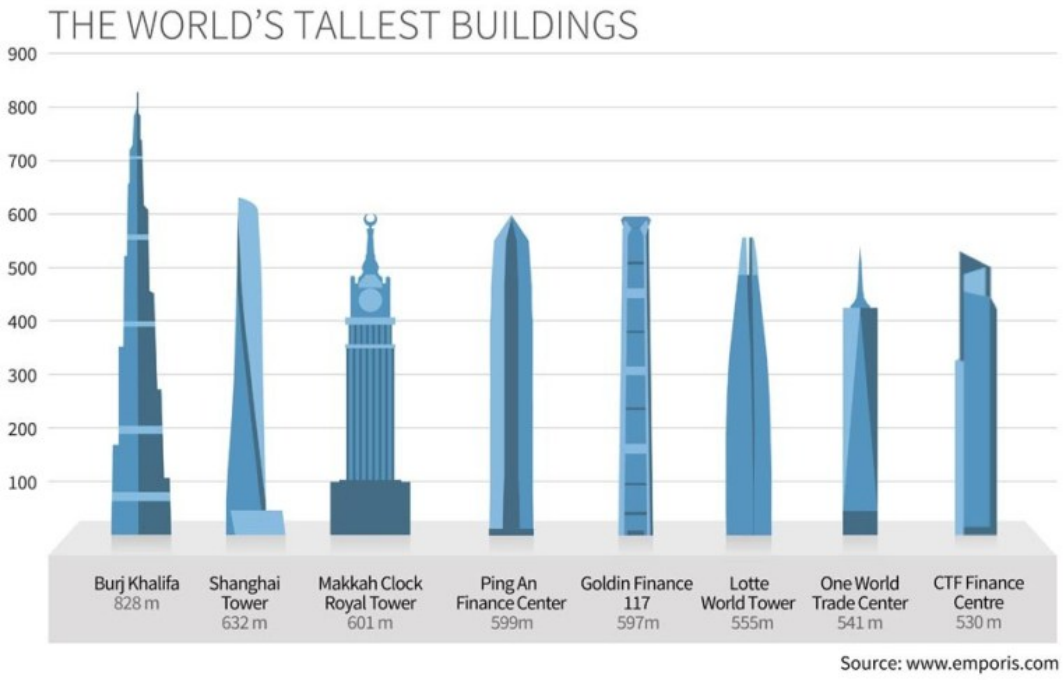

Figure 2.1: The tallest buildings in the world [12]

Development of high-rise buildings

The first high-rise buildings have been built in the late 19th century in the United States. Back then, high-rise bulidings were by far not as tall as high-rise buildings nowadays. The first skyscraper ever built is, arguably, the Home Insurance Building in Chicago in 1885 which was made of steel, cast iron and wrought iron. The reason for this material choice is the fact that masonry, which was primarily used at that time, was weak and inefficient so alternatives were desired [12]. The height of the building was 42.1 meters and structural integrity was given by a steel and iron frame.

After the first high-rise building was erected, many other high-rise buildings followed soon. Examples of these buildings are the Flatiron Building, Manhattan Life Insurance Building and American Surety Building in New York. New York City and Chicago had gotten into a high-rise building competition which is nowadays evident in their skylines as these are arguably one of the best skylines in the world [13] (figure 2.2). Soon after, a lot of skyscrapers were erected at different places in the world - first in Asia and South America and later also in Europe, Oceania and Africa. The rivalry between New York City and Chicago to build

(a)

(b)

Figure 2.2: Skyline of New York City (2.2a) and Chicago (2.2b) [14]

taller buildings has had its impact on other countries too as there is a desire to build higher and higher. The tallest building at the moment is the Burj Khalifa in Dubai with a height of 828 meters and soon there will be a building taller than 1 kilometer: The Jeddah Tower. Nowadays, almost every metropolitan city houses multiple high-rise buildings and high-rise buildings are in construction everywhere in the world as a result of global urbanization. Also the fact that there are a lot of technological developments in the building engineering sector may contribute to this trend.

2.1.2. Regulations, requirements and future vision

Governmental/institutional regulations

As the building types, methods and techniques have changed over the years, regulations and future perspectives have changed accordingly. In the Netherlands, the regulations have changed in the sense that the maximum allowable building height is continually increasing. A clear example of this the fact that in Utrecht a high-rise residential building is being developed which will be higher than the tower of the Dom church, which has been a controversial topic for years [15].

Not only the maximum building height is determined by municipalities and institutions, but also the locations where high-rise is allowed and to a certain extent, the architectural style, appearance and function of the building. This way, the structural design of the building is partly restricted, for example if large column-free spaces are desired.

Building requirements

According to Bhavikatti [16, p. 76], the fundamental requirements of a building are the following:

1. Strength and stability
2. Dimensional stability
3. Resistance to dampness
4. Resistance to fire
   (a) the structure should not ignite easily
   (b) building orientation should be such that spread of fire is slow
   (c) in case of fire, there should be means of easy access to evacuate the building quickly
5. Heat insulation
6. Sound insulation

7. Protection from termite
8. Durability
9. Security against burglary
10. Lighting and ventilation
11. Comfort and conveniences
12. Economy

For this research, the main focus is on criteria 1 and 2 as it is desired to find a structure that is strong and stable. In the preliminary design phase, a structure is normally analyzed on its strength, stability and behaviour [17]. The stiffness criteria can be found in limiting the deflections of the building. The strength guidelines and regulations are defined in the Eurocode and differ per material. Generally speaking, it can be stated that the design load should be smaller than the design capacity of the structural members. Criteria 8 and 12 are taken into account in the sense that the structural design should preferably durable and economic, the latter by reducing the material used.

Future vision and developments

A promising development in high-rise buildings is the use of timber as a structural material in high-rise buildings. The main driver for this is the fact that it is promoted by governments, also due to sustainability benefits of timber construction. A timber structure would reduce carbon emissions to only 10% of the carbon emissions for a similar steel structure, namely 4 kg to 40 kg of CO2 per square meter of office space respectively [18]. The use of Cross-Laminated Timber (CLT) allows construction of taller buildings due to its strength, stiffness, freedom of shape and sustainability benefits [19]. According to Block [20], building projects can be even more sustainable if materials like timber are used rather than concrete. However timber generally has a lower stiffness than steel which makes it more challenging if not impossible to build extreme high buildings from this material.

Another development in high-rise buildings is the concept of prefabricating elements, or even volumetric modules. This advancement does not only apply to high-rise buildings, but also lower and temporary buildings. This concept is further discussed in section 2.2.

2.1.3. Structural systems for high-rise buildings

Structural design and development of high-rise buildings is often complex as there are an unlimited number of possibilities regarding to structural systems, material choice, layout and dimensions of the structural members. In high-rise buildings, lateral loads due to wind pressure increase with height while vertical loads on the columns and foundation also increase as the building becomes taller. Currently, frequently used structural systems in tall buildings to accommodate these loads include core, outrigger, tube, diagrid and mega frame structures (figure 2.3). Diaphragm action of the floors, which entails that the floors will behave as slabs, is important in almost all systems listed and combinations of these systems are also possible. The chosen structural system generally depends on the geometry and dimensions of the building, especially the height and slenderness ratio (height/width). These buildings must be designed in such a way that they can sustain the loads acting on the building, while also providing sufficient comfort for building users. The latter can be defined as limiting deflections due to wind load and reducing vibrations in the building.

As the idea of building high-rise is still relatively new compared to other structures such as low-rise or other residential buildings, there are lots of challenges and opportunities. An example of this is the continuous desire to build higher and higher. This is evident in the fact 20 out of the 22 currently tallest buildings have been constructed in only the last two decades [22]. One of the reasons for this desire is the fact that high-rise buildings often function as a landmark and also aim to show a level of prestige. The fact that buildings keep getting taller and taller requires innovative structural designs as height is one of the critical factors in high-rise building design.

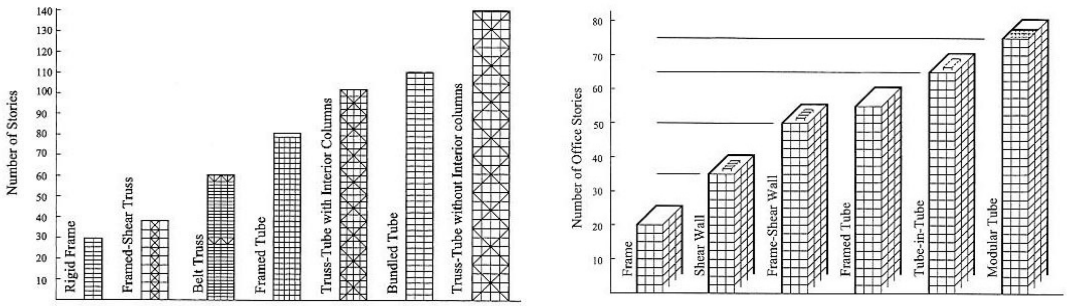

(**a**) Steel (**b**) Concrete

Figure 2.3: Structural Systems in High-Rise Buildings [21]

According to Halvorson and Warner [23], a structural system for a high-rise building should be designed according to these criteria:

- Resist overturning wind force by vertical elements placed as far apart as possible
- Channel gravity loads to those elements
- Link these elements together, creating rigid planes
- Resist lateral force with members loaded in axial compression rather than tension or bending

To ensure lateral stability, sometimes one structural system is not sufficient to provide a safe structure and so a combination of structural systems is used. The main structural systems used in high-rise buildings can be classified in the following groups [24]:

- Core structures
- Outrigger structures
- Facade tube structures
- Mega frame structures

In these conventional structural systems, the main principles listed by Halvorson and Warner [23] apply. However, each structural system behaves differently and there can be other innovative structural systems that will also meet these criteria. Also, within each structural system there are still an unlimited number of structural designs possible.

Examples of buildings with these main structural systems are displayed in figure 2.4, core (2.4a), outrigger (2.4b) and facade tube (2.4c) respectively. The core in figure 2.4a is inside the building, whereas figure 2.4b shows the outrigger trusses at about half of the height and at the top while the building in figure 2.4c is characterized by the thick facade columns. There are however a lot of different lateral stabilizing structural systems. Some of these have been depicted in figure 2.3.

It is difficult to say which structural system is the most suitable for a particular building. This depends on many factors such as building length, width and height, thus slenderness of the building, the functions and their layout as well as material choice. Generally, the building height is taken as governing: a rigid frame is assumed to be most economic for 5 to 10 stories, whereas a core is generally applied for buildings up to a height of 120 meters [25]. Structural members can also have multiple functions which is usually the case for a core, which also houses the elevator shafts, (emergency) staircases and other installations such as MEP services. At larger heights, tube structures, outriggers and mega frame structures are more suitable structural solutions, however they are usually combined with a structural core for functional reasons. In order to ensure cooperation with the core, diaphragm action of the floors is required to transfer the lateral loads.

(a) (b) (c)

Figure 2.4: Maastoren in Rotterdam (2.4a), New York Times Tower (2.4b) and Willis Tower in Chicago (2.4c) [26]

Also, a country-specific issue is the soft soil conditions in the major part of the Netherlands which is challenging for designing high-rise buildings. As a high-rise building is generally very heavy and encounters large bending moments at the base due to lateral loads on the building, a strong foundation with enough stiffness is required. For most high-rise buildings in the Netherlands, a piled raft foundation is used with generally very long piles (for example over 60m long piles in Zalmhaventoren [27]), while in other countries sometimes only a raft foundation is sufficient to support a similar type of building. For this research however, the foundation will not be considered and the main focus will be put on optimizing the superstructure.

Core structures

In a building with a core as stabilizing structure, the lateral forces must be transferred to the core. This is done through diaphragm action of the floors. Usually, the core is placed in the center (or close to the center) of the building. A building can also have multiple cores.

Examples of high-rise buildings which use a core as stabilizing system are the Maastoren and the Rembrandt Tower in Amsterdam as depicted in figures 2.4a and 2.5 respectively.

The core itself can be simplified to a large rectangular hollow section (RHS) which is usually made of reinforced concrete. A relatively good first approximation for the dimensions of the core is the height of the building divided by 10.

For an initial calculation, the moment of inertia of this rectangular hollow section can be calculated. In practice, the core is of course not a perfect rectangular hollow section as there are openings in the core for instance for the elevators, pipes and ducts. Also the dimensions (usually wall thickness) of the core may differ along the height of the building and the reinforcement is not yet taken into account. The building can be modelled as a cantilever beam loaded by a uniformly distributed load (lateral) which represents the wind load acting on the building. By using material properties (Young's modulus) and general rules of thumb for cantilever beams, the approximate beam deflection due to the wind load can be calculated.

Outrigger structures

When the situation occurs that a core only is not stiff enough to stabilize the building, an outrigger structure can provide extra stability to the core. One or multiple large trusses connect the core with the outriggers, which are generally placed at the edges of the building.

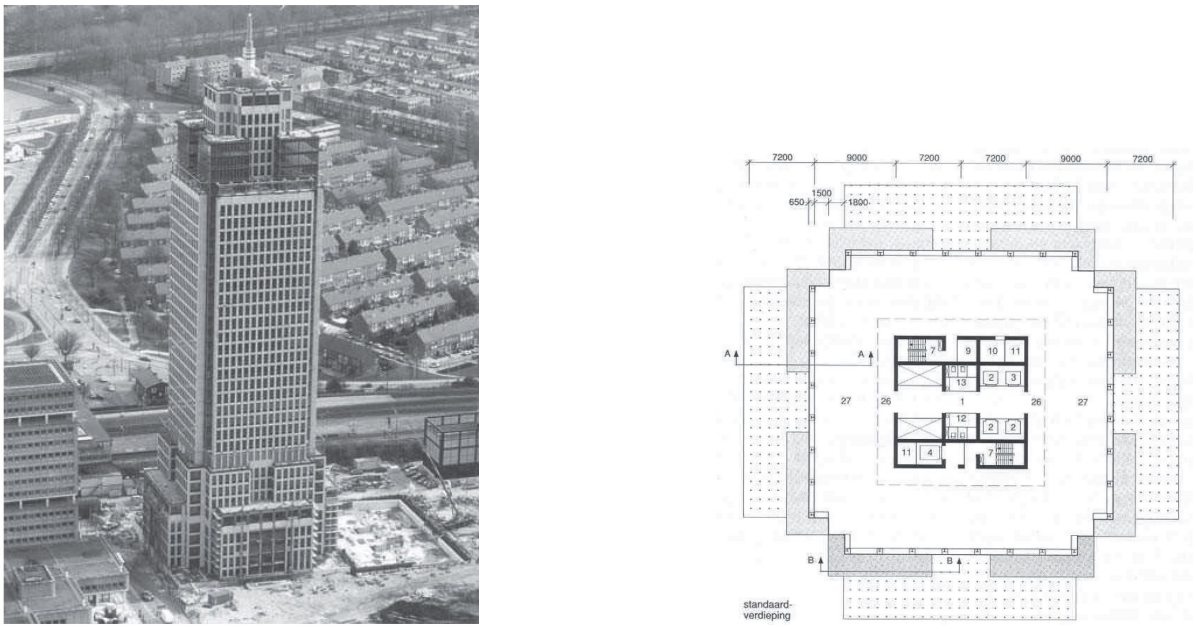

(a) (b)

Figure 2.5: Rembrandt Tower in Amsterdam (2.5a) and floor plan of Rembrandt Tower (2.5b) [28]

The idea behind an outrigger structure is the same as a person with a broken leg walking with crutches. As standing on one foot is quite unstable, leaning on the crutches will provide extra stability. In this case the core can be compared to the foot whereas the crutches are the outriggers. The forces in the outrigger will create a moment which counteracts the bending moment by the wind force. In order for the outriggers to have a significant effect, they must therefore be placed relatively far from each other in order to increase the internal lever arm and thus the moment. This principle is shown in figure 2.6. Also multiple trusses can be designed in a building in order to reduce the moment even further. Usually such trusses are relatively large and take up an entire floor (or sometimes even multiple floors), which is why these floors are usually mechanical floors that are used for services.

Facade tube structures

In a facade tube structure, the columns and beams are at the perimeter (or facade as the name says). The connection between these structural elements is usually rigid. When a facade tube structure also includes a structural core, the structural system is called a tube-in-tube structure as the core is referred to as the inner core. Generally facade tube (or tube-in-tube) structures have a higher stiffness because of the fact that the structural members are located at the perimeter of the building.

The stiffness of a facade tube structure can be approximated by assuming that the perimeter of the building is a rectangular hollow section with holes (for windows). Since the building perimeter is always bigger than the core, the stiffness is usually also higher, however this also depends on the number and size of the openings. The same calculation procedure as used for the core structure can be used to initially approximate the deflection of a tube (-in-tube) structure as well.

Mega frame structures

As the name might already reveal, mega frame structures are extraordinary large frame structures. Usually these type of structures have very large braces, as is evident in the Bank of China Tower in Hong Kong (figure 2.7). Typically, the connections between structural members in a mega frame structure are rigid. The mega frame structure often is a combination of multiple structural systems. Mega frame structures are generally very complex and only required to ensure the lateral stability of super- or mega-tall buildings.

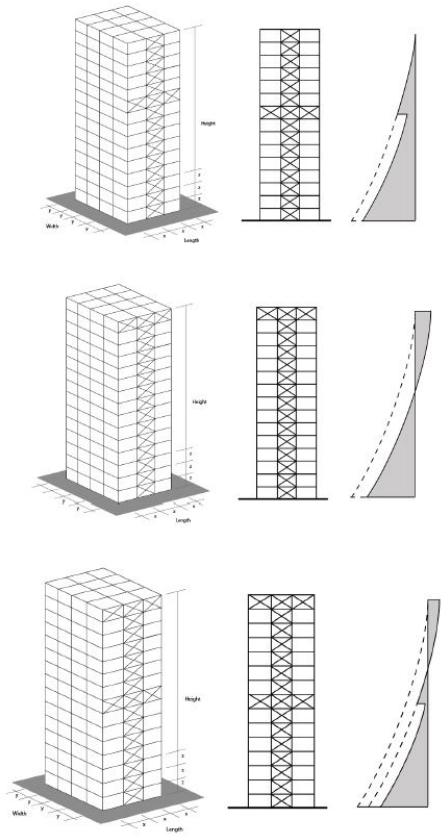

Figure 2.6: Outrigger system principle [25]

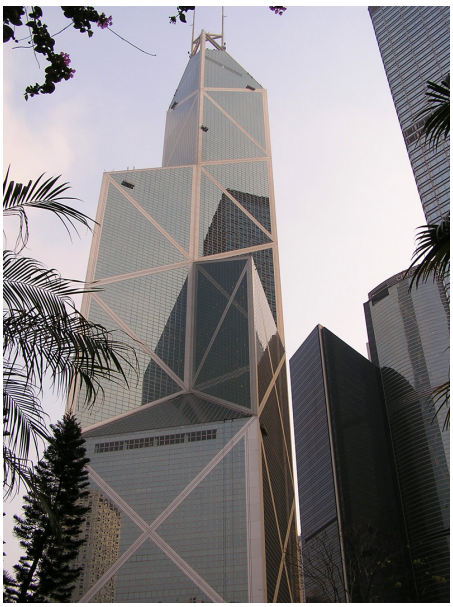

Figure 2.7: Bank of China Tower in Hong Kong [26]

2.2. Modular building concepts

2.2.1. Definition

Modular building can be understood as the act of building prefabricated modules, specifically repetitive volumetric units, off-site [29]. The modules are often constructed in a controlled environment and therefore less prone to uncertainties and delays. The completed modules are then transported to the building site where they can be installed. This building concept is different from the conventional building method, where most of the work is done on site. Another definition of modular construction according to Lawson et al. [30] is:

> "Three-dimensional or volumetric units that are generally fitted out in a factory and are delivered to the site as the main structural elements of the building."

The definition according to Lawson et al. [30] is a bit more extensive in the sense that the volumetric units are structural members of the building. Generally, this is almost always the case as the modules should be able to support themselves in order to be transported to the building site. However in high-rise buildings, an additional structural system may be required next to the self-supporting modular units in order to deal with the lateral load or the high compression loads which occur in the columns at lower floors.

Modular construction should not be mixed up with prefabricated construction. According to Generalova et al. [7], prefabrication is referred to as rapid construction of buildings where structural members are produced in a facility and assembled at the building site. Examples of these members could be columns, beams, floors and wall panels. Modular construction instead refers to prefabricated three dimensional blocks fabricated off-site, which has the advantage of speed of assembly, high quality control, work safety, noise reduction and lower construction waste [7]. Usually, these volumetric units have interior finishing as well in order to reduce the workload onsite.

Ideally, the modules should be replaceable and demountable too, which means that the building will be fully modular and that the modules can be replaced and reused. In an extreme example, this modular building may be compared to a vending machine in which an external frame can select an individual product (module) and remove it from the machine (building). This may cause some difficulties in the structural behaviour of the building, such as whether or not the modular structural elements will work together as a whole or not. A study by Lawson et al. [30] has shown the effect of the removal of modules by presenting the alternative load paths and force distributions in other structural members and shows that this can be feasible. At the same time, the added value of demountability should be considered too, as a high-rise building is not very likely to be deconstructed or demolished in shorter periods of time. Examples of this are the first high-rise buildings in New York City and Chicago, which have been standing for over a century and are still standing as of today.

While demountability can be questioned, throughout the world modular building has become increasingly popular. Some applications of modular buildings are elaborated in subsection 2.2.4.

2.2.2. Advantages and drawbacks to modular construction

Advantages

Modular housing is a method that allows a large number of new homes to be built in a short time period in urban areas [20]. According to Lacey et al. [29], the advantages of modular construction especially outweigh the drawbacks for hotel and residential buildings. These are often two important functions in high-rise buildings, which is why it is obvious that modular construction can be effective in these type of buildings. In general, the advantages of modular construction can be summarized as follows [30, p. 7]:

- Shorter build times
- Superior quality
- Economy of scale in production
- Excellent acoustic and thermal insulation

- Reduced design cost
- Lightweight, less material use, less wastage
- Increased productivity in factory production
- Safer construction
- Less disturbance to the neighbourhood
- Ability to dismantle the building

A study carried out by Kim [31] has found that a modular home consumes 4.6 percent less life cycle energy and emits 3 percent less greenhouse gases than traditional houses. The shortened building time and improved quality of the building also contribute to this reduction of energy consumption and greenhouse gas emissions. However, the study also mentions that transportation energy mainly depends on the locations of the building site and production facilities.

Also, Kamali and Hewage [32] mentions that modular construction is applicable to various types of buildings, including residential, commercial, educational and medical buildings and that in these types of buildings, the life cycle performance of such modular buildings is better among others. As sustainability in the building sector is becoming increasingly important, modular construction could be an important construction method for the future. The reason that modular construction, despite the listed benefits, has not yet been adapted on large scale globally mainly depends on aspects such as housing demand, labour demand and cost, efficiency in the building process and weather [33].

Disadvantages

Overall, it seems that there are a lot of advantages for modular construction and therefore modular construction can potentially be a viable contribution to the solution of global urbanization, while increasing safety at the building site and enhancing the quality of buildings. It is however not that simple as modular construction also brings about a lot of limitations and drawbacks, of which some are:

- Transportation limitations
- Hoisting limitations
- Limited module size and shape - poorer overall design [9]
- Complexity of connections
- Relatively new concept, little experience so far

The transportation and hoisting limitations generally define the maximum size and weight for the module. These limitations also depend on the local legislation and has been elaborated in section 2.2.2. An example of the fact that modular construction is relatively new and not yet fully understood is evident in the Atlantic Yards project, as discussed in section 2.2.4.

Limitations

Transportation regulations One of the main limitations for modular construction is the limited size of the module due to transportation regulations. The limitations of transport on the road differs per country or even per city. The maximum dimensions for special transport (also called oversized or exceptional transport) in the Netherlands and Belgium are listed in table 2.1.

The dimensions for transportation are thus quite limited, especially the width. The floor height, which is also the module height assuming that a module is one storey tall, usually does not exceed the maximum transportation limit of 4.00 meters. Also the length of a module usually will not exceed the maximum length for a truck with trailer. However, the width of a room in a residential building can easily exceed the maximum transportation limit of 3.00 meters. This means that for bigger rooms multiple modules may be needed. Usually, the

	Netherlands (RDW)	Rotterdam	Belgium
Height	4.25 m	4.00 m	5.00 m
Width	3.50 m	3.00 m	4.80 m
Length	27.5 m	22.0 m	35.0 m
Weight	100 tonnes	50 tonnes	120 tonnes

Table 2.1: Maximum transportation dimensions [34] [35] [36]

dimensions of a regular hotel room fit within the maximum transportation limitations, which is one of the reasons why modular construction is especially beneficial in hotels [30]. Other reasons are the speed of construction (and therefore faster return on investment) and the large amount of repetition.

It is also evident that the transportation limits within the city of Rotterdam (and possibly also in other cities) are more strict than the national regulations. This may be because of the limited space in the city, as well as the busy traffic. Therefore, municipalities may require this special transport to take place in a certain time slot and also that the transport must be guided by other vehicles [36].

Even though there are strict limitations, for some large building projects or other transportation demands, exceptions will be made. An incidental exemption may be applied for, which allows transportation of larger dimensions than the ones listed in table 2.1. In principle, there is no maximum dimension for which an exemption can be made [34]. However, requesting exemptions for these types of transport is not favourable as it can be time consuming and more expensive than regular transport.

Hoisting limitations Once the modular building blocks have been transported to the construction site, they have to be assembled. Usually, a crane is used to lift the module and put it in place. The load-bearing capacity and reachable height of the cranes therefore also define the module size and maximum building height.

One of the biggest cranes currently in use have a maximum load capacity of 1200 tonnes and a maximum hoisting height of 188 meters [37]. This load capacity is much bigger than the maximum load which is allowed to be transported on the road. Also, the maximum height of 188 meters is already higher than the currently tallest building in the Netherlands. Therefore, the hoisting limitations are assumed to have very limited influence on the design of a modular high-rise building.

Next to crane capacity, there are also regulations, standards and guidelines regarding the use of cranes. These standards are stated in the ISO 12480 norm.

Structural limitations Another limitation, and perhaps the most important one, is the structural limitation. As the structure is built up from individual modules, ensuring structural integrity and making sure the structure acts as a whole may introduce complications. Precast concrete modules generally do not have as stiff connections as in-situ concrete elements whereas bolted connections in steel are generally less stiff than welded connections. Additionally, constructing a building out of individual modules means that there are also a lot of double beams, columns or wall elements. This however depends on the type of module and is further elaborated in subsection 2.2.3.

In case of an external structure in which the modules are placed, the external structure will function as main load-bearing system. The modules can then be connected to the external structure with less stiff connections.

All in all, the main advantages and disadvantages of modular construction can be summarized as depicted in table 2.2.

Advantages:	Disadvantages:
About 10 to 15 % less construction waste [38]	Complexity of transportation of large modules
Less disturbance on site	Limited design freedom due to transportation limitations
Construction in (controlled) factory environment	Aesthetically less pleasing due to repeated modules
Safer construction (80% less accidents [38])	More material use due to double beams/-columns
Increased speed of erection due to repetition	
Recyclability of modules	
Less weather delays	
Great acoustic and thermal insulation [30, p. 7]	

Table 2.2: Advantages and Disadvantages of Modular Construction

2.2.3. Types of modules

Steel modules

Typically, there are three types of steel modules that are used in modular construction [38]. These are:

1. Four-sided modules
2. Corner-supported modules
3. Non-load-bearing modules

Four-sided modules are modules that are continuously supported by walls on the four sides of the module. It is possible to create some openings in the walls, for example for windows and doors.

Corner-supported modules deal with the vertical load by transferring these through edge beams to the columns that are located at the corners. The main advantage of corner-supported modules in comparison to four-sided modules is that there is more design freedom in the floor plan as the location of walls is not fixed. On the other hand, the dimensions of the edge beams may need to be larger as a result of the increased span compared to the continuously supported modules. The beams and columns used usually are angle- or C-sections, and square hollow sections (SHS). Angle and C-sections are however more sensitive to buckling and are less favoured for large compression loads.

Non-load bearing modules do not take any load, neither in vertical nor in horizontal direction and need a separate structure to support them. The structure of these type of modules will not be considered, however these type of modules can be placed in an external frame structure which is the primary load-bearing structure. The advantage of this is that demountability of the modules seems easier without affecting the main structure of the building. Lawson et al. [30] also refer to this type of structure as 'Hybrid Modular', where non-load-bearing modules are carried by beams or rest on concrete floors.

Precast concrete modules

Precast concrete elements are generally used as '1D' and '2D' elements such as beams, columns, walls and floors, however '3D' elements are relatively new. Most precast concrete modules include '2D' elements such as walls and ceilings (or floors) which are rigidly connected to each other. The base of the module can be left open such that the ceiling of the underlying module becomes the floor for the module on top. Walls can be left open as depicted in figure 2.9.

Generally, concrete modules are heavier than steel modules, especially corner-supported steel modules. A typical weight for precast concrete modules is about 20 to 40 tonnes [30].

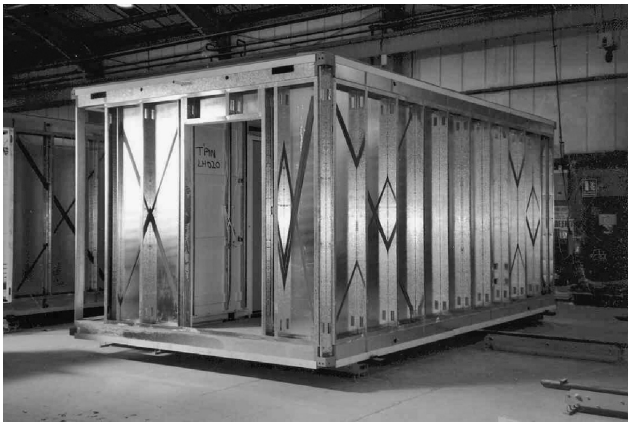

(a)

(b)

Figure 2.8: Four-sided (2.8a) and corner-supported (2.8b) steel modules [30]

Figure 2.9: Concrete module for school building [30]

Design considerations

According to Lawson et al. [30], the general principles for designing a modular building are the following:

- Decide whether four-sided modules or corner-supported modules will be used.
- Design building layout in such a way that the module size stays the same as much as possible.
- Choose module size according to transportation requirements.
- Decide stability system of the building: module bracing or concrete/steel core.
- Prefit services in the modules.
- Consider fire safety requirements and strategy.
- Determine cladding system of the modules.

The choice for each criterion may depend on function of the building, costs, other factors or personal preference. In high-rise buildings, so far the most modular high-rise buildings are stabilized by a concrete core. For lower buildings, usually rigid connections and in some cases additional bracing is sufficient. The type of module and module size also depends on material choice and local regulations.

2.2.4. Applications of modular construction

As the concept of modular construction is quite new, it has firstly been introduced in smaller projects, while after it has been proved successful, it has been applied in larger projects as well. Examples of noteworthy modular building projects include PPVC in Singapore, Spaceboxes in the Netherlands and 461 Dean Street in New York. Modular construction has only been applied in high-rise in the last few years, of which some examples are elaborated in this section.

Early modular construction projects

Throughout the world, modular building projects are increasing in popularity. An example of a modular housing project in Japan shows that modular buildings can also be designed to resist earthquake effects. In the UK, modular construction is especially popular in student housing. Also, in Scandinavia modular building is in the rise due to the short weather window for construction [30, p. 12]. An example very close to home is the Spacebox container student housing at the Delft University of Technology. These modules have been placed in 2003 and, after servicing for 12 years, were removed and sold in 2016, showing that this building is still in a good state and therefore reusable [39].

Figure 2.10: Spaceboxes in Delft [39]

461 Dean Street, New York

461 Dean Street in New York (figure 2.11) is another modular high-rise building project and is named the first ever modular high-rise building in the world. As it was completed in 2016, the idea of using modules in high-rise construction is still in its baby shoes. This building is part of the area development in Pacific Park, Brooklyn (also known as Atlantic Yards). The building is also known as ”B2” and is built up from steel modules, in total a number of 930 modules [26]. According to Tower et al. [40], volumetric modular construction changes the way of designing buildings.

The structure of this building in Atlantic Yards entails a steel frame. The dimensions of the modules are 4.57 meters wide, 3 meters high and the length varies between 6.10 meters and 15.24 meters [7]. Due to its large dimensions, special trucks were needed to transport the modules to the construction site.

However, the project was perceived as not so successful. ”Tolerance errors, misalignment problems, leaking gaskets and waterproofing failures” [6] occurred and lawsuits between the developer and contractor were filed. Part of the problems encountered during construction may be addressed to negligence of the involved parties, however this also shows that there is still some room for improvement in modular construction of high-rise.

101 George Street, Croydon

Completed in 2019, the 44-storey residential building in London held the record for tallest modular building in the world, before it was succeeded by the five meters taller Clement Canopy building in Singapore [20]. The same architect, main contractor and module supplier

Figure 2.11: 461 Dean Street, New York during construction [26]

also worked together on the Apex House is Wembley, which was the tallest modular tower in Europe before 101 George Street [26].

The sequence in which 101 George Street was built was first the concrete core, after which the volumetric prefabricated concrete modules were placed around the core to complete the building. This has been depicted in figure 2.12. In total, 1500 modules were used [41].

(a) (b)

Figure 2.12: 101 George Street, Croydon (2.12a) and its concrete cores (2.12b) [26][41]

Clement Canopy, Singapore
The main reasons to choose for modular construction in Singapore were improved productivity, better construction environment and improved quality control [42]. The Clement Canopy building in Singapore (figure 2.13) was a successful project that was originally planned for 36 months but eventually finished within 30 months, of which only 13 months were required to lift the modules and install them on site [43] [44]. The success of this project has resulted in the development of more off-site fabricated modular multi-storey residential buildings.

Figure 2.13: Clement Canopy Singapore [20]

A study by Chua et al. [45] has shown that PPVC high-rise buildings are robust enough to prevent progressive collapse. At the moment, the Clement Canopy, reaching a height of 140 meters, is the tallest modular building worldwide, taller than 461 Dean Street in New York, the first ever modular high-rise. The Clement Canopy is built up from 1899 off-site prefabricated concrete modules and accommodates 505 apartments [20]. The lightest module weighs 16800 kg whereas the heaviest module weighs 29000 kg [43]. Dimensions of the modules vary, but the largest of all has a dimension of 8.5 meters long by 3.2 meters wide by 3.15 meters height, which satisfies the transportation regulations in Singapore [44]. The crane used for the construction of this building had a capacity of 40000 kg and hook height of 88.4m [37] [43].

2.3. Structural optimization principles

2.3.1. Definition

According to Haftka and Gürdal [46], the definition of optimization is:

> ”Optimizing is concerned with achieving the best outcome of a given operation while satisfying certain restrictions.”

Another definition as given by Bruggi and Taliercio [47] is as follows:

> ”a design tool that allows a prescribed amount of material to be distributed over a given design domain to minimize a scalar objective function for a fixed set of constraints”

In terms of structural optimization, it is often strived for to minimize the costs or weight of the structure. The idea of minimizing weight especially holds in the aerospace engineering sector, while in the civil engineering branch usually a minimization of costs is desired for. However, as raw materials become more scarce, there is a need for lightweight structures, efficient and low cost structures [46]. This can be interpreted in the above given definition as finding a solution for a safe structure with a restricted amount of material or budget. Often, it is easier to express a structure in terms of weight than in terms of costs.

Generative design is often perceived as topology optimization, even though these are not the same. The definition of generative design given by Johan et al. [48] is given as ”the

process of defining high-level objectives and conditions to, using computation, search for solutions that meet the specified objectives and conditions". The high-level objective could be to minimize structure weight, whereas the outcome of generative design could be *a range of* solutions which meet the boundary conditions.

There are many methods for structural optimization. According to Leiva [49], the types of structural optimization that can be distinguished are:

- Topology optimization
- Sizing optimization
- Topometry optimization
- Shape optimization
- Topography optimization
- Freeform optimization

Where topometry optimization is perceived as a generalization of size optimization and topography and freeform are special applications of shape optimization. Thus, the three methods commonly used for structural optimization are size optimization, shape optimization and topology optimization [50] [51].

2.3.2. Size optimization

Srivastava et al. [50] state that size optimization is the simplest form of the listed optimization methods. In size optimization, only the size of structural members are varied with. Typically, these are only geometric parameters such as the thickness of a plate or the cross-sectional dimensions of a beam [49]. Such optimization can also be carried out manually using hand calculations. For example, by using rules of thumb to find the maximum deflection of a simply supported beam and calculating the stress in a beam by using classical mechanics formulae, the cross-section of a beam can be adapted accordingly:

For example, a beam is assumed with span length L, uniform load q, Young's modulus E and yield strength f_y. The ideal dimensions for this beam can be found as follows:

Deflection of a simply supported beam loaded by a uniformly distributed load should be lower than the deflection limit:

$$w_{\max} = \frac{5}{384}\frac{qL^4}{EI} \leq \frac{L}{250} \tag{2.1}$$

This means the moment of inertia I which corresponds to the maximum allowable deformation can be computed:

$$I_{\text{required}} \geq \frac{5}{384}\frac{qL^4}{E}\frac{250}{L} = \frac{1250}{384}\frac{qL^3}{E} \tag{2.2}$$

The stress due to bending is calculated by using standard mechanics formulae:

$$\sigma = \frac{M}{W} = \frac{\frac{1}{8}qL^2}{W} \leq f_y \tag{2.3}$$

To satisfy the stress condition, the section modulus W_{required} can be found:

$$W_{\text{required}} = \frac{\frac{1}{8}qL^2}{f_y} \tag{2.4}$$

With the known required moment of inertia and section modulus, a choice can be made from available beams which satisfy these criteria. For more complex structures, more sophisticated tools are preferred over calculations by hand. Currently, there are many software tools available for this type of cross-section (size) optimization.

An example of a tool which can be used for size optimization is Karamba3D Cross Section Optimizer. This tool finds the optimal cross-section for beams and shells depending on input

parameters which can be for instance maximum displacement or utilization. A more detailed study on this method and especially this tool is presented in chapter 3.

An existing building in which a similar method of optimization has been applied is the Dutch National Military Museum, as depicted in figure 2.14. In this building, the roof is a space frame structure from which aeroplanes are hung. Using cross-section optimization, the ideal cross-section for each structural member has been found. In figure 2.15, the left image shows the utilization before optimization whereas the right image shows the utilization after optimization. It is obvious that after the optimization most members are much better utilized and thus that the structural members do not have larger dimensions than necessary.

Figure 2.14: Dutch National Military Museum [52]

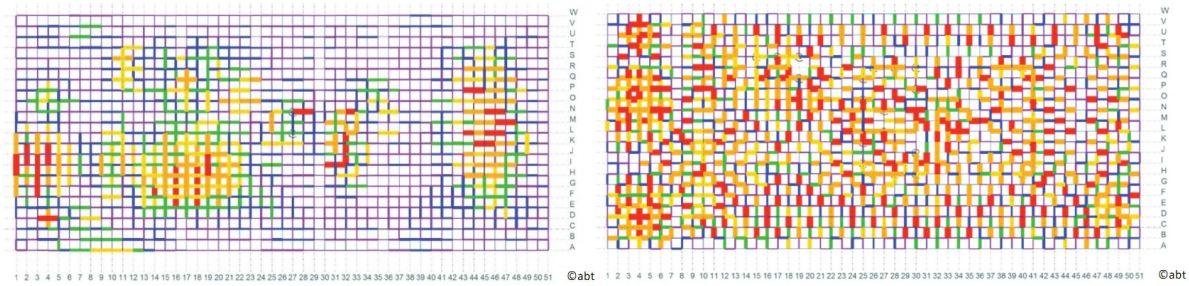

Figure 2.15: Before (left) and after (right) size optimization in Dutch National Military Museum [52]

For statically indeterminate structures, it is more complex to compute the optimum cross-section of a beam element as the force distribution is dependent on the section properties of each element. Therefore, an iterative procedure is needed in which the section forces are checked again after updating the cross-sections.

Strain Energy Density optimization

Another method is to optimize the cross-sections using the strain energy density. These members will contribute the most to the stiffness and deformation capacity of the structure. The highest strain energy density in a beam indicates that changing the cross-sectional area of this beam (assuming that the length remains unchanged) has the biggest influence on the stiffness of the structure. The strain energy density is defined as the strain energy divided by the volume (of the beam). For a beam loaded by axial force only as depicted in figure 2.16, the strain energy U is defined as follows:

$$U = \int_0^{x_1} P dx \tag{2.5}$$

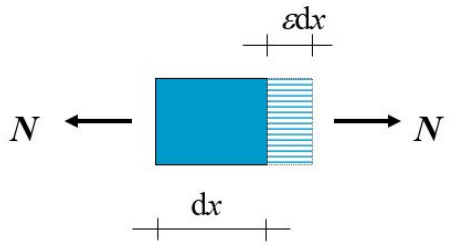

Figure 2.16: Beam element loaded by axial force

The strain energy density is defined as the strain energy divided by a volume. Assuming that the cross-section of each member is constant along its length, this volume can be interpreted as the cross-sectional area multiplied with the length of the beam element. Hence, the following equation results for the strain energy density u:

$$u = \frac{U}{V} = \frac{\int_0^{x_1} P dx}{AL} \tag{2.6}$$

As $\frac{P}{A} = \sigma_x$ and $\frac{x}{L} = \epsilon_x$ hence $\frac{dx}{L} = d\epsilon_x$, this gives:

$$u = \int_0^{\epsilon_1} \sigma_x d\epsilon_x \tag{2.7}$$

With $\sigma_x = E * \epsilon_x$ and therefore $\epsilon_x = \frac{\sigma_x}{E}$, the final definition for the strain energy density becomes:

$$u = \int_0^{\epsilon_1} E\epsilon_x d\epsilon_x = E\int_0^{\epsilon_1} \epsilon_x d\epsilon_x = \frac{1}{2}E\epsilon_x^2 = \frac{1}{2}E(\frac{\sigma_x^2}{E^2}) = \frac{\sigma_x^2}{2E} \tag{2.8}$$

With a constant Young's modulus, it appears that the strain energy density is quadratically related to the axial stress in the beam elements. However there may also be other stresses, which will have their influence on the strain energy density. According to equation 2.7, the strain energy density for axial force is:

$$u = \int_0^{\epsilon_1} E\epsilon_{xx} d\epsilon_{xx} = \frac{1}{2}E\epsilon_{xx}^2 = \frac{1}{2}\sigma_{xx}\epsilon_{xx} \tag{2.9}$$

Similarly, for stresses in y- and z-direction, the strain energy density is $\frac{1}{2}\sigma_{yy}\epsilon_{yy}$ and $\frac{1}{2}\sigma_{zz}\epsilon_{zz}$ respectively. With shear stresses, for example in the xy-plane, and given the stress-strain relation by Hooke's law, the strain energy density is described as follows:

$$u = 2\int \sigma_{xy} d\epsilon_{xy} = \sigma_{xy}\epsilon_{xy} \tag{2.10}$$

Thus, for an element loaded by arbitrary stresses, the strain energy density function becomes:

$$u = \frac{1}{2}(\sigma_{xx}\epsilon_{xx} + \sigma_{yy}\epsilon_{yy} + \sigma_{zz}\epsilon_{zz}) + (\sigma_{xy}\epsilon_{xy} + \sigma_{yz}\epsilon_{yz} + \sigma_{zx}\epsilon_{zx}) \tag{2.11}$$

For an element loaded under pure bending, the strain energy can be expressed similarly:

$$U = \int_0^L \frac{M^2}{2EI} dx \tag{2.12}$$

And thus the strain energy density for bending can be found likewise:

$$u = \frac{U}{V} = \int_0^L \frac{M^2}{2EI}\frac{1}{AL} dx \tag{2.13}$$

By increasing the cross-section of the members with high strain energy density (instead of the members with high utilization), extra stiffness is added to the structure. This way, the structure can be optimized for stiffness. Again, this should be an iterative procedure where the stresses and displacements must be checked afterwards.

2.3.3. Shape optimization

Shape optimization focuses on finding the optimal shape of the structure, given an objective function such as minimizing costs or weight [50]. This is also the case in size optimization, however in shape optimization there is more freedom as the design variables are the coordinates of the boundary. The steps in shape optimization are as follows [53]:

1. Define geometry of the structure
2. Generate mesh and run finite element analysis
3. Compute sensitivity of constraints and objective function
4. Convergence criteria met - optimization problem solved

This means that the topology is predefined in step 1. By changing the boundaries, a more optimal shape can be found within the same topology. An example of shape optimization versus topology optimization is displayed in figure 2.17. In the top figure, the topology changes into something different whereas in the bottom figure, the topology is still the same but only the shape is smoothened out at the re-entrant corner.

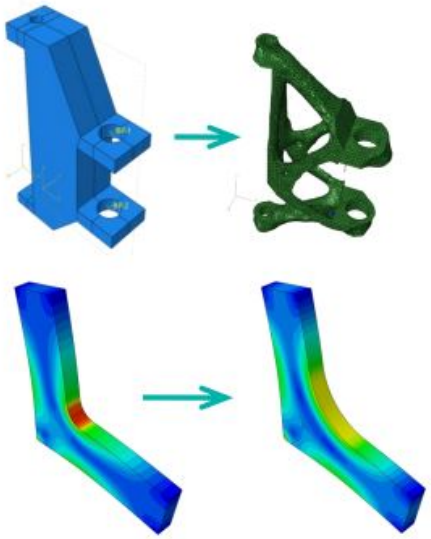

Figure 2.17: Topology optimization (top) vs. shape optimization (bottom) [54]

Topography and freeform optimization are considered as special forms of shape optimization, in which freeform optimization is sometimes also referred to as topology optimization. In shape optimization, the topology is fixed, which is why topology optimization is often used to overcome this limitation.

2.3.4. Topology optimization

The definition of topology optimization as stated earlier is as follows [47]:

> ”a design tool that allows a prescribed amount of material to be distributed over a given design domain to minimize a scalar objective function for a fixed set of constraints”

Topology optimization goes a step further than shape optimization in the sense that not only the shape can vary, but also the topology. In fact, often the topology of the structural member is defined through this optimization technique. The design variables in topology optimization resemble a volume fraction or elements in a mesh with material properties which are included or removed from the model [49]. Thus no initial topology is required, but only a design space in which the solution must be found. It is seen as the most general structural optimization technique, but also perhaps as the most difficult one [50]. Topology optimization often results

in complex shapes that are difficult to manufacture. An example of complex geometries that derive from topological optimization can be found in the biomedial industry in the production and manufacturing of prostheses for maximized comfort. New techniques such as 3D printing or additive manufacturing (AM) can allow production of shapes that were not feasible before and therefore be used in multiple applications [55]. Some topology optimization methods are listed below [51]:

- Evolutionary Structural Optimization (ESO) method
- Bi-directional ESO (BESO) method
- Solid Isotropic Material with Penalisation (SIMP) method
- Homogenization method
- Level set method

Evolutionary Structural Optimization (ESO) method One of the popular techniques for topology optimization is the Evolutionary Structural Optimization (ESO) method [51]. The general idea of the ESO method is that the structure can be optimized by removing ineffective (or less effective) parts from a specified design domain [56]. Usually, parts with low stress or strain energy are considered to be less effective and can therefore be removed. This method is an iterative process: first, a FE analysis is carried out after which parts are removed. Subsequently, the analysis is run again in order to see which parts are ineffective in the new topology. This process continues until the convergence criteria are met. As the number of elements decreases with each iteration, the stiffness matrix for the FEA becomes simpler (a removed element has zero stiffness). Therefore, the computation time decreases with each iteration [51].

Bi-directional ESO (BESO) method An extension of the ESO method is the Bi-directional ESO (BESO) method. The main difference of this method compared to ESO is the fact that not only parts can be removed, but also added however only in the given design space. This means that BESO can be initiated with a minimum amount of material and can be optimized by adding material only where needed [57]. The (B)ESO method is quite time efficient and therefore has been applied in multiple FEA packages, of which an example is depicted in figure 2.18a.

Solid Isotropic Material with Penalisation (SIMP) method In the SIMP method, elements have a density which is a value between 0 and 1. Zero density means that material will be removed whereas a density of value 1 means that material will be added. Since values in between zero and one can occur, these will be penalized such that they will converge to zero or one, thus adding or removing material.

TO tools With many TO tools available, topology optimization is now more accessible than before. One relatively simple example of this is BESO2D by Xie and Huang [51]. An example of topology optimization making use of the BESO method for a high-rise building modelled as a cantilever beam loaded by a horizontal distributed load has been displayed in figure 2.18a.

Another tool developed by Xie and Huang [51] is called Ameba, a plugin for Grasshopper. This tool is based on the same BESO technique for TO.

In Karamba3D, there are also tools available for BESO, namely BESO for beams and BESO for shells. This tool is also applicable for beam elements and has been studied extensively in chapter 3. A study on BESO for beams for a simple cantilever beam is further elaborated in appendix A.1.

Besides the available tools, an own method and implementation can be (visually) programmed as well using the GHPython component (and other components) in Grasshopper. This way, the optimization can be controlled as the input, data stream and output can be specified more precisely than in existing tools. The implementation and study of these available tools have been elaborated in chapter 3.

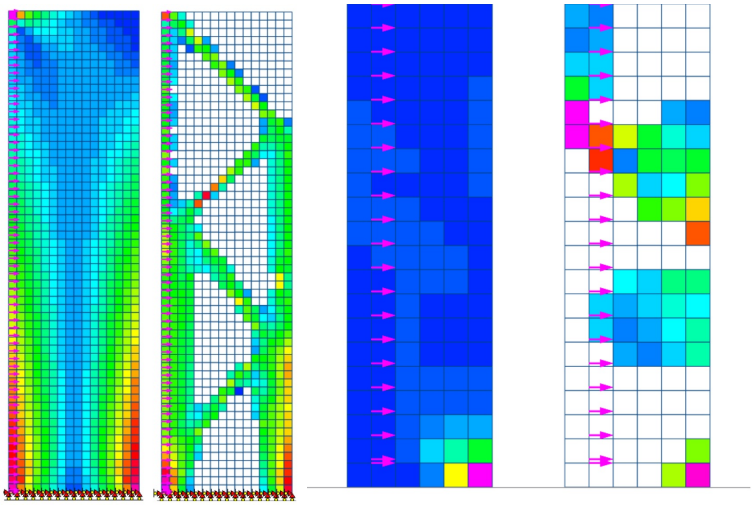

(a) (b)

Figure 2.18: Topology optimization of a cantilever beam in BESO2D [51] for different mesh sizes

Example of TO for (modular) high-rise

In high-rise buildings, the lateral load is governing and the structural system must be able to take this load. However, it is not necessary that all modules in the modular building contribute to carrying the lateral load or have the same stiffness. Therefore, a distinction could for example be made between two types of modules:

1. Load-bearing (braced) modules
2. Non-load-bearing (unbraced) modules,

in which the load-bearing modules have a higher lateral stiffness in order to account for the lateral load acting on the buildings as well as the vertical load, whereas the non-load-bearing modules can be seen as volumetric units that are only self-supporting. Thus, the non-load-bearing modules actually carry a load, however only the vertical load. In corner-supported modules, the load-bearing modules can be seen as regular modules with the addition of (partial) diagonal braces. In case of four-sided modules, the walls of the module give lateral stiffness to the module.

By defining two types of modules, the structural system of the modular building can be compared to the result of topology optimization. The value of each element's stiffness according to the SIMP method must be either 0 or 1 at the end of the optimization. In a modular high-rise building design, the value of 0 or 1 can be compared to a non-load-bearing or load-bearing modules respectively, or the addition or removal of bracing in the modules. The same holds for the BESO method. This way the result of the topology optimization somehow resembles the structural design for high-rise building.

When the mesh size increases, which is normally the case if assumed that modules have realistic dimensions similar to reference projects, unless the building is extremely large, convergence is sometimes not found. This has been illustrated in figure 2.18b. A possible solution to overcome this problem is to use a smaller mesh size while increasing the filter radius. The influence of the filter radius can be seen in figure 2.19. Usually, the filter radius is chosen as two to three times the mesh size, in order to prevent to get a checkerboard pattern as result [51]. A study by Aremu et al. [58] shows that increasing the filter radius decreases the geometric complexity but results in less optimal topologies.

As seen in figure 2.18a, the result of the topology optimization also matches one of the criteria for design of structural systems for high-rise given by Halvorson and Warner [23], namely the fact that the elements must be placed as far apart as possible. Normally, the result of topology optimization gives shapes that are difficult to fabricate, however if each

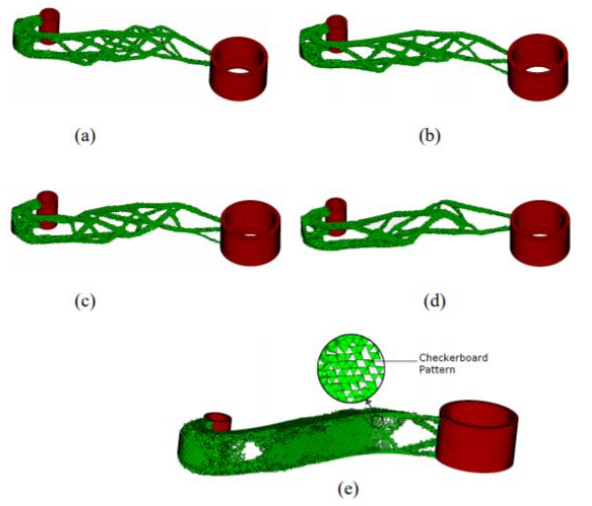

Figure 8: Optimum topologies for FR Experiment (ER=5%)
(a) FRF=1.5, (b) FRF=2.0, (c) FRF=2.5, (d) FRF=3.0 (e) Unfiltered

Figure 2.19: Influence of Filter Radius on TO [58]

element in the mesh resembles a module, the fabrication process becomes much simpler and the result would look like a more realistic structural design. Yet it must be considered that also a value in between 0 and 1 can also be represented by partial bracing, for example on one side of the module, or by varying the stiffness of the bracing element. Also, the columns and beams can also contributed to the lateral stiffness of the structure as a whole, albeit limited. Therefore it makes more sense allow modules with *some* lateral stiffness as well, thus starting with a design space in which elements can have a specific stiffness which is beneficial for the overall lateral stiffness of the structure.

This result presented here is still quite abstract but does give an indication of the possible outcomes of TO and its potential. In chapter 3, a more detailed and concrete study on TO methods is carried out in which the results are easier to grasp and projected on the application in modular high-rise buildings.

3

Comparison of existing optimization methods

This chapter discusses the study performed on structural optimization using various methods and under different conditions. Firstly, the methods are discussed individually after which the considered cases are presented along with their results. The results found in this chapter are used for the new proposed optimization method described in chapter 4.

3.1. Objective

As presented in section 2.3, there are various methods and tools that can be used to optimize a structure. In order to understand the behaviour of the different optimization methods, a study is carried out on optimizing modular frame structures using different methods for different cases. For this purpose a parametric model is set up in Grasshopper and the plugin Karamba3D is used for structural analysis. By parametrizing the structural model, the outcomes of the different analysis and optimization methods can be quickly compared to each other for different types of structures. The main objective of this study is to understand the procedure of optimization methods and to find which tool and method are the best ones to use when it comes to material saving of frame structures.

The considered cases include optimization of a 2D frame structure with (partial) or without braces using various different methods. This way, each module can have its own specific lateral stiffness which could be beneficial to the overall stiffness of the building, rather than having zero or maximum lateral stiffness for a module such as found in figure 2.18.

3.2. Optimization tools and methodology

As mentioned in section 2.3, there are several types for structural optimization, subdivided in size, shape and topology optimization. In this study, the main optimization methods that are studied are the following:

1. Cross-Section (CS-)optimization (size)
2. BESO for beams (topology)
3. BESO for beams + Cross-section (CS-)optimization (topology + size)

One of the motivations for using these optimization methods is the fact that these tools can make use of Karamba and therefore are simple to implement in a parametric model. By using 1D (beam or truss) elements instead of 2D elements, computation time is also reduced. Additionally, the frame structure fits well with the idea of modular construction as the modules can be placed in the structural frame, similarly to the 461 Dean Street building in New York City.

3.2.1. Cross-section optimization

The first method that is used is Cross-Section (CS-)optimization. CS-optimization is a type of size optimization and therefore a relatively simple optimization type. This method only changes the size of the cross-section of each structural member, which are in this case only beam or truss elements. The method also works for shell elements (by varying thickness), however these elements are not considered in this study.

This method is implemented by using the Karamba3D Cross Section Optimizer. This is a Grasshopper component called 'OptiCroSec' which aims to find the optimal cross-section of each structural member within a given range. The input parameters for this component are specified in table 3.1.

Boundary conditions and input

The method considers the following boundary conditions:

1. Maximum utilization (default at 1.0)
2. Maximum displacement (default none, manually inputted)
3. Maximum number of iterations for utilization (in case of no convergence)
4. Maximum number of iterations for displacement (in case of no convergence)

Utilization is defined as the unity check of steel members according to EN 1993-1-1. The check is performed in ULS whereas the deformation is checked in SLS. To verify the structure, the loads are inputted without load factors, while the maximum utilization is limited to $1/\gamma$, in which γ represents the load factor. A rough approximation for this combined factor for dead and live load is 1.4, which yields that the utilization must be limited to $1/1.4 \approx 0.7$ [59]. Tthe utilization has been limited to 0.5 as an early design stage is regarded and some extra margin could be beneficial later on in the project. This means the obtained displacement and utilization are in SLS, whereas the utilization limit is set strictly so that it would still suffice in ULS. The maximum deformation is set to h/750, a common limit for high-rise building design.

The cross-section family from which cross-sections can be picked is specified by inputting a certain range of cross-sections. A convenient component by Karamba for this matter is the Cross Section Range Selector, which specifies a certain range of cross-sections, according to shape and maximum dimensions, however it is also possible to input a manually created list of cross-sections. The input for cross-sections from which the optimizer can choose from is a list of cross-sections, sorted by favourability of the cross-section. Thus, in order to save material, the list should be sorted by weight of the cross-section. This is done automatically if only profiles from a certain family selected (e.g. I-shaped profiles are sorted from small to large height).

The input parameters used are displayed in talbe 3.1. The full list of cross-sections used is presented in appendix A.2.

MaxUtil	0.5	Maximum utilization ratio
MaxDisp	h/750	Maximum displacement in cm
ULSIter	5	Maximum number of iterations for ULS calculation
DispIter	5	Maximum number of iterations for displacement
nSamples	3	Number of sample points for cross-section design
Elast	True	Elastic cross-section design
gammaM0	1	Material safety factor
gammaM1	1	Material safety factor buckling

Table 3.1: Input parameters cross-section optimization

Optimization procedure

The process of the cross-section optimizer is depicted in figure 3.1. Firstly the initial structure is analyzed. This outputs the section forces in all elements. Subsequently, the smallest cross-section within a cross-section family, which satisfies the boundary condition for utilization, is chosen for each member. This process is an iterative process which stops when the cross-sections do not change anymore or when the maximum number of iterations has been reached (no convergence) [59].

This component always tries to satisfy the utilization boundary condition first. It is not possible within this component to consider the displacement condition first, however, assuming that the displacement will be governing, a possible workaround could be to set the maximum utilization to an unreasonably large number which in practice will never be reached. This will result in very small sections initially, after which they are increased in order to reach the displacement criterion. Nevertheless, this way the intended maximum utilization (0.5) criterion may not always be met.

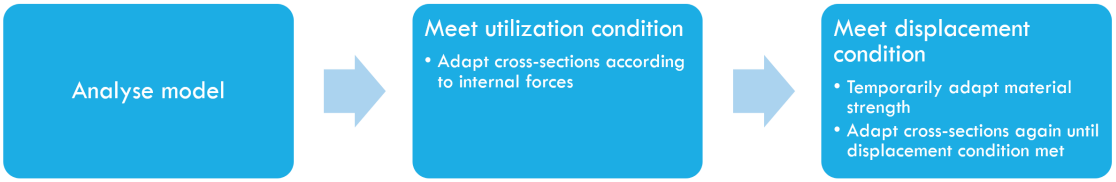

Figure 3.1: Schematic overview of CS-optimization procedure

The procedure to find a solution which meets the deformation condition differs slightly from the procedure for the utilization condition. While the first boundary condition is met by picking structural members according to the utilization based on their section forces, the optimizer now has to quantify the contribution of each element to the global stiffness of the structure as a whole and increase (or decrease) the cross-sections accordingly. The cross-section optimizer adapts the material strength temporarily which may lead to inefficient structures in case the maximum deformation only occurs in a small part of the structure [59]. As Karamba iteratively adapts the material strength, it seems logical that if the material is weakened, a higher member utilization results. The members with the highest utilization will probably exceed the utilization limit and therefore the cross-section of these members will be increased. This way, the cross-section satisfies the utilization condition again and additional stiffness is added to the structure, decreasing the maximum displacement. The next step in this iterative procedure is to find the displacement in the new situation and check whether this is within the limit. If not, the material strength is again decreased, while if the boundary condition is already met, the algorithm might increase the material strength slightly in order to find a more economical solution.

3.2.2. BESO for beams

Secondly, the structure can be optimized using BESO for beams, a form of topology optimization in which elements are removed (or added). BESO for beams is implemented in a Grasshopper component in Karamba and therefore easy to apply to the same structural model. The principle of the BESO method and some applications have been elaborated in section 2.3.4.

The implementation of BESO for beams in Karamba applies itself to beam elements, meaning that the design space only exists of the beam (or truss) elements rather than a mesh such as in figure 2.18a. In Karamba, there is also a component called BESO for shells which is in essence similar to BESO2D by [51]. As the structural model is built up from beam elements only, the BESO for shells component is not relevant for this study.

Optimization procedure

The BESO for beams method analyzes the structure, finds and removes the elements that are least strained and therefore least effective [59]. This is done in each iteration step. The

number of elements that are removed per step can be specified. As this is a BESO approach, this method also allows the addition of new members to the structure, albeit within the initially given design space.

For BESO for beams, reduction of elements continues until the specified Target Ratio (TR) has been reached. Therefore BESO for beams does not consider a utilization or deformation criterium similar as in CS-optimization and the results have to be manually checked afterwards whether or not these conditions are satisfied. The input parameters for the BESO optimization are displayed in table 3.2. Again, a maximum number of iterations is specified as boundary condition in case no convergence can be found.

ElemIds	diag	Elements for BESO analysis
TargetRatio	1.0 to 0.1	Target mass ratio relative to initial mass
MaxChangeIter	10	Maximum number of iterations for adding/removing elements
MaxConvIter	20	Maximum number of iterations for reaching convergence
WTension	1	Weight factor for tension
WCompr.	1	Weight factor for compression
WShear	0	Weight factor for shear
WMoment	0	Weight factor for moments
BESOFac	0	BESO factor (number of elem. per half step)
MinDist	0	Minimum distance between changing elements
WLimit	0	Limit ratio weight of element : mean weight

Table 3.2: Input parameters BESO optimization

The removal of elements in the BESO method is based on the stress in the elements. As failure of a structure occurs because of excessive stress, an optimum structure is considered as a structure in which each member has the same stress level [60]. Therefore, the elements are removed based on their relative stress level.

By applying the BESO for beams method on the diagonal bracing elements, the lateral stiffness of each module can theoretically become 0 (all diagonals removed), 1 (no diagonals removed), or approximately 0.5 (single diagonal removed).

3.2.3. BESO for beams + Cross-section optimization

A combination of BESO for beams and CS-optimization combines the benefits of both methods. As CS-optimziation cannot remove elements, BESO for beams may be more beneficial, however CS-optimization can change the dimension of each (remaining) member. As CS-optimization also takes into account deformation and utilization conditions, a combination of these methods seems like a practical solution.

It can be argued which analysis should be performed first. First performing CS-optimization and then BESO for beams means that the cross-sections will be optimized first, taking into account the deformation and utilization limits, after which beam elements may be removed. This sequence of analyses does not make sense practically as the deformation and utilization will most likely exceed their limits after BESO for beams is performed, leaving an unsafe design.

Therefore, performing BESO for beams first and afterwards CS-optimization of the remaining structural members is more practical. This way, non- (or very limited) utilized members are removed first after which the other members can be optimized, still satisfying the utilization and deformation criteria. The procedure of performing this combination of optimizations is depicted in figure 3.2.

A challenge in this optimization method is to find the ideal TR for the BESO for beams. Specifying a very low TR will expectedly save a lot of material during BESO, however then during CS-optimization some material must be added by enlarging cross-sections in order to satisfy the boundary conditions. On the other hand, choosing a very high TR might mean that even after CS-optimization, some members, despite their small cross-section, are still not utilized too much nor crucial for the global stiffness of the structure.

In order to find the ideal TR, an evolutionary solver can be used such as Galapagos or Octopus. Both are plugins for Grasshopper and can therefore be integrated with the existing

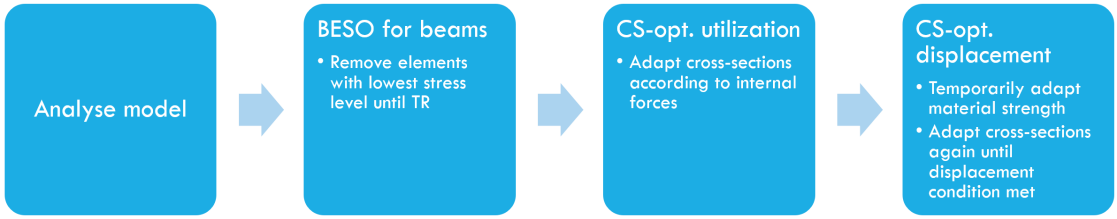

Figure 3.2: Schematic overview of BESO>CS-optimization procedure

structural analysis model. Both solvers need as input a genome and a fitness. As genome, the TR can be specified and as fitness, the total mass of the structure can be inputted. The solver will then try to minimize the fitness (weight) and find the corresponding genome (TR), as shown in figure 3.3. However, to understand the influence of the TR on the mass and behaviour of the structure, a 'brute force' method is used, thus all combinations (within a certain range limit) are calculated and plotted in a diagram.

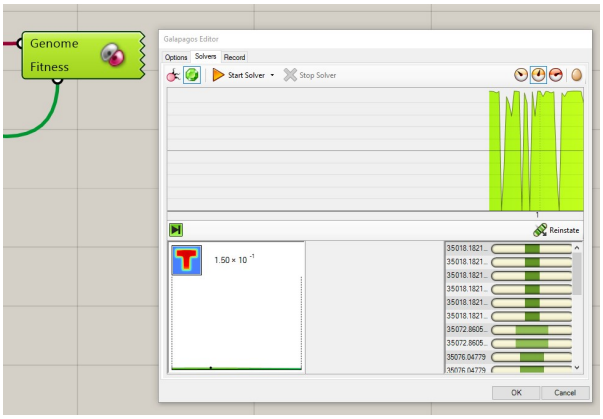

Figure 3.3: Galapagos solver in order to find ideal Target Ratio by minimizing fitness (weight)

3.3. Test cases

The test cases that are considered are all steel frame structures, however the layout of the structures differs from case to case. The cases considered are in 2D initially to simplify the analysis and optimization. The expectation is that more or less similar results will be found when the analysis is carried out in 3D.

3.3.1. Assumptions

The starting point of the analysis is a 2D frame structure (with or without bracing) in an XZ-plane, built up from modular blocks of 3 x 3 meters (figure 3.5, 3.6, 3.7). The number of modules in X-direction is 4 and the number of modules in Z-direction is 20. Steel corner-supported modules are assumed. The dimensional parameters can later on be modified in order to analyze different cases. In order to make the analyses comparable, cross-section (1) has been chosen such that the initial weight of the structure remains approximately the same for all structural systems considered. The distribution of this weight however differs per type of structural system. For cross-section (2) and (3), different initial cross-sections are taken in order to see the sensitivity for differences in initial input.

The following load combinations are considered:

1. Wind load only

2. Wind load and vertical load (live + dead load)

Dimension X [m]	3
Dimension Y [m]	3
Dimension Z [m]	3
Number of modules X-direction [-]	4
Number of modules Z-direction [-]	20
Total building height [m]	60
Corresponding wind load [kN/m^2]	1.53

Table 3.3: Initial parameters test cases

For the wind load, the values for the peak pressure are taken from the Eurocode, depending on building height. The calculation of the wind load has been further elaborated in section 5.2.1 and also a Python script is developed for the calculation of the wind load (appendix B.1), which gives the same values are table NB.5 from NEN-EN 1991-1-4+A1+C2. The assumption is that the building is situated in wind area I and the terrain category is III (urban). The wind pressure q_p from the Eurocode is multiplied with the Y-dimension of the module in order to obtain a load per length [kN/m] rather than a load per area [kN/m^2].

Secondly, the combination of wind load and vertical load consisting of live load and dead load is analyzed. For the vertical load, a value of 10 kN/m^2 is assumed. This load is built up from a live load ($4kN/m^2$, congregation or shopping area assumed) and a dead load ($6kN/m^2$, 200mm solid slab floor assumed with finishing). This loads acts in negative Z-direction and is also multiplied with the Y-dimension of the module in order to obtain a line load which can be modelled in the 2D model.

The structure is verified based on the following criteria:

1. The utilization of the structural members must be smaller than 0.5 (Ratio SLS/ULS with additional margin)

2. Maximum deformation equals h/750 in which h is the total building height (extra margin for rotation of foundation)

These requirements are inputted in the cross-section optimzer. Additional requirements such as the maximum deformation per storey are not regarded as this is a preliminary study and no local peak stresses or deformations are expected in the considered cases.

Furthermore, the utilization in Karamba is checked according to the Eurocode. Equation 6.2 from NEN-EN 1993-1-1+C2+A1 yields as follows:

$$\frac{N_{\mathrm{Ed}}}{N_{\mathrm{Rd}}} + \frac{M_{\mathrm{y,Ed}}}{M_{\mathrm{y,Rd}}} + \frac{M_{\mathrm{z,Ed}}}{M_{\mathrm{z,Rd}}} \leq 1 \tag{3.1}$$

While this is a relatively conservative approach for calculating the utilization value. For interaction of loads (e.g. bending and shear, bending and axial force), different interaction formulas must be applied. The general formula that is applied to verify the elastic capacity of the member is stated in formula 6.1 of EN1993:

$$(\frac{\sigma_{\mathrm{x,Ed}}}{f_y/\gamma_{\mathrm{M0}}})^2 + (\frac{\sigma_{\mathrm{z,Ed}}}{f_y/\gamma_{\mathrm{M0}}})^2 - (\frac{\sigma_{\mathrm{x,Ed}}}{f_y/\gamma_{\mathrm{M0}}})(\frac{\sigma_{\mathrm{z,Ed}}}{f_y/\gamma_{\mathrm{M0}}}) + 3(\frac{\tau_{\mathrm{Ed}}}{f_y/\gamma_{\mathrm{M0}}})^2 \leq 1 \tag{3.2}$$

in which $\sigma_{\mathrm{x,Ed}}$ is the design value of the stress in longitudinal direction, while $\sigma_{\mathrm{z,Ed}}$ is the design value of the stress in transverse direction. tau_{Ed} is the design value of the shear stress. γ_{M0} is the partial factor and its value is 1.00 according to the Eurocode. This is however for a later design stage and a conservative approach suffices for now.

The steel grade is assumed to be S235 with a yield strength of 235 N/mm^2, however the steel grade can be changed in the model later on if desired. Since a linear analysis is carried out, the material strength parameter does not influence the deformation behaviour of the building but only impacts the utilization factor.

3.3.2. Rigid frame structure

First of all, a rigid frame structure is considered. The model is depicted in figure 3.5a and 3.5b. This model does not have any diagonals and therefore a rigid frame structure remains. The expectation is that the rigid frame structure only satisfies for buildings with a limited height or needs very large cross-sections in order to satisfy. In the latter case, the structure would be somewhat similar to a facade tube structure.

For this case, it does not make sense to run a BESO analysis as there are no diagonals. Running a BESO for beams analysis would therefore simply make the building smaller as depicted in figure 3.4, which is not the objective of the optimization. Therefore, only CS-optimization is applied.

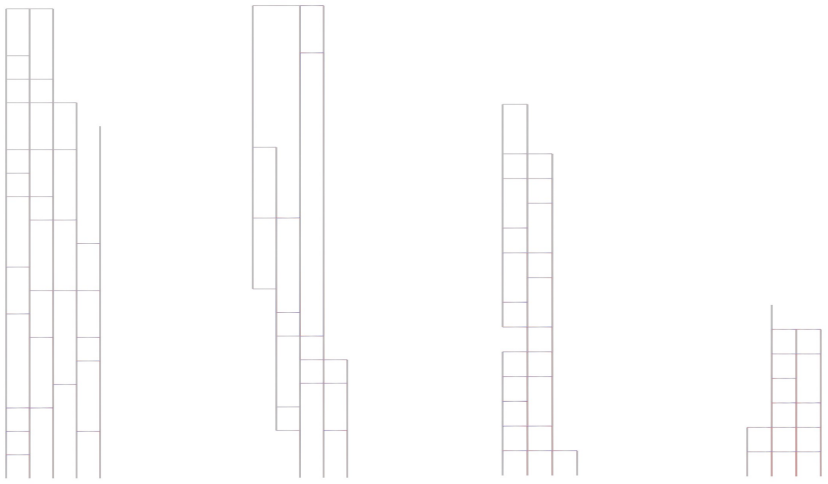

(a) (b) (c) (d)

Figure 3.4: BESO analysis for Rigid Frame model with TR=0.8, 0.6, 0.4 and 0.2 respectively

The initial design of this structure is based on rules of thumb. For steel columns, a recommended cross-sectional height between $l/7$ and $l/18$, l being the span length [61]. HD wide flange columns have been chosen as they are relatively easy to be placed on top of each other. For steel beams, a recommended value for the cross-sectional height of HE beams is between $l/15$ and $l/20$ [61]. The cross-sections are designed based on rules of thumb and have been enlarged slightly after the initial analysis showed that the structure did not satisfy the criteria for deformation and utilization (cross-section 1). In order to see the influence of the starting point for CS-optimization, starting points with extremely small (cross-section 2) or large (cross-section 3) cross-sectional dimensions are also considered. An overview of the assumed cross-sections is listed in table 3.4.

Structural member	Cross-section (1)	Cross-section (2)	Cross-section (3)
Columns	HD 400x262	HD 260x54.1	HD 400x1299
Beams	HEA 400	HEA 100	HEA 1000
Diagonals	N/A	N/A	N/A
Total structure weight [tonnes]	110.3	20.5	457.2

Table 3.4: Cross-sections rigid frame model

3.3.3. Braced frame structure

The braced frame structure is initially a structure with braces all across the building, thus in modular construction, bracing in each module. However, these diagonal braces are not

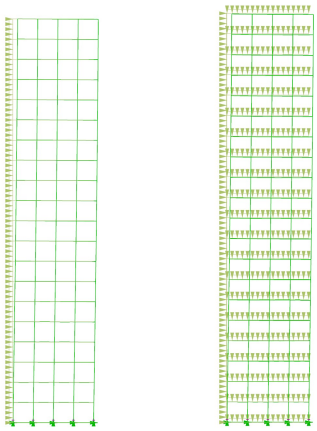

(a) (b)

Figure 3.5: Rigid frame model for wind load and wind+vertical load

always necessary and therefore it may be desired to remove some of these diagonals from an aesthetic or functional point of view. All three optimization techniques are applied. The cross-sections that are taken for the initial model are listed in table 3.5. For the BESO for beams and BESO+Cross-Section optimization methods, BESO is limited to diagonal members only. CS-optimization can change the cross-section of all members (within a certain cross-section family). The braced frame model is displayed in figure 3.6a and 3.6b. Cross-section (1) matches the initial weight of the rigid frame model, whereas cross-section (2) is a more realistic starting point with generally smaller sections.

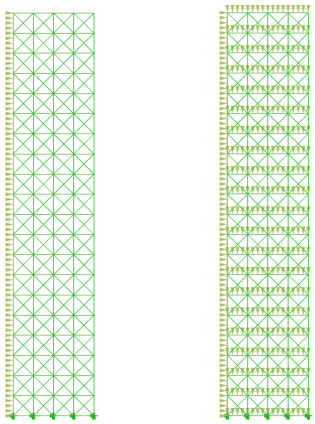

(a) (b)

Figure 3.6: Braced frame model for wind load and wind+vertical load

3.3.4. Core structure

The core structure is a structure which has a stiff steel core with diagonal bracing, while the remaining members have smaller dimensions. The core is situated at the centre of the building. There are no braces on the outer sides of the building, which could also be a better solution functionally as well as aesthetically. The internal diagonal bracing could also represent walls, which is quite common for high-rise buildings. All three listed optimization methods are applied. The cross-sections that are taken for the initial model are listed in table 3.6. The number of diagonals is half the number of diagonals in the braced frame structure.

Structural member	Cross-section (1)	Cross-section (2)
Columns	HD 320x245	HD 320x198
Beams	HEA 300	HEA 200
Diagonals	HEA 120	HEA 100
Total structure weight [tonnes]	109.2	81.4

Table 3.5: Initial cross-sections braced frame model

An overview of the structural model is given in figure 3.7a and 3.7b.

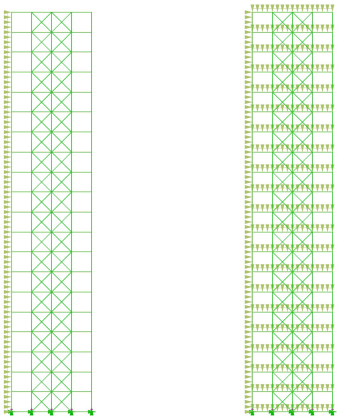

(a) (b)

Figure 3.7: Core model for wind load and wind+vertical load

Structural member	Cross-section (1)	Cross-section (2)
Columns core	HD 320x245	HD 320x198
Outer columns	HD 320x245	HD 320x198
Beams	HEA 240	HEA 240
Diagonals core	HEA 240	HEA 200
Initial structure weight [tonnes]	109.1	89.0

Table 3.6: Initial cross-sections core model

3.4. Results

This section discusses the most important results from the considered cases. The full results can be found in appendix A.3. In the colour plots, blue represents members in tension whereas the red-coloured members are in compression. The deformation scale is set to 100. The diagrams display the results for CS-, BESO and BESO>CS-optimization versus the TR of the BESO-analysis, in which the boundary conditions for displacement and utilization are represented by red-dotted lines.

3.4.1. Rigid frame structure

For the rigid frame structure, only cross-section optimization has been carried out. This result is comparable to a BESO>CS optimization with TR=1.0 (no elements added or removed).

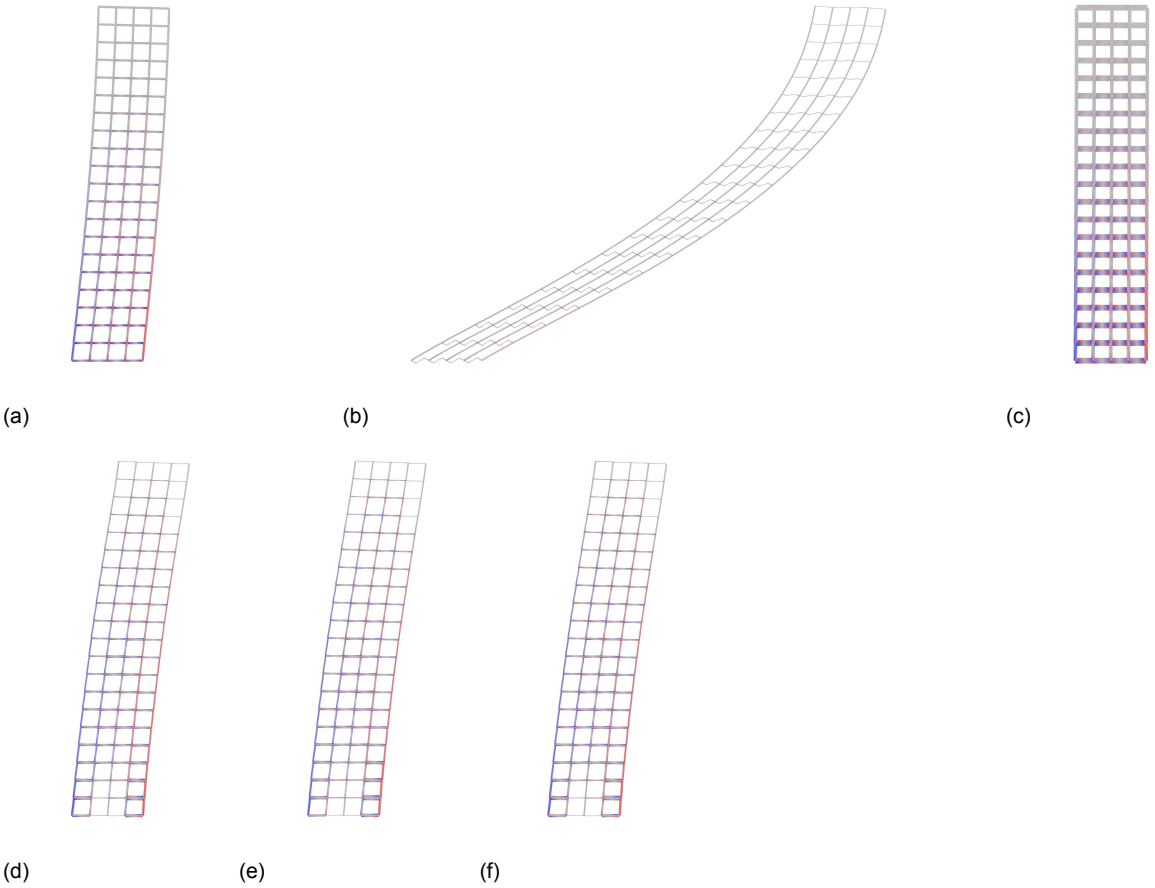

Figure 3.8: Rigid Frame structure under wind load, Cross-section (1), (2), (3) (a,b,c) and CS-optimization results (d,e,f)

Analysis	Max. displ. UC [-]	Weight [tonnes]	Max. util.	Avg. util.	Min. util.
Initial (1)	0.56	110.3	0.18	0.075	0.0046
Initial (2)	28.2	20.5	22.8	2.93	0.077
Initial (3)	0.086	457.2	0.039	0.015	0.0010
CS optimized (1)	0.99	66.4	0.16	0.12	0.016
CS optimized (2)	1.00	65.5	0.16	0.13	0.017
CS optimized (3)	1.00	66.0	0.16	0.13	0.015

Table 3.7: Rigid frame analysis results wind load

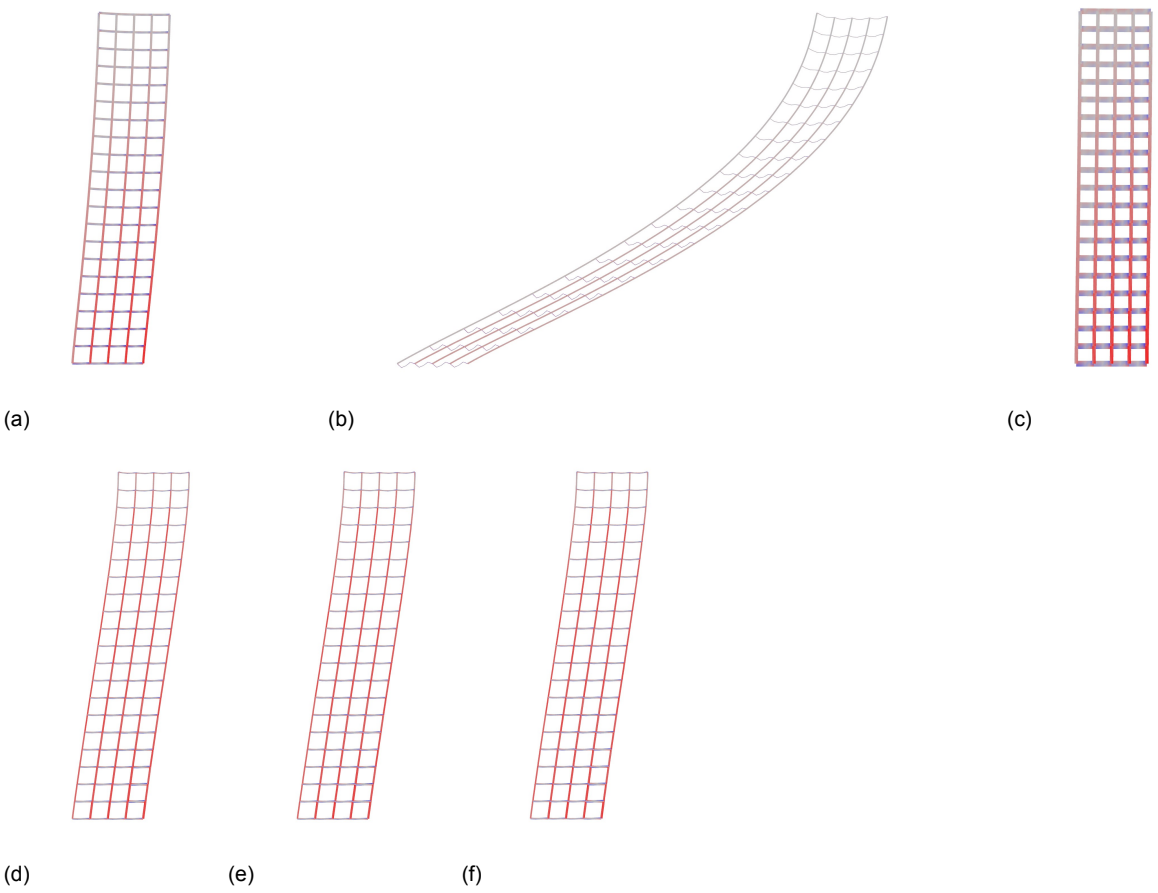

Figure 3.9: Rigid Frame structure under wind+vertical load, Cross-section (1), (2), (3) (a,b,c) and CS-optimization results (d,e,f)

Analysis	Max. displ. UC [-]	Weight [tonnes]	Max. util.	Avg. util.	Min. util.
Initial (1)	0.57	110.3	0.34	0.17	0.022
Initial (2)	28.2	20.5	680.7	178.8	0.17
Initial (3)	0.088	457.2	0.067	0.037	0.0039
CS-optimized (1)	0.99	77.1	0.31	0.27	0.11
CS-optimized (2)	0.99	77.5	0.31	0.26	0.10
CS-optimized (3)	1.00	76.7	0.30	0.27	0.11

Table 3.8: Rigid frame analysis results wind+vertical load

In both load cases, CS-optimization succeeds to satisfy the conditions for maximum displacement and utilization. The unity check for displacement being approximately 1.00 suggests that displacement is governing in this situation. For each initial cross-section (1, 2 and 3), about the same solution is found with the similar structural weight and displacement and utilization. The solutions therefore are stable solutions which are not sensitive to the initial cross-sections, as long as the same cross-section library is regarded. There is a large variety in cross-sections which may cause difficulties in connecting the members. This could be prevented by defining extra boundary conditions.

3.4.2. Braced frame structure (wind load)

Cross-section 1

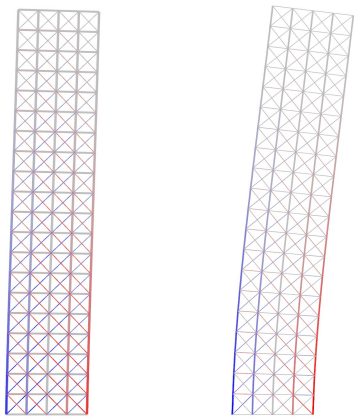

(a) (b)

Figure 3.10: Braced frame under wind load, before (a) and after (b) CS-optimization

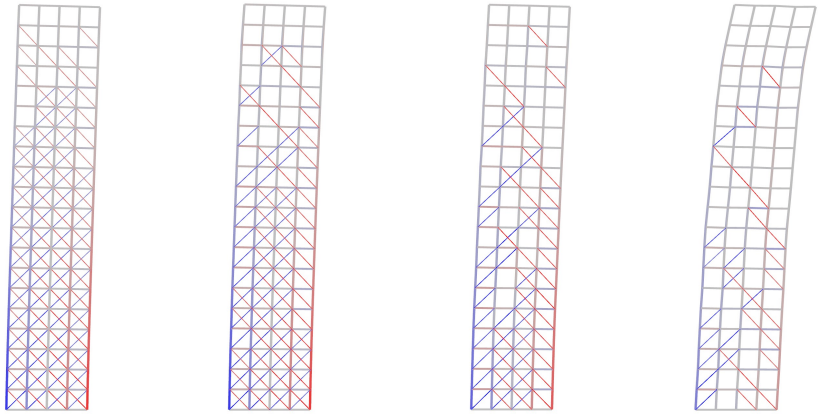

(a) (b) (c) (d)

Figure 3.11: Braced frame under wind load after BESO, TR=0.8, 0.6, 0.4 and 0.2 respectively

BESO is limited to removing diagonals from the model so beams and columns remain. Generally, the lowest stress occurs in the diagonals in the upper part of the structure as these elements are removed in BESO.

TR is linearly related to the mass of the structure after optimization. This is expected as TR is defined as the ratio between the final and initial mass (of the diagonals). CS-optimization reduces the weight much more as it is also able to adapt the sections of all members. Combining BESO and CS-optimization gives an extra reduction of material, with an optimum at TR≈0.3. All optimization methods generally show an increase in displacement. (BESO+)CS-optimization generally succeeds in finding a solution for which the unity check for the displacement is close to 1.0 (boundary condition).

The maximum and average utilization for BESO>CS-optimization starts at 1.0 and then generally decreases, proving that displacement becomes governing after removing some diagonals. In BESO, the maximum utilization increases above the limit as it is not a boundary condition. The minimum utilization in all methods is very low, thus there will always be underutilized members for this case.

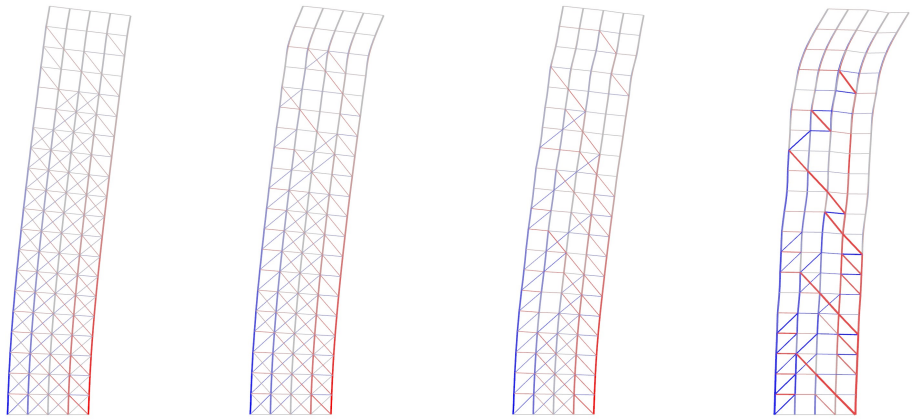

(a) (b) (c) (d)

Figure 3.12: Braced frame under wind load after BESO>CS, TR=0.8, 0.6, 0.4 and 0.2 respectively

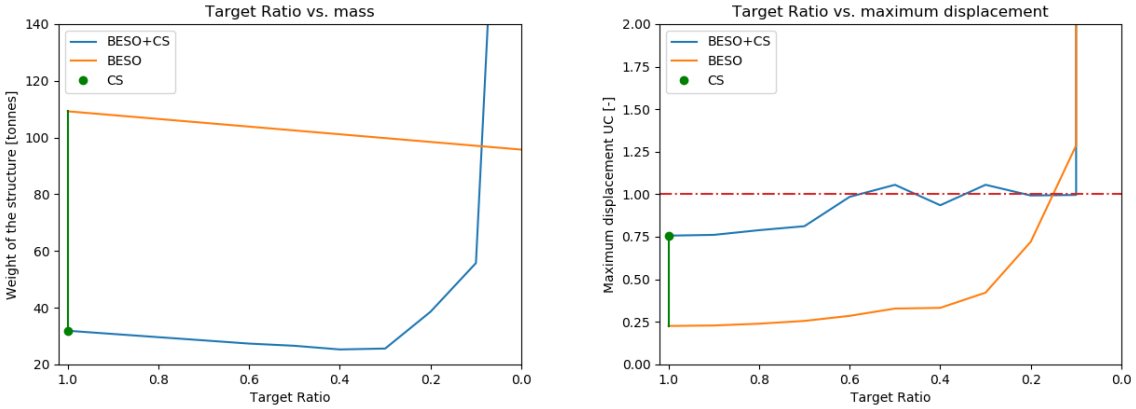

(a) (b)

Figure 3.13: Braced frame structure under wind load, TR versus mass and displacement

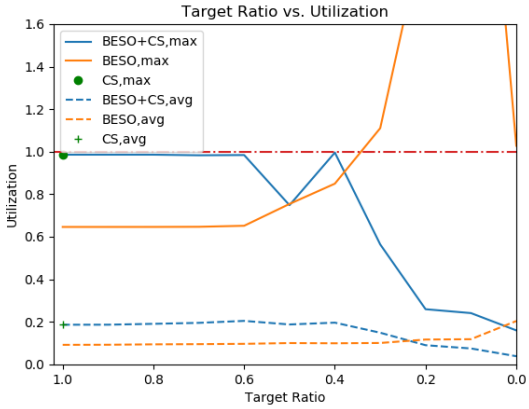

Figure 3.14: Braced frame structure under wind load, TR versus utilization

3.4.3. Braced frame structure (wind+vertical load)

Cross-section 1

Now, the same cases is considered but vertical load is added.

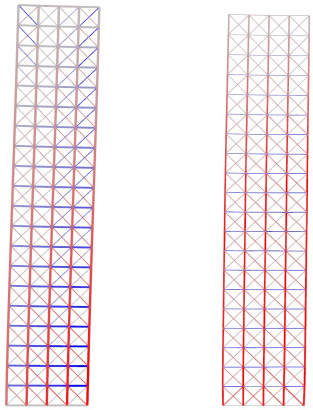

(a) (b)

Figure 3.15: Braced frame under wind+vertical load, before (a) and after (b) CS-optimization

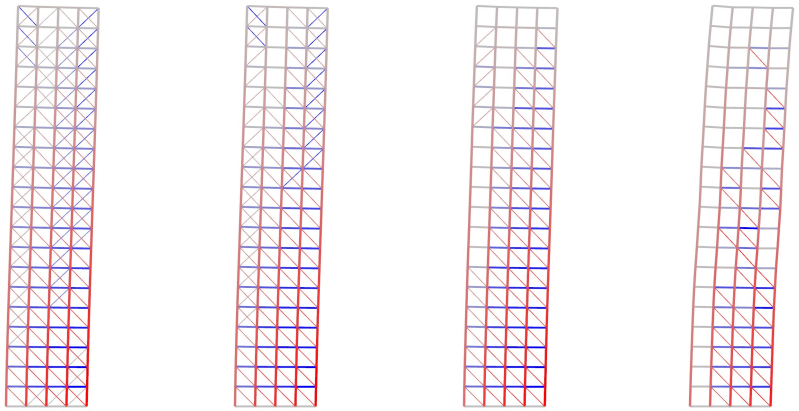

(a) (b) (c) (d)

Figure 3.16: Braced frame under wind+vertical load after BESO, TR=0.8, 0.6, 0.4 and 0.2 respectively

The TR versus mass curve is similar to earlier results, however the displacement curve is different. It appears that the displacement is no longer governing for higher TR. Due to the vertical load, the maximum utilization has become governing for higher TR. The average utilization is also much higher than the average utilization in the case with wind load only. As TR becomes smaller, the maximum displacement increases while the utilization decreases, thus displacement becomes governing and the problem becomes a stiffness problem again which is evident at TR<0.2.

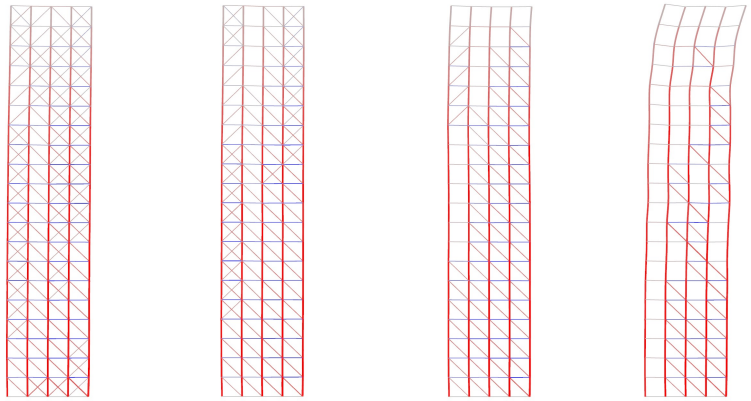

(a) (b) (c) (d)

Figure 3.17: Braced frame under wind+vertical load after BESO>CS, TR=0.8, 0.6, 0.4 and 0.2 respectively

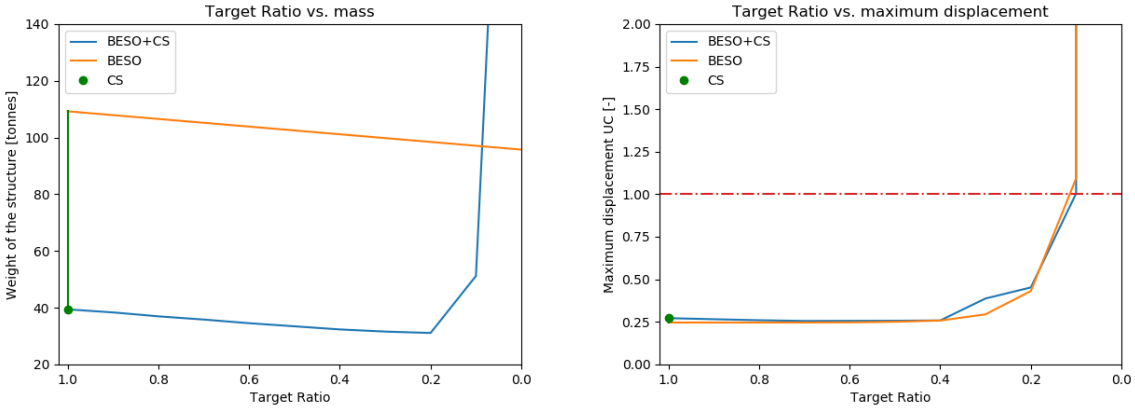

(a) (b)

Figure 3.18: Braced frame structure under wind+vertical load, TR versus mass (a) and displacement (b)

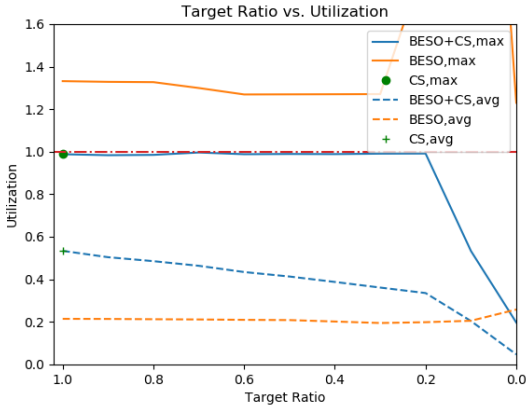

Figure 3.19: Braced frame structure under wind+vertical load, TR versus utilization

3.4.4. Core structure (wind load)

Cross-section 1

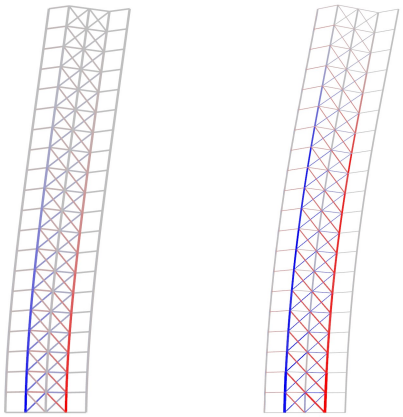

(a) (b)

Figure 3.20: Core structure under wind load, before (a) and after (b) CS-optimization

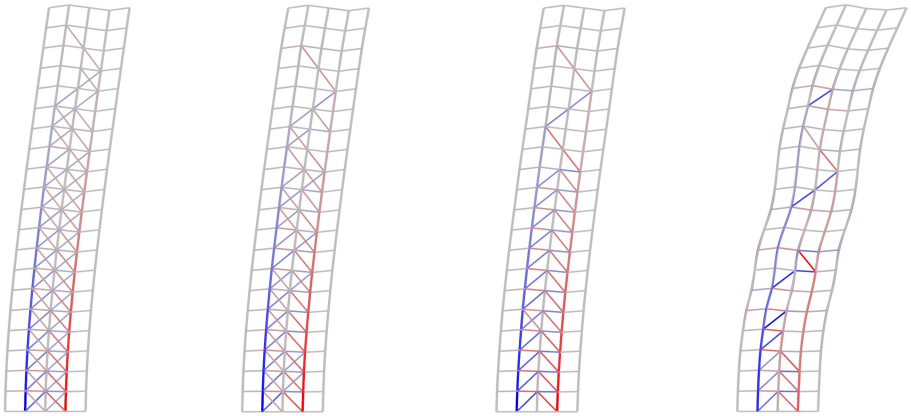

(a) (b) (c) (d)

Figure 3.21: Core structure under wind load after BESO, TR=0.8, 0.6, 0.4 and 0.2 respectively

In the core structure under wind load, displacement is governing. BESO>CS finds a solution for which the displacement unity check is approximately equal to 1.0 for TR>0.2. The TR with lowest structure weight is approximately 0.8, however differences in structure weight are very limited with TR between 0.4 and 1.0. The fact that TR=0.8 is found as optimum can be related to the result of the braced frame structure. In the braced frame structure, an optimum TR of approximately 0.3 was found, which is 40% of diagonals, given that there were diagonals in *each* module. At the same time, the core structure starts with diagonals only in the center of the building, thus only 50% of the modules include diagonals. Therefore a TR of 0.3 in the braced frame structure means the same number of diagonals at a TR of 0.6 in this core structure. Placing diagonals in the center results in an optimum with more diagonals and therefore the considered braced frame structure is more optimal than the core structure.

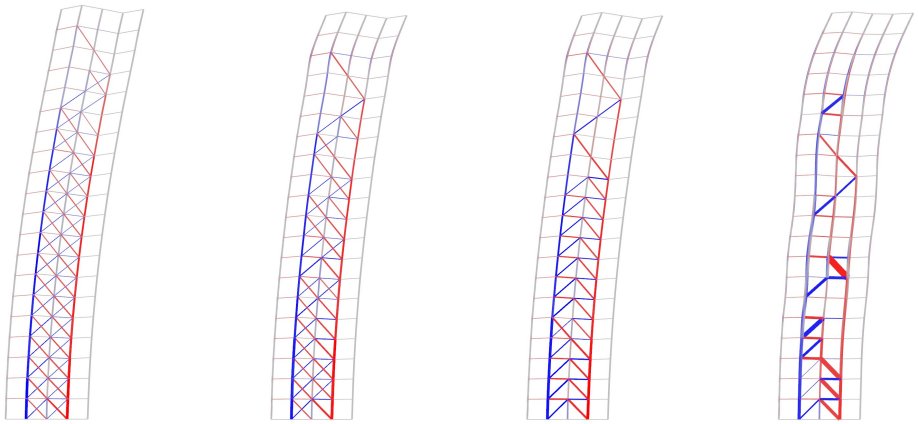

(a) (b) (c) (d)

Figure 3.22: Core structure under wind load after BESO>CS, TR=0.8, 0.6, 0.4 and 0.2 respectively

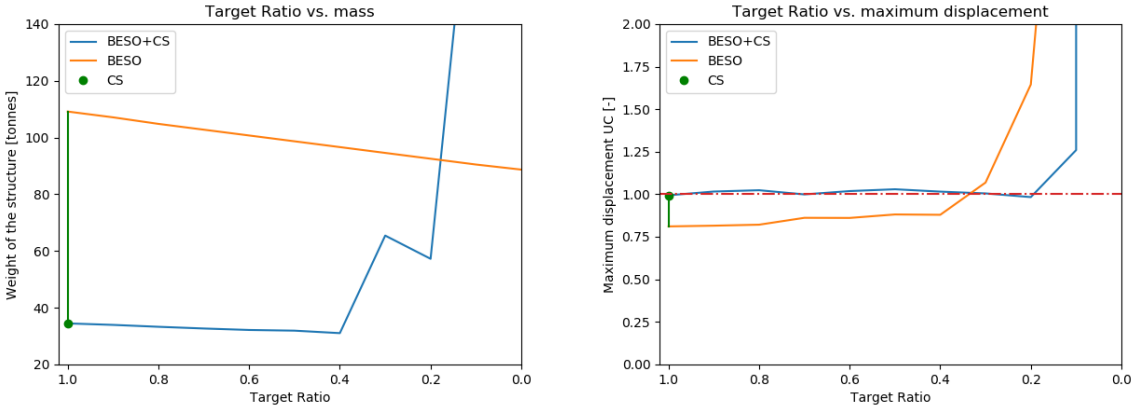

(a) (b)

Figure 3.23: Core structure under wind load, TR versus mass (a) and displacement (b)

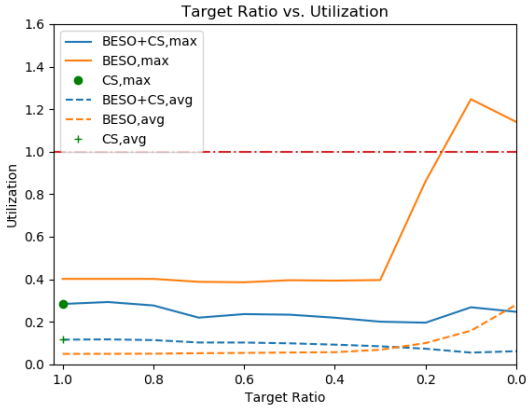

Figure 3.24: Core structure under wind load, TR versus utilization

3.4.5. Core structure (wind+vertical load)

Cross-section 1

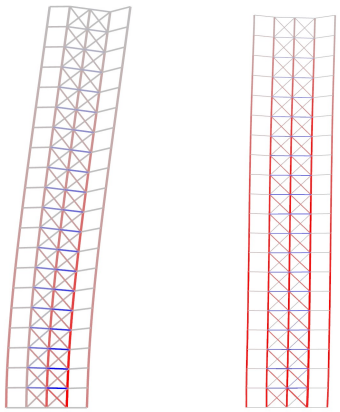

(a) (b)

Figure 3.25: Core structure under wind+vertical load, before (a) and after (b) CS-optimization

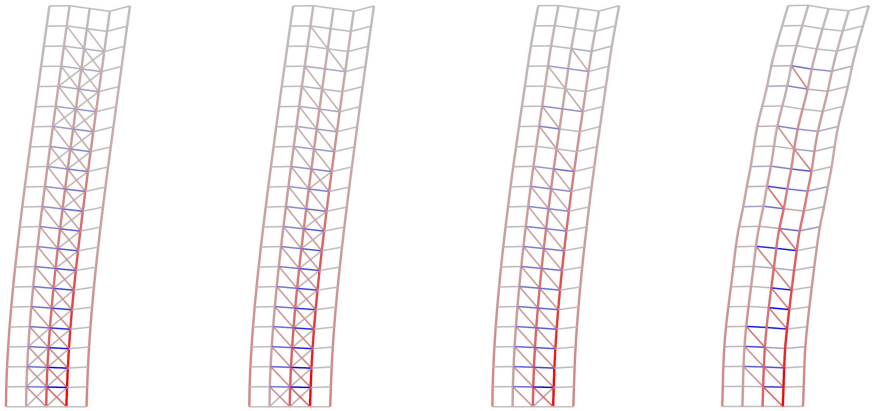

(a) (b) (c) (d)

Figure 3.26: Core structure under wind+vertical load after BESO, TR=0.8, 0.6, 0.4 and 0.2 respectively

Including vertical load in the core structure seems to create strength problem at higher target ratios, after which the problem becomes a stiffness problem when TR decreases. This is again evident in the increasing displacement unity check and decreasing maximum and average utilizations as TR decreases.

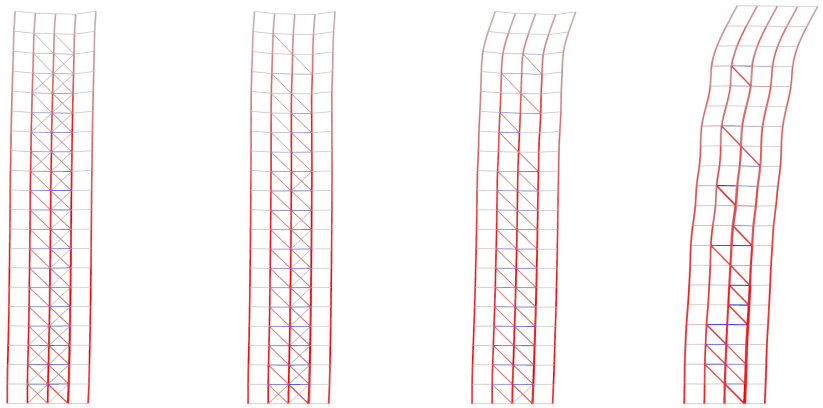

(a) (b) (c) (d)

Figure 3.27: Core structure under wind+vertical load after BESO>CS, TR=0.8, 0.6, 0.4 and 0.2 respectively

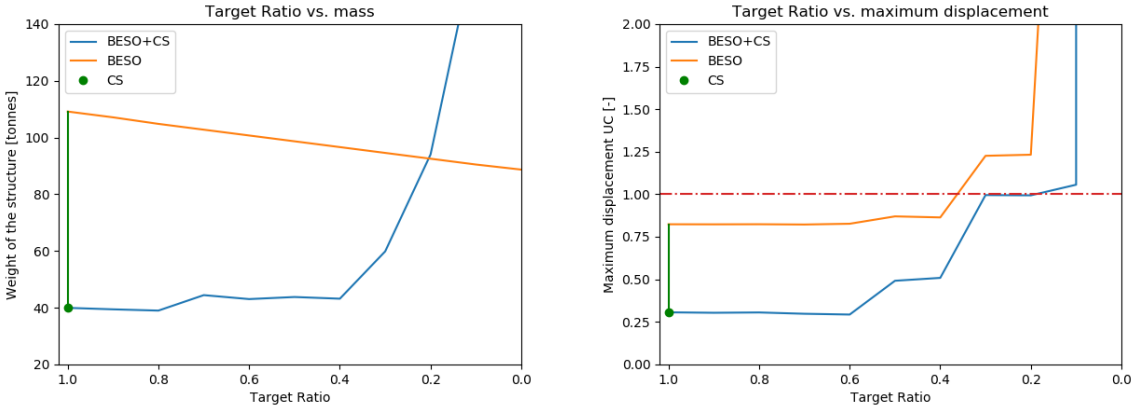

(a) (b)

Figure 3.28: Core structure under wind+vertical load, TR versus mass (a) and displacement (b)

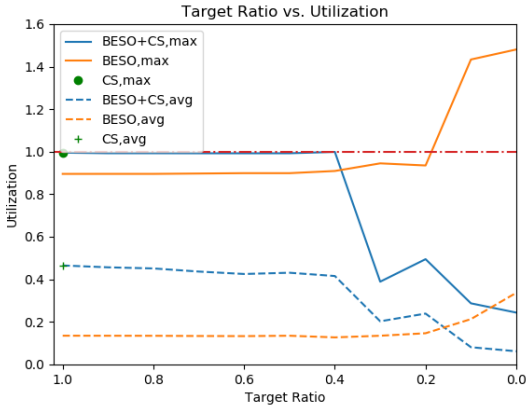

Figure 3.29: Core structure under wind+vertical load, TR versus utilization

3.5. Preliminary discussion

3.5.1. Optimization methods

In general, it is observed that all considered methods succeed in reducing the weight of the structure. In the rigid frame structure, no elements can be removed and the CS-optimization shows an increase in utilization and deformation (within the predefined boundaries) and a significant decrease in material use. The initial input of cross-sections is not very important for the final outcome of CS-optimization as final weight and unity checks are approximately similar.

CS-optimization is much more efficient than applying BESO only (regardless of TR) as it takes into account the boundary conditions of utilization and deformation. By combining the two optimization methods, the weight of the structure can even be further diminished, however, an ideal TR must be found. The ideal TR differs per structure and load case, however in the considered cases it was found that removing diagonals to a certain extent decreased weight or did not significantly increase the structure weight. By using the combined method, therefore the number of elements and therefore connections, which are generally costly, is reduced while decreasing or increasing weight within an acceptable limit.

At a low TR, the weight of the structure significantly increases for BESO>CS method, while for the BESO-only method the weight keeps linearly decreasing but the maximum deformation increases greatly. This behaviour is caused by the fact that BESO>CS has to meet the boundary condition for maximum displacement and therefore adds material by increasing the cross-sections of the remaining structural members, while BESO keeps removing elements, even if the structure is not able to meet these safety criteria. The increase in weight could be interpreted as the price which has to be paid for removing elements which is a trade-off.

For the BESO>CS method, the average and maximum utilization generally decreases slightly whereas the average and maximum utilization for the BESO method slightly increases as structural members are removed. At a certain point removing additional structural members causes a big increase in maximum utilization. For both methods, the minimum utilization is close to zero, regardless of the target ratio. This suggests that there will always be underutilized members for the considered cases.

3.5.2. Structure types

In the structures loaded by wind load alone, tensile stresses occur in the lower columns which create a counteracting moment. This is expected not to be a problem as in a real design situation, vertical load will be taken into account and no tensile stresses (as found in the considered cases) will act on the foundation of the building.

In the rigid frame structure, it does not make sense to apply BESO and only Cross-Section optimization is applied. Using size optimization on this structure shows that the weight can significantly be decreased, however the exact amount of material that can be saved depends on the initial input. Overall, the material will be much better utilized and deformation and utilization requirements are met.

The considered braced frame and core benefit from the combination of BESO and Cross-Section optimization. In order to find the lowest weight structure, the optimum TR must be found. For the braced frame structure, this TR lies around 0.3, whereas for the core structure, the TR lies around 0.8. The core structure starts with 50% less diagonals than the braced frame structure but the lowest structural weight is encountered at a larger number of diagonals. Also, the minimum weight of the core structure is higher than the weight of the braced frame structure (table 3.9). A braced frame is therefore more efficient than a core structure, which Halvorson and Warner [23] also suggest by resist the load by vertical elements placed as far as possible, thus bracing in modules at the edges.

While the graphs show a great reduction in structure weight, it is hard to interpret the geometry of the structure after BESO>CS optimization. Generally, there are more diagonals in the bottom part of the structure which seems logical as these members will have to account for a greater shear force. However, the placement of the diagonals seems somewhat arbitrary, despite the fact that the optimization procedure removes elements based on quantitative results, namely stress level.

Load case	Structure	Weight [tonnes]
Wind load	Rigid frame	66.0
	Braced frame	25.3
	Core	31.1
Wind+vertical load	Rigid frame	76.7
	Braced frame	31.1
	Core	39.0

Table 3.9: Minimum structure weight after optimization

3.6. Preliminary conclusions

In short, the most important findings for the considered cases are the following:

- CS-optimization result does not depend on initial input
- CS-optimization more efficient than BESO
- BESO depends on initial input of cross-sections
- BESO>CS-optimization leads to additional decrease of material
- (Too) low TR: displacement governing and material use increases again
- (Too) high TR: too many elements and material use could be reduced
- Optimum TR differs per type structure and load case
- Braced frame structure more efficient than core structure
- Rigid frame structure inefficient compared to core and braced frame
- Different cross-sections for beams and columns make it hard to standardize modules

Therefore, the combination of BESO and CS-optimization shows the greatest potential. Yet, in order to create a structural design for a modular high-rise concept, the method must be adapted and various other factors and boundary conditions must be taken into account such as standardization of structural elements, placement of diagonals and design for multiple load cases. This is further elaborated in chapter 4.

4

Proposed optimization method

The results from chapter 3 are used in order to propose a structural optimization method and implementation. This chapter describes the proposed optimization method and presents test cases to verify the performance of the proposed method and to compare the results to the earlier studied methods.

4.1. Relevance

As concluded in chapter 3, there are several methods that can be used to minimize the weight of a frame structure. Each method has its own advantages and disadvantages and each method may be more suitable for specific cases. For example, BESO is not applicable in the considered rigid frame structures so cross-section optimization must be applied which was proven effective in reducing weight. However, CS-optimization was found more effective than BESO, while the combination of BESO and CS-optimization succeeds to further bring down the weight of the structure in the consdiered braced frame and core structures.

Some disadvantages of the BESO>CS optimization procedure are the fact that it is more time consuming than Cross-Section optimization only and especially the fact that it is a combination of two methods applied in sequence. An integral approach by coupling the two methods could lead to more accurate and efficient results. The idea is therefore to write a script that performs both optimizations within each iteration. The main objective is again to reduce the structural weight and number of elements by removing them from the structural model. The two methods are schematically laid out in figure 4.1 and the coupled method is further elaborated in section 4.2.

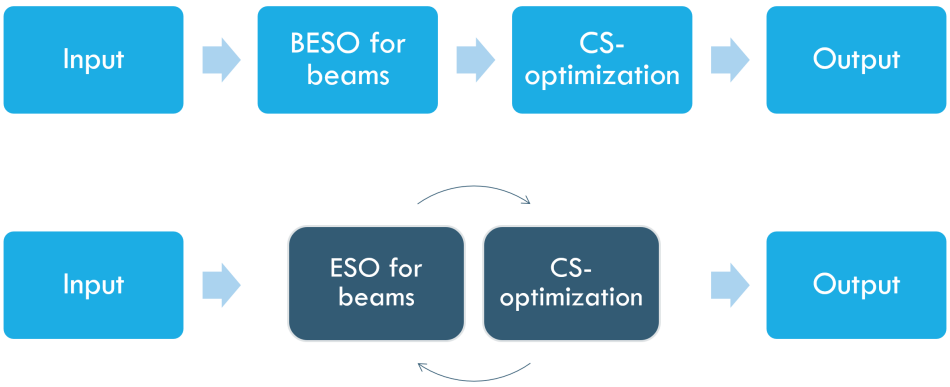

Figure 4.1: Overview procedure of (existing) sequential BESO>CS (top) and (new) coupled ESO<>CS method (bottom)

4.1.1. Random Structure Generator

A similar optimization technique has been applied before during the design of the Northwest Corner Building at Columbia University in New York City. This building entails diagonal bracing at rather odd places, which could be compared to the results obtained in chapter 3. The 14-storey building was designed using a 'Random Structure Generator' which randomly deleted bracing members. Initially, a structural analysis was ran, after which all bracing members in compression were removed, while tensile members were classified in three groups: highly loaded, moderately loaded and lowly loaded. Subsequently, respectively 10, 40 and 70 percent of the members of the corresponding group were removed randomly. Consequently, the method in essence is an ESO method. By alternating the percentage of members removed from each group, different designs could be obtained. The main findings were that removing lowly loaded members gave a realistic, rational load path while removing highly loaded members gave some unpredictable results [62]. In collaboration with the architect of the building, a solution was found for the final design of the building.

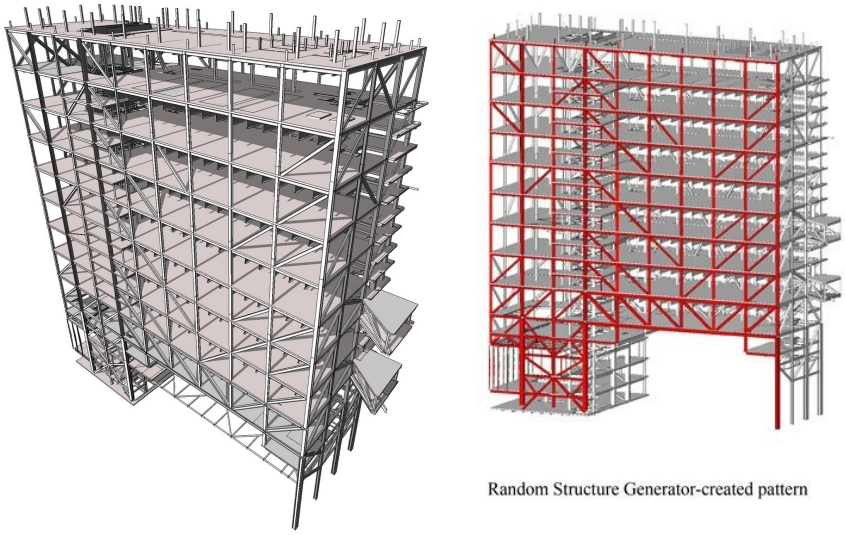

(a) (b)

Figure 4.2: Columbia University Northwest Corner Building structure and Random Structure Generator pattern

The structural design of this existing building shows that by applying bracing only where necessary, a lot of members can be removed. However, removing members randomly might not lead to the optimal design with the lowest structure weight. Yet, it does give multiple options which was found helpful for the architect of the building. Despite this, the main objective of the study for now is to minimize the structure weight and limit the number of connections (and therefore diagonals). The proposed ESO method therefore removes members, though not randomly but instead by using a more theoretical background as described in section 2.3.

4.2. Coupled ESO<>Cross-Section optimization method

4.2.1. Description

As the existing methods for BESO have their limitations regarding adjusting and adapting the iterative process, it is more convenient to manually write an iterative process as it gives more insight in the procedure and adaptability of the method.

For stiffness optimizations, regarding the strain energy density as explained in section 2.3.2 is more logical than weighing the stress or strain level. It is important not to confuse the strain energy with the strain energy *density*. The difference between these terms is elaborated in section 2.3.

The ESO-part (addition of members is not included) of the coupled ESO<>CS-method considers the strain energy density in each member. As a high-rise building design is often governed by deformation limits rather than stress levels, it seems more obvious to remove the members which contribute the least to the stiffness of the overall structure first, rather than the members that are least utilized in terms of stress. The advantage of scripting this method is the fact that the removal criteria for the elements can be easily controlled and adapted.

The general idea and procedure of the script is as follows:

1. Analyze initial structure using Karamba
2. Find deformation energy for axial force and bending
3. Sort the strain energy density levels from low to high
4. Remove N element(s) with the lowest strain energy density
5. Update the structural model
6. Repeat until i number of iterations have been performed

The main input parameters for this method are:

1. N: number of elements removed per iteration
2. i: number of iterations

The strain energy and strain energy density in the diagonal members are directly proportional as all diagonals have the same length and cross-sectional area initially. However this is not always the case, and thus the list of strain energy densities is re-sorted again in each iteration. This is especially important when Cross-Section optimization is implemented in each iteration.

Coupled ESO<>CS-optimization

Similarly to BESO for beams, running and ESO analysis alone may not make sense as the utilization and deformation criteria are not considered as boundary conditions. Therefore, coupling the ESO and cross-section optimizer will likely give better or more realistic results than ESO alone. Thus, the full optimization procedure would be as follows:

1. Analyze initial structure using Karamba
2. Increase/decrease cross-sections until utilization criterium is met
3. Increase/decrease cross-sections until displacement criterium is met
4. Find deformation energy for axial force and bending
5. Sort the strain energy density levels from low to high
6. Remove N element(s) with the lowest strain energy density
7. Update the structural model
8. Analyze updated model with reduced number of elements
9. Repeat from step 2 until i number of iterations have been performed

The procedure is schematically displayed in figure 4.3.

The main advantage over the BESO>CS-optimization method is that now, in each iteration step, the cross-sections are updated which may lead to differences in strain energy density. Hence, the method is called (two-way) coupled ESO<>CS-optimization. In the BESO>CS-optimization method the BESO was carried out first and after reaching the objective (Target

Ratio), CS-optimization was applied. As the problem considered are generally statically indeterminate problems, the internal forces in the structural elements are dependent on their section properties. The end result in BESO>CS-optimization is therefore more dependent on the initial input or starting point. For the coupled ESO<>CS-optimization method this is not the case as CS-optimization is also carried out in each iteration. As shown in chapter 3, CS-optimization is not very sensitive to its initial input as regarding a very heavy or a very lightweight structure approximately resulted in the same structure after CS-optimization.

4.2.2. Implementation

By implementing the proposed optimization method in the existing script, the same structural model can be used. In order to make the optimization script work, Anemone, a Grasshopper plugin, is needed. This plugin allows loops in the script as Grasshopper as standard does not allow recursive data streams. Other plugins which are used are Karamba3D for the structural analysis and GHPython for acquiring and managing data from the structural analysis output.

In each iteration loop, the (updated) structural model is disassembled and the elements are sorted by their strain energy density. The strain energy has two contributions: axial deformation energy and bending deformation energy. The sum of these energies represents the total elastic energy, however the bending deformation energy is zero for truss elements. The diagonal elements with the lowest strain energy density are removed, with a multiple of n in each iteration. Subsequently, the model is rebuilt, analyzed and cross-section optimized again which results in an updated model to be used in the next iteration. The iterative process continues until the desired number of iterations has passed. Optionally, the process can also be stopped after the cross-section optimizer fails to meet the boundary conditions for displacement or utilization. In this case, the analysis has been set to continue until all diagonals have been removed.

The full explanation of the script is presented in appendix B.3.

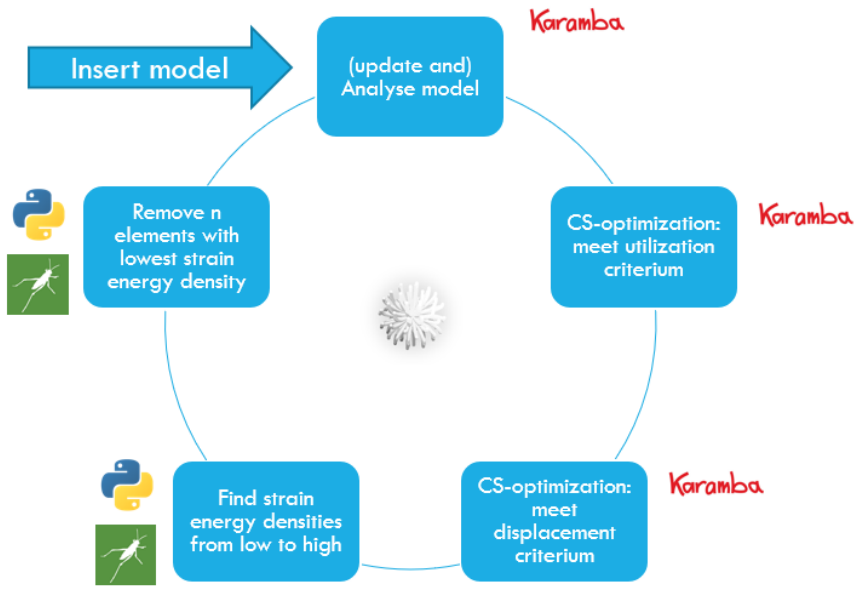

Figure 4.3: Overview procedure of the coupled ESO<>CS-optimization method

4.3. Test cases

4.3.1. Assumptions

The considered test cases are more or less comparable to the test cases in chapter 3. A rigid frame structure is not considered as it was concluded that this structure was not efficient and only CS-optimization was applicable to this type of structural system. Also, for the cases considered, which include a 'mid-rise' and 'high-rise' structure, it is assumed that a rigid frame might not be sufficient to ensure lateral stability and an additional bracing system is required. A core structure was found less favourable than a braced frame structure as there is less restriction in the placement of diagonals. Thus, only the latter structural system is considered for a mid- and high-rise case under wind and wind+vertical loading.

The initial cross-sections chosen are similar to cross-section (1) in each case considered. However it must be noted that as CS-optimization is also included, the optimized structure is not very sensitive to the initial cross-sections that are picked as long as the cross-section library remains the same. Keeping the cross-sections the same in both analyses yet gives a fair starting point. The loads and support conditions are also identical to the wind load cases from chapter 3, thus using NEN-EN 1991-1-4+A1+C2 to calculate the height-dependent wind load. The loads are listed in table A.1.

	mid-rise	high-rise
Dimension X [m]	3	3
Dimension Y [m]	3	3
Dimension Z [m]	3	3
Number of modules X-direction [-]	4	4
Number of modules Z-direction [-]	20	40
Total building height [m]	60	120
Corresponding wind load [kN/m^2]	1.53	1.85
Vertical load [kN/m^2]	10	10

Table 4.1: Initial parameters test cases mid-rise and high-rise

The verification criteria for the structure are similar to the verification criteria in chapter 3, namely:

1. Maximum utilization ≤ 0.5
2. Maximum displacement $\leq h/750$

Braced frame structure

For the braced frame structure in 2D, each module includes diagonals. There are in total 2 diagonals in each module, which coincide at the middle node in each module. As there are a total of $4 * 20 = 80$ modules, this brings the total number of diagonals is $80 * 2 = 160$.

The number of diagonals removed in each iteration is set to 1. This means that the total number of iterations is $n_{\text{diagonals}} + 1 = 161$. The first iteration is regarded as the initial analysis in which no diagonals are removed.

For the high-rise structure, the number of diagonals is twice as much, thus the number of iterations is 321. It can however also be opted for increasing the number of elements removed per iteration step in order to speed up the optimization process, however this might decrease accuracy of the result.

4.3.2. Influence of N-parameter

Lastly, the influence of the N-parameter (number of elements removed per iteration) is tested by analyzing the same case with a varying value for N. This has been done for the high-rise braced frame structure, of which the total number of diagonals is 320. The case considered is depicted in figure 4.4b. The number of iterations is directly proportional to the number of elements removed per iteration. The main objective is to find a good balance between analysis speed and accuracy of the results.

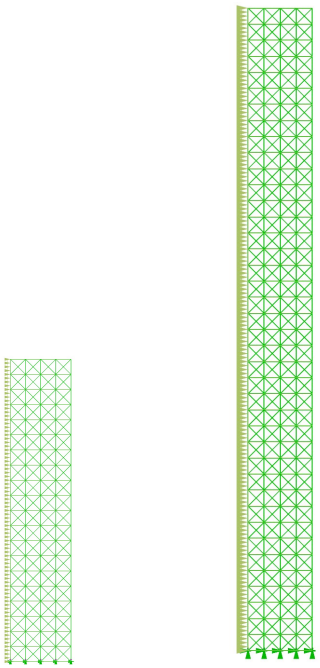

(a) (b)

Figure 4.4: Considered cases for 'mid-rise' and 'high-rise' braced frame structure

Number of elements removed per iteration	Total number of iterations
1	321
4	81
16	21

Table 4.2: Test cases for N-parameter

4.4. Results

4.4.1. Mid-rise braced frame structure (wind load)

The results found are primarily compared to the BESO>CS method from chapter 3.

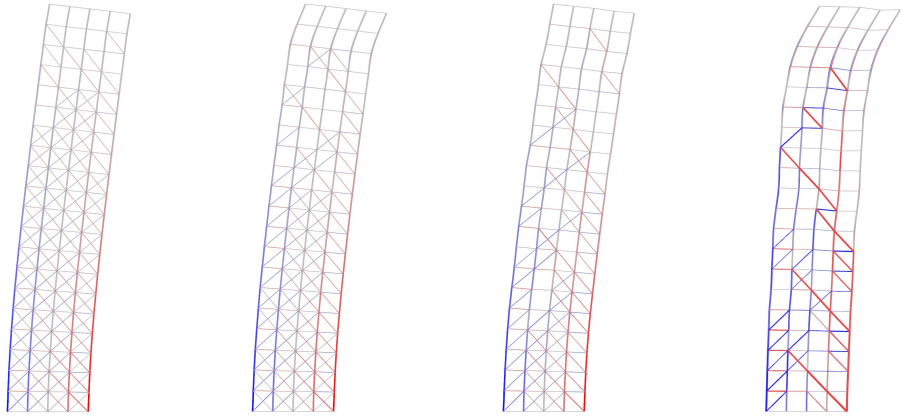

(a) (b) (c) (d)

Figure 4.5: Braced frame under wind load after BESO>CS, TR=0.8, 0.6, 0.4 and 0.2 respectively

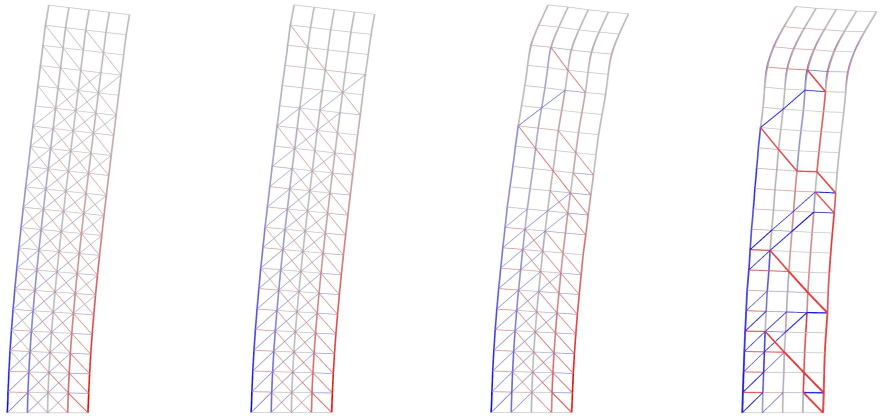

(a) (b) (c) (d)

Figure 4.6: Braced frame under wind load after ESO<>CS, fraction of diagonals remaining 80%, 60%, 40% and 20% respectively

The results of the ESO<>CS method are close to the results of the BESO>CS-optimization. The fact that the ESO<>CS-optimization curve is less smooth than the BESO>CS curve can be explained by the greater number of data points for the first-mentioned method, but also by implicitly updating the cross-sections in each iteration. In both methods, at lower TR it is observed that there are no diagonals in the top floors which therefore deflect much more than other floors. For both cases, the internal drift criterium of h/300 is not met as it was not considered as boundary condition. The reason for absence of diagonals is explained by the fact that lateral loads are taken by bending of the columns in this part of the structure. If truss elements would be used, each floor would include diagonals.

The minimum weight of the structure occurs at a TR of around 0.3, while at lower TR, the structure weight greatly increases, which is quite similar to the BESO>CS curve. The same explanation as found in chapter 3 yields for this, that is, the fact that too many diagonal members have been removed that the remaining members must large increase in size to meet the boundary conditions.

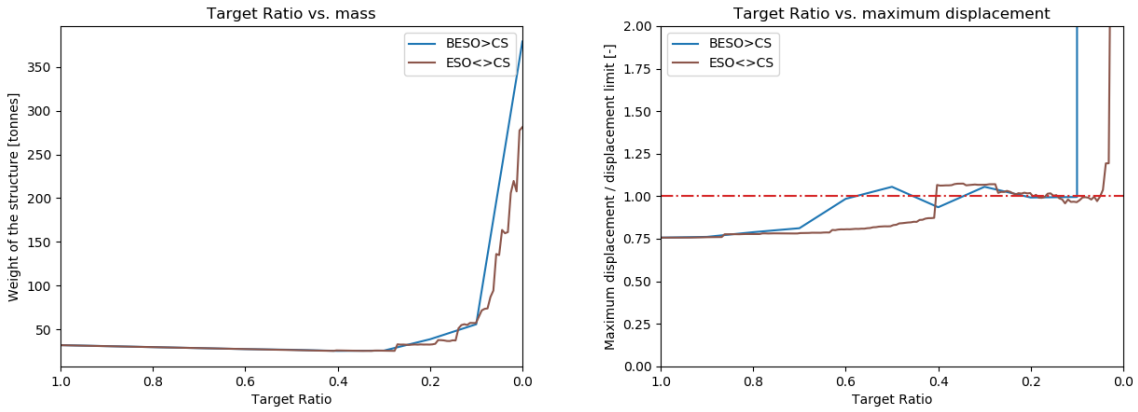

(a) (b)

Figure 4.7: Braced frame structure under wind load, TR versus mass and displacement

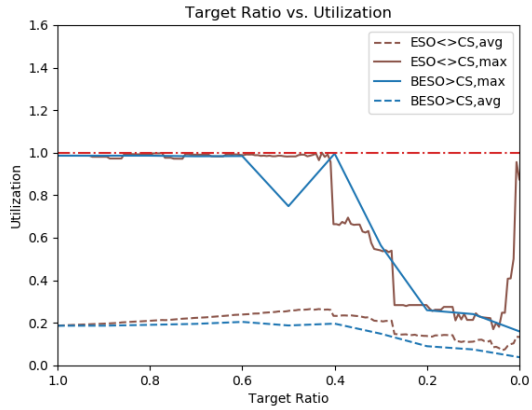

Figure 4.8: Braced frame structure under wind load, TR versus utilization

Overall, the observation is that the structure weight is approximately similar for both methods, however at TR < 0.2, ESO<>CS results in a lower structural mass. It is also evident that at approximately the same TR, displacement in the structure is governing. The suggestion that is created is therefore that when displacement is governing, thus for stiffness problems, the ESO<>CS method is slightly favoured.

4.4.2. Mid-rise braced frame structure (wind+vertical load)

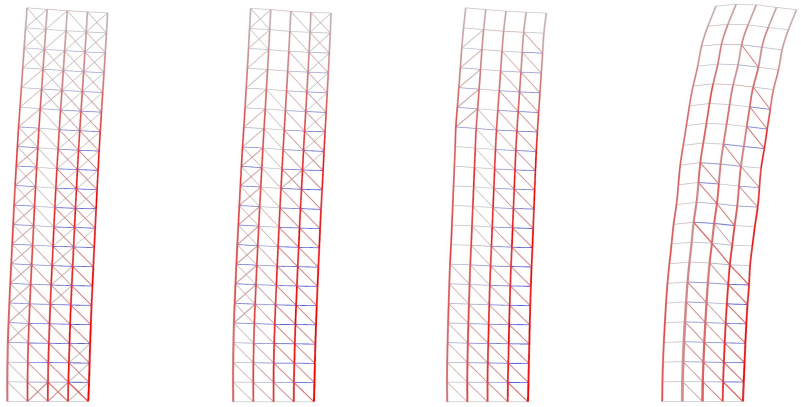

(a) (b) (c) (d)

Figure 4.9: Braced frame under wind+vertical load after BESO>CS, TR=0.8, 0.6, 0.4 and 0.2 respectively

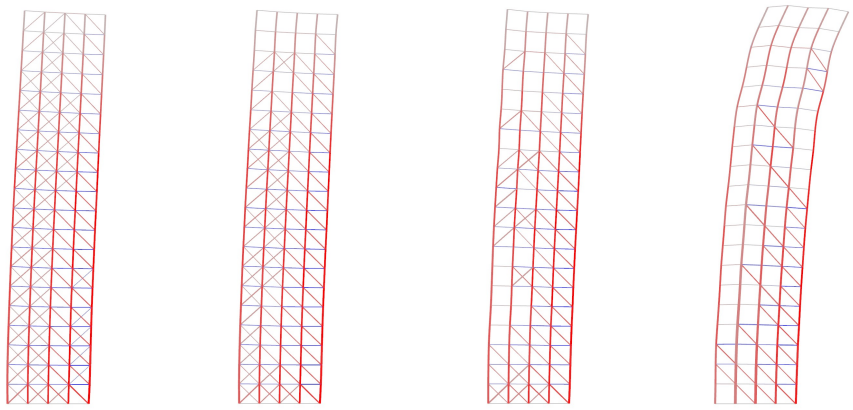

(a) (b) (c) (d)

Figure 4.10: Braced frame under wind+vertical load after ESO<>CS, fraction of diagonals remaining 80%, 60%, 40% and 20% respectively

For wind+vertical load, it appears that for both methods, at lower TR, only compression bracing remains. It seems like a part of the vertical load is taken by the diagonals. This means that diagonals in tension due to wind load are loaded by compression due to vertical load, which counteract each other. Thus the strain energy density (which is linearly related to the stress for these truss elements) is relatively low and therefore these elements are removed in both methods. The diagonals that remain are the diagonals which are loaded by compression due to wind load and additional compression due to vertical load.

Furthermore, at a TR of 0.4, when displacement starts to become governing, ESO<>CS results in a slightly lower structural weight. In the utilization graph, it appears that the average utilization of ESO<>CS is higher than for BESO>CS, which indicates that members are generally better utilized.

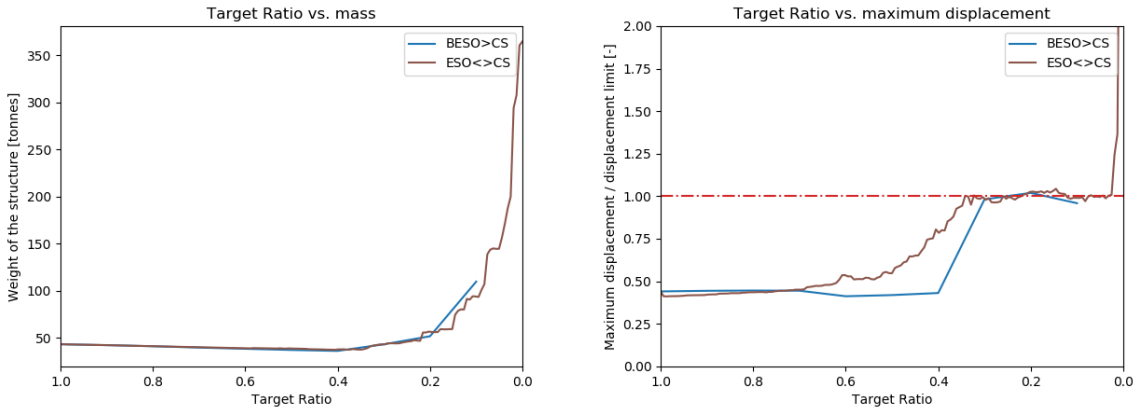

(a) (b)

Figure 4.11: Braced frame structure under wind+vertical load, TR versus mass and displacement

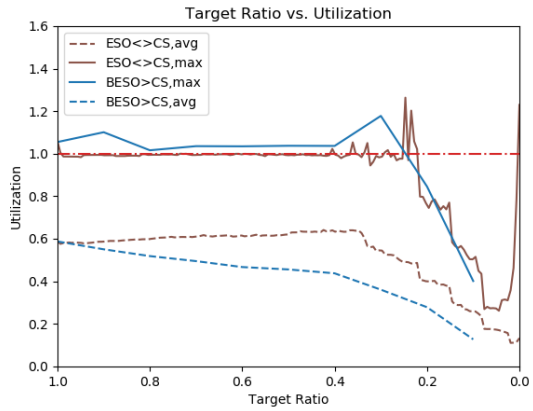

Figure 4.12: Braced frame structure under wind+vertical load, TR versus utilization

4.4.3. High-rise braced frame structure (wind load)

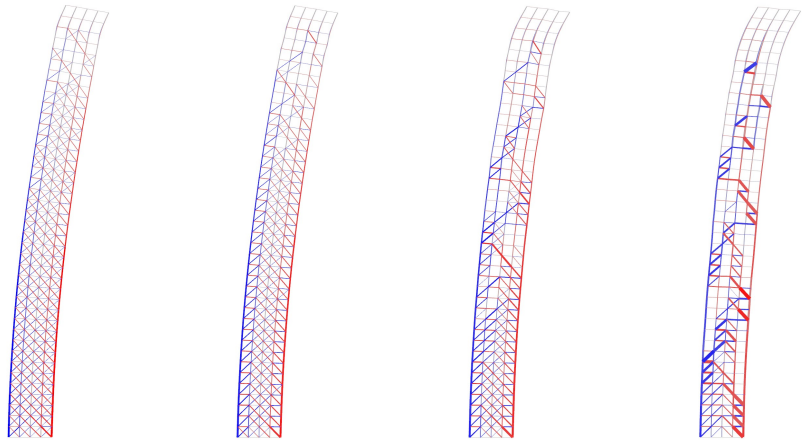

(a) (b) (c) (d)

Figure 4.13: High-rise braced frame under wind load after BESO>CS, TR=0.8, 0.6, 0.4 and 0.2 respectively

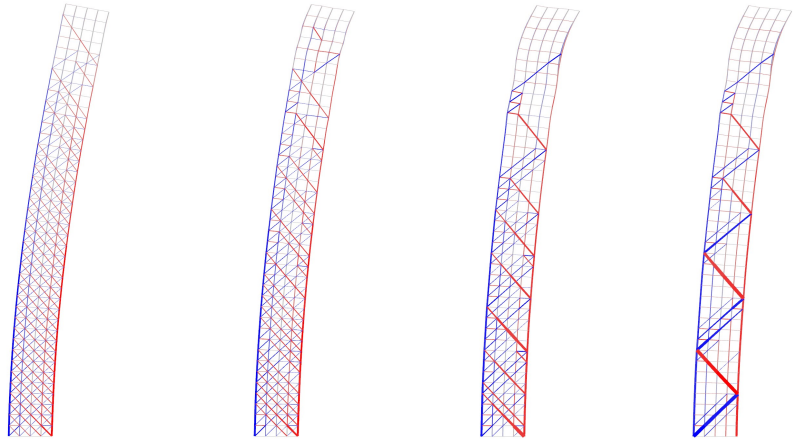

(a) (b) (c) (d)

Figure 4.14: High-rise braced frame under wind load after ESO<>CS, fraction of diagonals remaining 80%, 60%, 40% and 20% respectively

In the high-rise braced frame case, it appears that displacement is always governing regardless of TR. The ESO<>CS method generally has higher average member utilization and results in lower structural weight, however the difference is most obvious at TR from 0.3 to 0.1, just before the cross-section optimizer fails to meet the boundary conditions. This result confirms the suggestion that for the considered stiffness problems, the ESO<>CS method is favoured.

It also seems that ESO<>CS creates a truss-like structure in the form of a mega frame, with larger diagonals at the bottom and smaller diagonals near the top. This shape is most evident at a TR of 0.2 and intuitively seems like a much more efficient structure than the result of BESO>CS at similar TR.

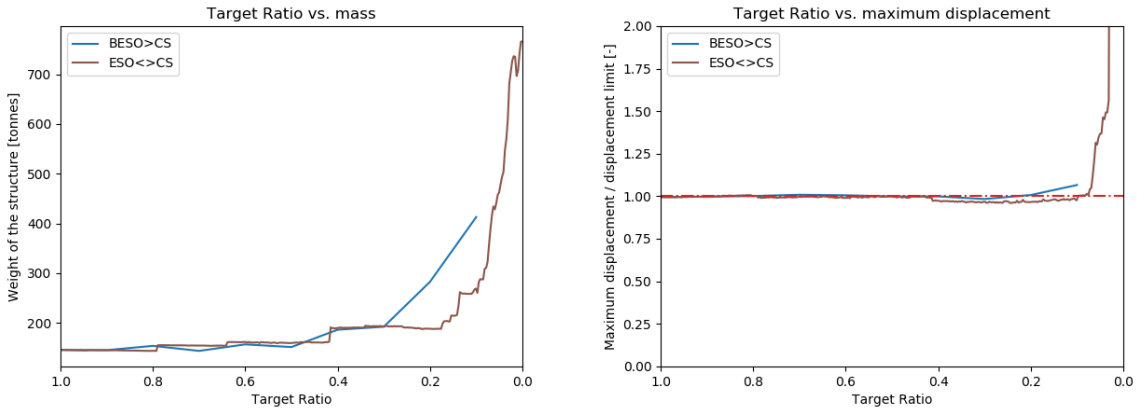

(a) (b)

Figure 4.15: High-rise braced frame structure under wind load, TR versus mass and displacement

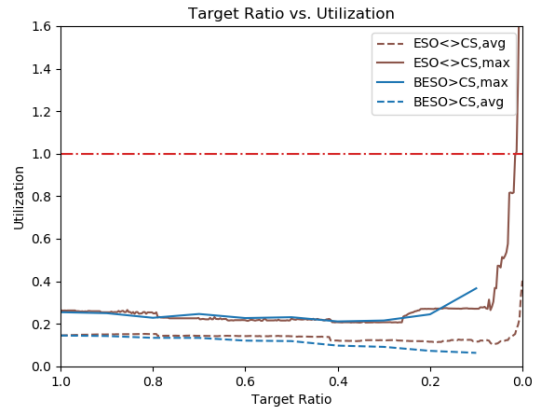

Figure 4.16: High-rise braced frame structure under wind load, TR versus utilization

4.4.4. High-rise braced frame structure (wind+vertical load)

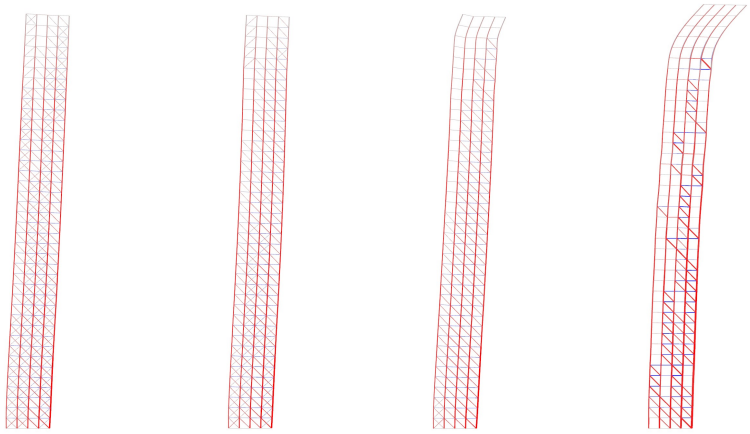

(a) (b) (c) (d)

Figure 4.17: High-rise braced frame under wind+vertical load after BESO>CS, TR=0.8, 0.6, 0.4 and 0.2 respectively

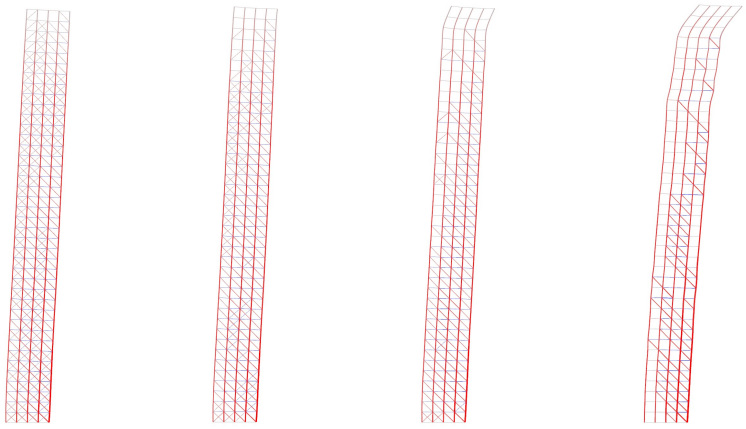

(a) (b) (c) (d)

Figure 4.18: High-rise braced frame under wind+vertical load after ESO<>CS, fraction of diagonals remaining 80%, 60%, 40% and 20% respectively

For wind+vertical load in the high-rise structure, displacement is no longer governing at all TR, but only at TR lower than 0.35. Again, it is observed that at this TR, the mass for ESO<>CS is lower and the members are on average more utilized.

It appears that vertical load is partly taken by diagonal bracing again, and that therefore only compression bracing remains. Also, the cross-section optimizer gives relatively small dimensions to the columns on the windward side whereas the columns on the leeward side have larger dimensions. This is again explained by the fact that the columns on the windward side encounter tension due to wind load and compression due to vertical load, which compensate each other.

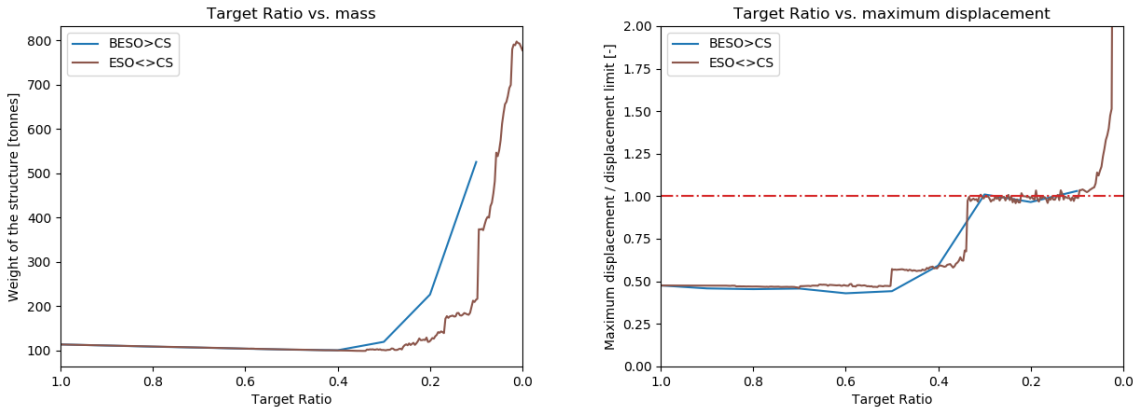

(a) (b)

Figure 4.19: High-rise braced frame structure under wind+vertical load, TR versus mass and displacement

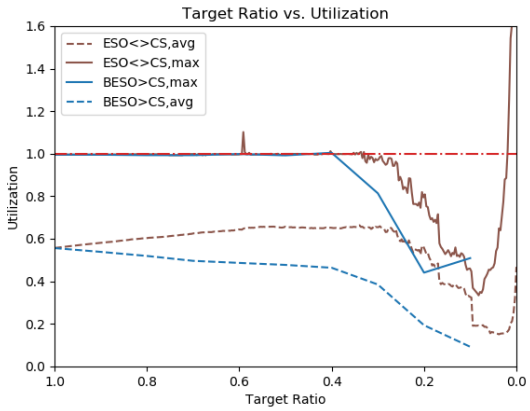

Figure 4.20: High-rise braced frame structure under wind+vertical load, TR versus utilization

4.4.5. Influence of N-parameter

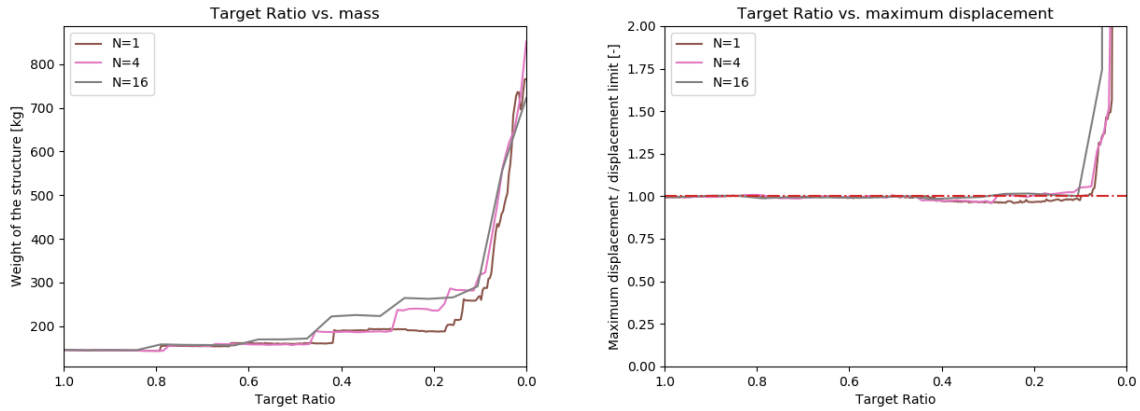

(a) (b)

Figure 4.21: High-rise Braced frame structure under wind load, TR versus mass and displacement for various N-values

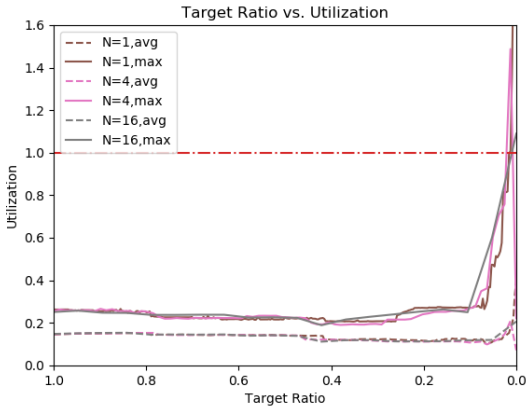

Figure 4.22: High-rise Braced frame structure under wind load, TR versus utilization for various N-values

It appears that the greater the number of elements removed per iteration, the higher the weight of the structure is. Displacement is governing in all considered cases, as the displacement stays around the limit, regardless of N-parameter or TR.

For utilization, also very minor differences are found in maximum as well as average utilization. This suggests that picking a larger number for N might be beneficial as it speeds up the analysis without losing too much accuracy, however the best results occur when the value of N is lower.

However, taking a closer look at the geometry of the optimized structures might suggest differently. The intuitively optimal truss-like mega frame which was found for N=1 seems to become less optimal as N increases and the result for large values of N starts to look like a somewhat arbitrary placement of diagonals such as for the BESO>CS method in chapter 3. Therefore picking a lower value for N not only results in a lower structural weight but also in solutions which are intuitively more sound.

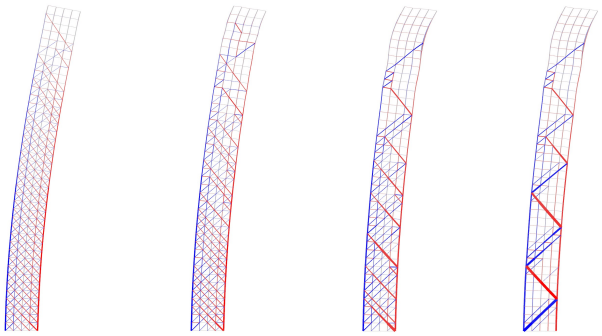

(a) (b) (c) (d)

Figure 4.23: High-rise braced frame under wind load after ESO<>CS (N=1), fraction of diagonals remaining 80%, 60%, 40% and 20% respectively

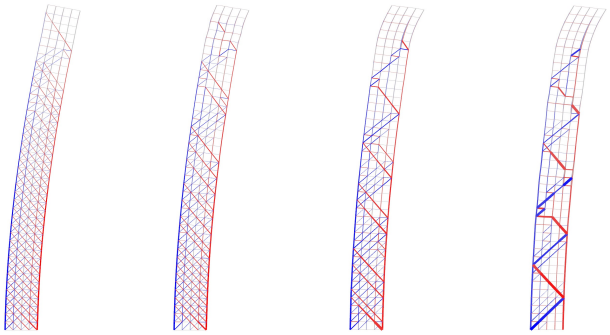

(a) (b) (c) (d)

Figure 4.24: High-rise braced frame under wind load after ESO<>CS (N=4), fraction of diagonals remaining 80%, 60%, 40% and 20% respectively

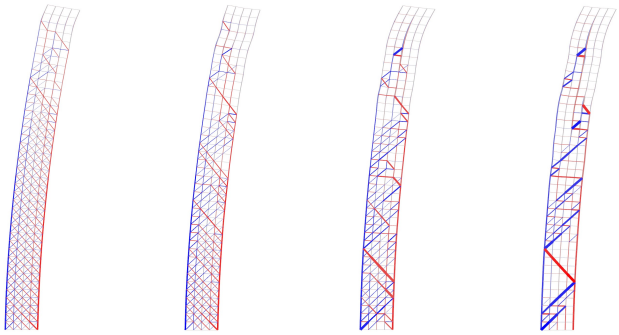

(a) (b) (c) (d)

Figure 4.25: High-rise braced frame under wind load after ESO<>CS (N=16), fraction of diagonals remaining 80%, 60%, 40% and 20% respectively

4.5. Discussion

4.5.1. General findings

For the considered cases it is found that the coupled ESO<>CS-optimization method is favoured and results in a lower weight for stiffness problems where displacement is governing. Updating the cross-sections in each iteration seems beneficial compared to the existing BESO>CS method and therefore choosing a small value for N is desired. As the cross-sections are updated in each iteration, members which are highly utilized are increased in size. As their section properties increase, they will likely take more load in the next iteration. Thus, the utilization remains relatively high which means the element will not be removed but instead will increase in size again and therefore take even more load in the next iteration. This way, there is a positive feedback loop in which members with high strain energy density will keep increasing in size and take more load. In the existing BESO>CS method, adaptation of the cross-sections only happens after BESO is completed with a specified TR, which means there is no positive feedback loop and element removal is only based upon stress level in the case with initial cross-sections. The benefits of the coupled ESO<>CS method are most evident in the single load case with wind.

For the cases with wind+vertical load, it is observed that mainly compressive bracing remains, while column dimensions on windward and leeward side are smaller and larger respectively. When the wind direction changes, tensile forces in bracing may change to compression and vice versa. Therefore, (single) bracing should be able to take tension and compression, however they should not take the vertical load. In practice, this cannot always be avoided, but the diagonals should not be designed to take vertical load. Possible ways to prevent this are:

- Eliminate all compression bracing
- Change angle of bracing
- Design/optimize for multiple load cases (separately)

4.5.2. Tension/Compression eliminator

It can be opted for to remove all diagonals under compression so that a structure with only diagonals under tension will remain. This could be desirable as the heavily loaded tensile members will remain after ESO instead of the heavily loaded compression members (which were also loaded by vertical load). This way, the diagonals primarily carry the lateral load whereas the columns primarily carry the vertical load. An additional advantage is that buckling effects no longer have to be considered when the members are in tension.

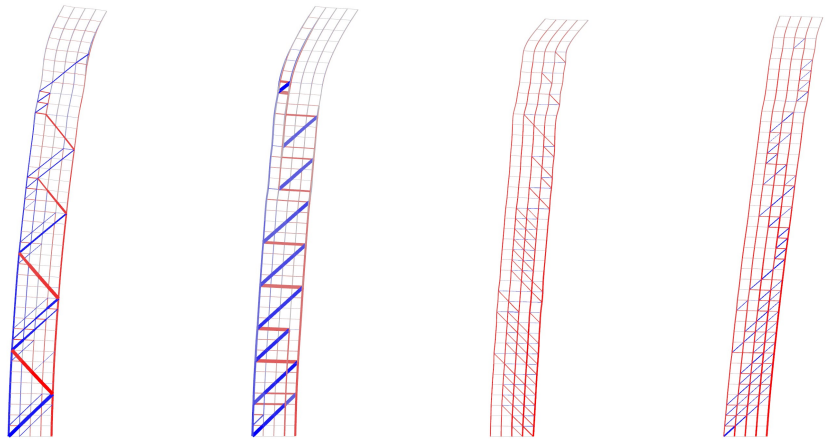

(a) (b) (c) (d)

Figure 4.26: High-rise braced frame under wind (a,b) and wind+vertical (c,d) load after ESO<>CS (N=1, fraction of diagonals remaining 20%), with (a,c) or without (b,d) compression diagonals

However, by only allowing tensile forces in the bracing elements, it appears that the beams are heavily loaded in compression in order to account for the tensile forces induced by the diagonals. This would create a vertical Pratt-truss-like structure in which the beams act as compression members. This is undesirable as the dimension of the beams and columns should stay the same as much as possible in order to standardize the modules. Also, when the structure is loaded by wind from opposing direction, the diagonals in figure 4.26b will be loaded in compression, or the structure should be mirrored. Therefore designing the braces such that they can handle compression as well as tension reduces the number of diagonals needed and is a sensible design strategy for the diagonal bracing system, unless the bracing system only includes X-bracing. With X-bracing systems, it is assumed that the compression brace will buckle and all the lateral load is taken by the tensile brace.

When the structure is loaded by wind and vertical load, it seems that the main difference between tensile and compressive bracing is the direction of the forces in the beams. When braces are in tension, beams will be in compression and vice versa. It is preferred to have the tension in bracing and beams in compression. A reason for this is the fact that the buckling length of the beam is smaller than the one of the diagonal. This is evident in figure 4.27 in which the cross-sections for the beams are larger in the tension bracing model, whereas the diagonals have larger dimensions in the compressive bracing model. Also, beams usually have considerable dimensions already as they have to carry vertical loads and limit vertical deflections and larger beams are visually less disturbing than large diagonal members.

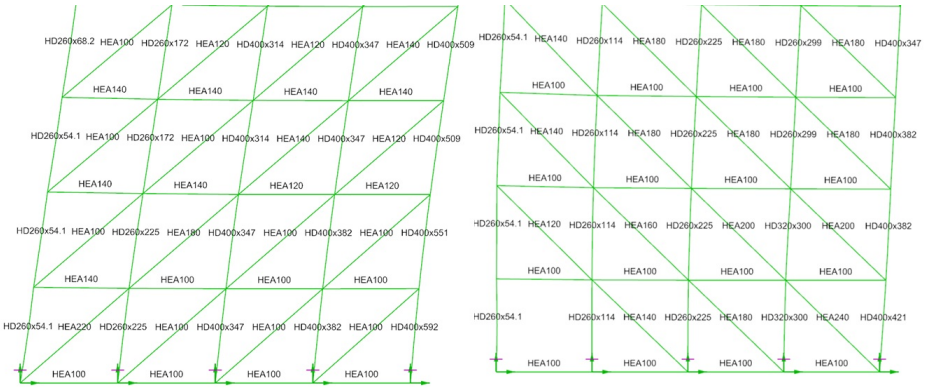

Figure 4.27: Cross-sections for high-rise braced frame structure under wind+vertical load for tensile (left) and compressive (right) bracing after CS-optimization

4.5.3. Angle of bracing

By varying the angle of the braces, the portion of vertical load which enters the braces can be controlled when the structure is loaded by vertical and lateral load. A bracing system with a large angle with the horizontal will result in more vertical load, whereas an angle close to 0 leads to (almost) 0 vertical load and solely lateral load. As square modules were assumed earlier, the angle of the braces was set at 45 degrees.

Figure 4.28 shows much more elements in tension at a smaller angle. Choosing a smaller angle is therefore preferred if it is strived for to eliminate the vertical load from the bracing elements. Bracing systems with a smaller angle are generally wider and therefore more stable [63]. Yet, the bracing angle ultimately depends on the module dimensions which is governed by external factors such as function and transportability and should not be a boundary condition for eliminating vertical load from the diagonal members.

4.5.4. Multiple load case design

Separately considering load cases

As diagonals should take the lateral load whereas the columns should take the vertical load, a possible design strategy could be:

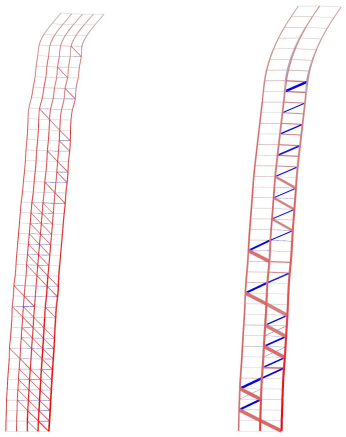

(a) (b)

Figure 4.28: High-rise braced frame under and wind+vertical load after ESO<>CS (N=1, fraction of diagonals remaining 20%), diagonals at 45 degrees (a) and 27 degrees (b)

1. Design bracing system for wind load
2. Design columns and beams for vertical load

For example, the truss-like structure in figure 4.29a is optimized for wind load using coupled ESO<>CS and seems like a sensible solution. If this structure is then loaded by vertical load whilst CS-optimizing the columns and beams, a structure is found which satisfies both load cases (4.29b). On the other hand, another structure is found when applying the coupled ESO<>CS method for the combination of wind+vertical load (4.29c). This structure already satisfies the boundary conditions for the case with wind+vertical load and has a lower structural weight as presented in table 4.3.

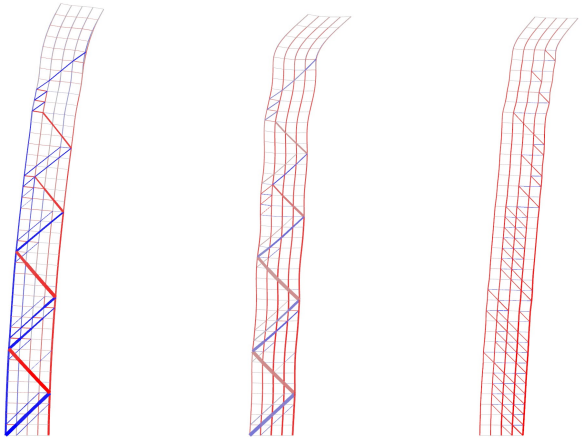

(a) (b) (c)

Figure 4.29: Truss-like structure optimized under wind (a) and wind+vertical (b) load, wind+vertical load optimized structure (c)

Considering wind load only for the design of the bracing system and the vertical load only for design of the columns and beams generally leads to a structure which satisfies, but is not necessarily results in the lowest structural weight. The reason for this is that wind load only is a more critical load case and more material is needed in order to satisfy the displacement (and/or utilization) criterion. The relevance of this load case can however be doubted as in practice there will never be only wind load on the building, but also dead load

Structure	Max. displ. UC [-]	Weight [tonnes]	Max. util.	Avg. util.
Truss-like (a) (wind load)	0.98	187.9	0.28	0.12
Truss-like (b)	0.98	186.2	0.54	0.34
Optimized for wind+vertical (c)	0.98	129.6	0.74	0.52

Table 4.3: Results of multiple load case design for wind+vertical load

and in most of the time, live load. When designing for wind+vertical load, using the coupled ESO<>CS-method (4.29c) results in about 43% lower structural weight in this case and is therefore preferred over using the method for wind load only and separately applying vertical load (4.29b).

Combining simultaneous load cases

Eventually, the building must be verified while being loaded by permanent load and leading variable loads. This includes vertical load as well as wind load. Optimizing the structure directly for these load cases results in the lowest structure weight instead of considering various loads separately. Therefore it is suggested to directly consider the combination(s) for which the structure must be verified and optimize for these load combinations, which are mostly wind+vertical load, considering wind from multiple directions separately.

By considering wind from multiple directions separately and optimizing for these cases, all columns are designed to withstand the 'worst-case-scenario'; vertical load and additional compression from wind load.

4.6. Conclusion

It can be concluded that especially in case of stiffness problems the coupled ESO<>CS-method is more effective than the existing BESO>CS method. This indicates that the application of this method is a viable optimization procedure for high-rise buildings. The main difference is that cross-section optimization now is included in each iteration, which gives much more accurate results. This is especially evident in the case with wind load only, which results in a truss-like mega frame. A low value for N (elements removed per iteration) gives more accurate results but increases the iteration time.

When considering the case with wind and vertical load however, it seems like vertical load is partially taken by the diagonal members. This is not a characteristic of the optimization method as it also occurs in the existing method, but a design issue that should be taken care of, for example by specifying boundary conditions. In the case of modular high-rise construction, reasonable boundary conditions are:

- Standardize cross-section of all beams
- Standardize cross-section of columns (or little variation)
- Consider multiple load cases (wind+vertical, multiple directions)

By specifying these boundary conditions, modular construction is made more accessible as the modules can have standardized dimensions. Also, by standardizing the cross-section of the columns, the column size is no longer dependent on wind direction as all columns are designed for the worst-case-scenario. A subdivision for column groups is made as shown in figure 4.30. The columns in each group have the same cross-section and are optimized using the cross-section optimizer in the coupled ESO<>CS-method. The expectation is that columns in the lower segment of the building will have larger cross-sections. The list of element groups is presented in table 4.4.

The beam dimensions are based on rules of thumb as they all have the same span, take the same load and have the same support conditions (hinged). The optimization is hence sped up as the beams do not participate in cross-section optimization and can be modelled as truss elements, while the resulting forces act on the nodes instead of on the elements.

The load cases which must be considered are the cases with wind+vertical load. All wind directions must be considered as separate load cases:

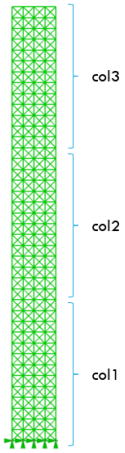

Figure 4.30: Subdivision of columns

Element group	Included elements	Cross-sections	Element type
col1	Columns $0 \leq z \leq h/3$	similar in group after CS-opt	beam
col2	Columns $h/3 < z \leq 2h/3$	similar in group after CS-opt	beam
col3	Columns $2h/3 < z$	similar in group after CS-opt	beam
beams	All beams	similar in group, based on rules of thumb	truss
diag	All diagonals	may vary per element after CS-opt	truss

Table 4.4: Element groups in structural model

1. Vertical load + wind (left) (LC0)
2. Vertical load + wind (right) (LC1)

For a 3D-model, two additional load cases are taken into account:

3. Vertical load + wind (front) (LC2)
4. Vertical load + wind (back) (LC3)

The coupled ESO<>CS-method will result in a range of solutions, starting with solutions with many diagonals to solutions with less diagonals. All solutions meet the displacement and utilization boundary conditions and the analysis is terminated after these boundary conditions can no longer be met. This is the case when too many diagonals have been removed that the remaining elements must have larger cross-sections than defined in the cross-section list in appendix A.2.

5

Case study

After defining a structural optimization method, the method is implemented in a parametric script which allows any type of building volume to be translated into a structural model which is analyzed and optimized. The implementation of the optimization method and application of the design script is discussed in this chapter.

5.1. Objective

The objective of the script is to translate a randomly given building volume into a modular structural concept. The input parameters are the building volume and module dimensions, which can be determined by for example transportation requirements or convenience for fabrication. The building volume is then divided in modular volumetric blocks by the specified dimension. This idea can be compared to a potato slicer which cuts potatoes into french fries.

Subsequently, a structural model is drawn, analyzed and optimized. Thus, a rough layout of the structural design is aimed for by simply pressing a button. For this purpose, a user interface is designed which enables controls the parameters and optimization and presents the obtained results. The user interface is displayed in figure 5.1 and further elaborated in appendix B.4.

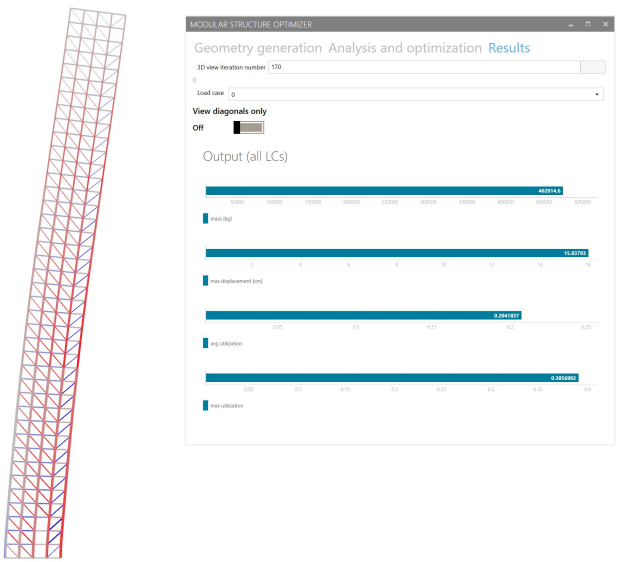

Figure 5.1: User Interface for modular structure optimizer

5.2. Assumptions

5.2.1. Loads

The main loads acting on the building are live load, dead load and wind load. The magnitude and application of these loads is stated in Eurocode NEN-EN 1991. The assumption is that high-rise buildings are designed in consequence class CC3. The corresponding K_{FI} factor is 1.1.

Vertical loads

Vertical loads on the building include dead load and live load. Other vertical loads such as snow load are not considered important in this design stage.

It is assumed that the building is multi-purpose and the use should be flexible. Possibilities for the use of the building could be residential, office or shopping. Therefore, the highest live load should be assumed.

Function	Live load [kN/m^2]
Office	2.5 to 3
Residential	1.75 to 2
Shopping	4

Table 5.1: Live loads according to the Eurocode

The dead load of the building is automatically modelled as point loads on the nodes in the finite element model. The dead load of the floor slabs can be assumed by choosing a certain type of floor. The assumption has been made for a solid slab floor.

Floor type	Dead load [kN/m^2]
Solid slab including finishing	6

Table 5.2: Floor load assumptions

Horizontal loads

The horizontal load on the building is considered from 4 sides separately and follows from NEN-EN 1991-1-4. The Dutch National Annex to the Eurocode provides a table with peak pressure, however the peak wind pressure as a function of building height z can also be calculated with the following formulae from the Eurocode.

First, the basic wind speed is calculated with the following formula from the Eurocode (NEN-EN 1991-1-4 formula 4.1):

$$v_b = c_{\mathrm{dir}} * c_{\mathrm{season}} * v_{\mathrm{b},0} \tag{5.1}$$

in which the directional wind factor c_{dir} is given in the National Annex and has a recommended value of 1.0. The same holds for the seasonal factor c_{season} which also has a recommended value of 1.0. The fundamental value of the basic wind speed $v_{\mathrm{b},0}$ can be found in the National Annex and depends on the wind area.

Wind area	I	II	III
$v_{b,0}$ [m/s]	29.5	27.0	24.5

Table 5.3: $v_{\mathrm{b},0}$ for application in the Netherlands

The mean wind velocity $v_m(z)$ as a function of height z is described as follows in NEN-EN 1991-1-4 formula 4.3:

$$v_m(z) = c_r(z) * c_o(z) * v_b \tag{5.2}$$

in which $c_r(z)$ is the terrain roughness factor and $c_o(z)$ is the orography factor. The terrain roughness factor depends on the height above ground level and the terrain roughness on the

windward side of the building. The orography factor c_0 can be taken as 1.0.

$$c_r(z) = \begin{cases} k_r * \ln(\frac{z}{z_0}), & \text{for } z_{\min} \leq z \leq z_{\max} \\ c_r(z_{\min}) & \text{for } z \leq z_{\min} \end{cases} \tag{5.3}$$

in which z_0 is the roughness length and $z_{\min}$ is the minimal height, of which both can be found in NEN-EN 1991-1-4 table 4.1. The Dutch National Annex prescribes different values for z_0 and $z_{\min}$ in table NB.3-4.1. The values that are used for calculation of the wind pressure are taken from the Dutch National Annex and listed in table 5.4 and 5.5.

Terrain category	z_0 [m]	z_{min} [m]
0	0.005	1
II	0.2	4
III	0.5	7

Table 5.4: Terrain categories and parameters according to Dutch National Annex

$z_{0,II}$	0.05 [m]
z_{max}	200 [m]
k_I	1.0 [-]

Table 5.5: Other parameters for calculation of wind pressure

The terrain factor k_r can be calculated with NEN-EN 1991-1-4 formula 4.5:

$$k_r = 0.19 * (\frac{z_0}{z_{0,\text{II}}})^{0.07} \tag{5.4}$$

Subsequently, the turbulence intensity $I_v(z)$ is determined as function of height z according to NEN-EN1991-1-4 formula 4.7:

$$I_v(z) = \begin{cases} \frac{\sigma_v}{v_m(z)} = \frac{k_I}{c_o(z) * \ln(\frac{z}{z_0})}, & \text{for } z_{\min} \leq z \leq z_{\max} \\ I_v(z_{\min}) & \text{for } z < z_{\min} \end{cases} \tag{5.5}$$

Eventually, the peak wind pressure $q_p(z)$ can be determined (NEN-EN1991-1-4 formula 4.8):

$$q_p(z) = (1 + 7I_v(z)) * \frac{1}{2} * \rho * v_m^2(z) = c_e(z) * q_b \tag{5.6}$$

in which: ρ is the density of air and has a recommended value of $\rho = 1.25\ [kg/m^3]$

$$q_b = \frac{1}{2} * \rho * v_b^2 \tag{5.7}$$

As it follows from the formulae, the peak wind pressure is not only a function depending on the height of the building but also on other variables such as wind area and terrain. The formulae have been programmed in python such that the peak wind pressure $q_p(z)$ is calculated according to the given input, namely the building height z, wind area and terrain category. An overview of this script is found in section B.1.

The wind load distribution is not constant along the height of the building. According to the Eurocode, the wind load must be distributed as depicted in figure 5.2.However for the early design stage, a peak pressure of $q_p(h)$ is taken across the entire height of the building, which is an overestimation and therefore leaves room for additional material reduction in the detailed design stage.

Furthermore, the external pressure coefficients must be taken into account. It is assumed that the building has a rectangular floor plan and a vertical facade, meaning table 7.1 from NEN-EN 1991-1+A1+C2 can be used. The factors for pressure and suction are distributed as depicted in figure 5.3. The relevant coefficients are listed in table 5.6.

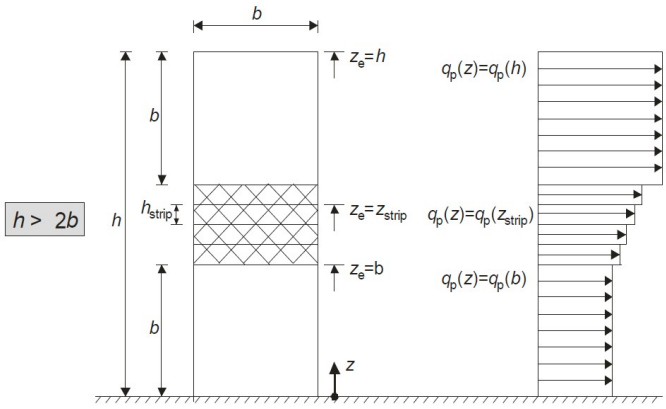

Figure 5.2: Wind pressure distribution according to NEN-EN 1991-1+A1+C2 figure 7.4

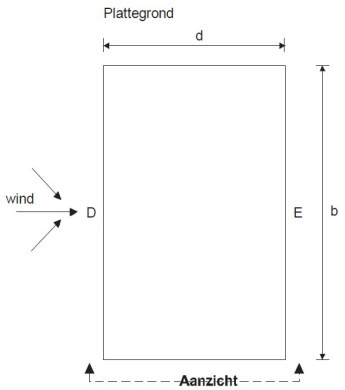

Figure 5.3: Zone distribution of wind pressure for rectangular buildings with vertical facade

The assumption is that it entails a high-rise building for which the ratio h/d is always bigger than 5. The corresponding factors are +0.8 on the windward side and -0.7 on the leeward side. A simplification is made by modelling a factor or +1.5 on the windward side.

The factor $c_s c_d$ is assumed to be 1.0 for low-rise buildings but for high-rise buildings, a detailed calculation is required. The formula for $c_s c_d$ is expressed in formula 6.1 in EN 1991-1-4:

$$c_s c_d = \frac{1 + 2 * k_p * I_v(z_s) * \sqrt{B^2 + R^2}}{1 + 7 * I_v(z_s)} \tag{5.8}$$

This is however a relatively complicated formula which include many unknown factors for such an early design stage. Therefore, a value of 1.0 is assumed for $c_s c_d$ which is a conservative approximation according to Vrouwenvelder and Steenbergen [64, p. III-18].

Other loads

Other loads that could act on a high-rise buildings are snow load and incidental blast loads. It is assumed that snow loads do not have a significant influence on the overall structural system of the building. The chance of blast loads occurring is assumed to be small and preference is given to other measures to prevent these loads on the structure rather than designing the structure specifically for these types of loads. These loads are therefore not taken into account in the analysis for the whole building.

Load combinations

The load combinations that can be distinguished comprise of live load, dead load and wind load. In Ultimate Limit State (ULS), load factors have to be applied for permanent and variable

Zone	D	D	E	E
h/d	$c_{pe,10}$	$c_{pe,1}$	$c_{pe,10}$	$c_{pe,1}$
5	+0.8	+ 1.0	-0.7	-0.7
1	+0.8	+ 1.0	-0.5	-0.5
$\leq$ 0.25	+0.7	+ 1.0	-0.3	-0.3

Table 5.6: Recommended values for external pressure coefficients for vertical facades in rectangular buildings

loading. The factors for permanent load and the leading variable load must be multiplied with K_{FI} for unfavourable actions. The resulting factors are listed in table 5.7.

Design situation	Permanent loads unfavourable	Favourable	Variable loads leading	Other
1	1.485	0.9	-	1.65
2	1.32	0.9	1.65	1.65

Table 5.7: Load factors in ULS [17]

For ULS, the governing load combinations are determined by the following formula:

$$\gamma_G * G_k + \gamma_{Q;1} * Q_{1;k} + \sum(\gamma_{Q;i} * \Psi_{0;i} * Q_{i;k}) \tag{5.9}$$

For SLS, the governing load combination is determined as follows:

$$G_k + \gamma * Q_{1;k} + \sum(\Psi_{0;i} * Q_{i;k}) \tag{5.10}$$

The ”combined” load factor for permanent and variable load with the assumed load using formula 5.10 and 5.9 is described as the ratio between ULS and SLS:

$$\frac{\gamma_G * G_k + \gamma_{Q;1} * Q_{1;k} + \sum(\gamma_{Q;i} * \Psi_{0;i} * Q_{i;k})}{G_k + \gamma * Q_{1;k} + \sum(\Psi_{0;i} * Q_{i;k})} \tag{5.11}$$

The four load combinations considered are all situations with wind and vertical load, with wind load varying from direction. An overview of all load combinations is depicted in figure 5.4.

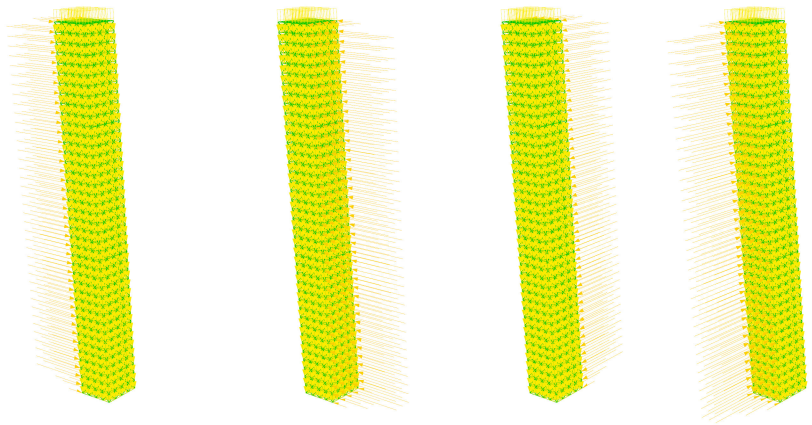

(a) (b) (c) (d)

Figure 5.4: Load cases LC0, LC1, LC2 and LC3

5.2.2. Material and geometry

For the beam elements, a steel grade of S235 is assumed. The steel grade properties are given in the table below:

Steel grade	Yield Strength (N/mm^2)	Young's modulus (GPa)
S235	235	210

It can also be opted for using other steel grades such as S275, S355 or S460. This is a parameter which can be changed by the designer, but is assumed to be S235 by default.

5.2.3. Verification criteria

Strength

The strength of the structural members must be verified in ULS. Depending on the ratio between variable and permanent load, the factor described in formula 5.11 is at least 1.485 and at most 1.65 when both design situations in table 5.7 are considered. As the characteristic loads are used to verify the deformation, the maximum utilization for the ULS check would be $1.0/1.65 = 0.61$.

By taking a utilization limit of 0.5, similar to the limit set in the studies in chapter 3 and 4, some extra safety is added.

Stiffness

The stiffness of the building is verified in SLS. The maximum allowed deformation for multi-storey buildings as stated in the Dutch National Annex to the Eurocode NEN-EN 1990 as follows:

- h/300 per storey
- h/500 for the entire building

Again, h/750 is taken in order to allow some additional displacement due to settlement of the foundation.

5.2.4. Geometry generation and structural optimization

The inputted building shape and module dimensions are used to prepare the geometry of the structural model. The main procedure is displayed in figure 5.5 and further elaborated in appendix B.2. Simply stated, the volume is divided in blocks which include beams, columns and diagonals in each plane. Diagonals in the horizontal plane represent diaphragm action of the floors while diagonals in the vertical plane carry lateral loads. The geometry of a block is presented in 5.6. The general modular concept is an external structure which is built up from building blocks as depicted in figure 5.6, in which modules can be placed as described in section 2.2.

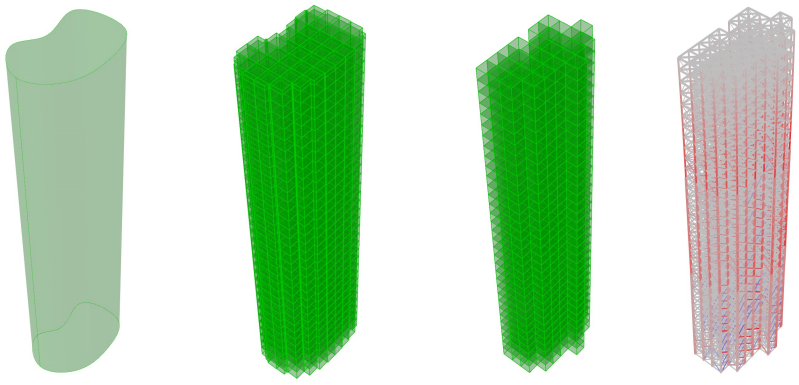

(a) (b) (c) (d)

Figure 5.5: Procedure from BRep to structural model, analysis and optimization

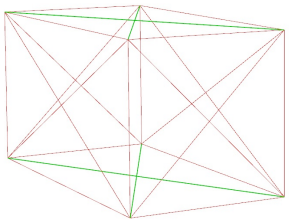

Figure 5.6: Geometry of a building block from the external frame structure

Optimization procedure

After generating the geometry and defining the input for the structural analysis, the structural model is analyzed and optimized using the coupled strain-energy based ESO and CS-optimization method with the boundary conditions and assumptions as concluded in chapter 4. Due to the large number of elements in the model, the optimization script might take some time as the number of iterations is larger as well as the time per iteration.

By using this optimization procedure, the optimizer finds a range of solutions which all satisfy the specified boundary conditions. The optimum solution could be a trade-off between number of elements and mass, and therefore could be found by for example specifying a price per connection and cost per kilogram.

5.2.5. Modular concept

Depending on the choice of structural members, the structure could be a modular self-supporting structure or an external structure in which modular units are placed.

Self-supporting modular structure

In case of a modular self-supporting structure, for example SHS columns and channel or angle sections for edge beams can be taken. An example of connection of such modules is depicted in figure 5.7.

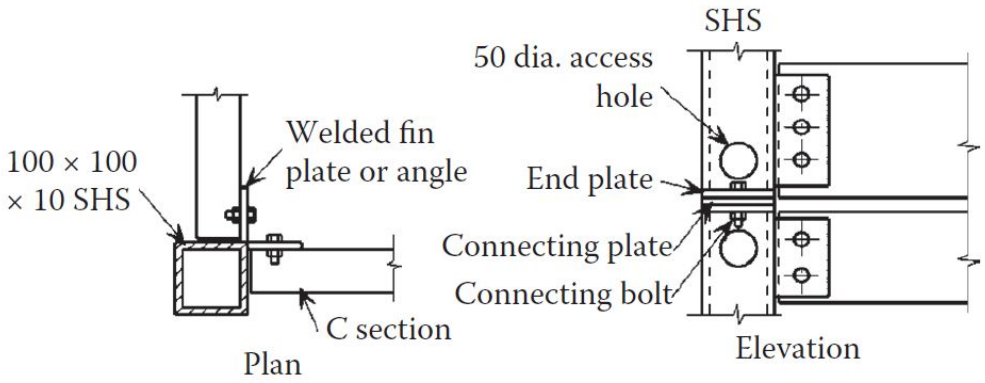

Figure 5.7: Connection of steel module with SHS and C-sections [30]

However, this type of structure is only applicable to lower buildings. For tall buildings, preference is given to an external main load-bearing structure in which modules can be placed. This was also the case in the 461 Dean Street Building.

External structure with modules

An external structure in which modular units are placed can be built up from regular standardized wide flange beams and columns such as HEA-, IPE- and HD-sections. In the external frame structure, modular units can be placed. The general idea is that corner supported

modules are carried by the external frame structure and therefore the modules themselves only need to be self-supporting and can be fabricated out of lighter angle or channel sections. This is similar to 461 Dean Street, of which a module is depicted in figure 5.8. The modules in this building are supported on steel columns with additional transverse crossbars [7]. The modules in this building are not all corner-supported modules, but also four-sided

Figure 5.8: Module in 461 Dean Street Building [7]

modules are included. In the considered case studies, only corner-supported modules are assumed while diagonals could represent a wall panel. The steel modules are bolted to the frame structure and therefore easier to install than prefabricated concrete modules, which often require wet connections.

Earlier (section 2.2), a vending-machine-like concept in which modules can be replaced was mentioned. This concept is generally known for providing snacks and soft drinks but has been applied in automated car parks (figure 5.9) throughout the years. Applying this concept in buildings could be considered unnecessary as the frequency of module replacement is rather low, however it would be a great way to renew a high-rise building and lengthen its life span. By designing an external frame structure and bolting the modules to the structure, module replacement is possible to a certain extent.

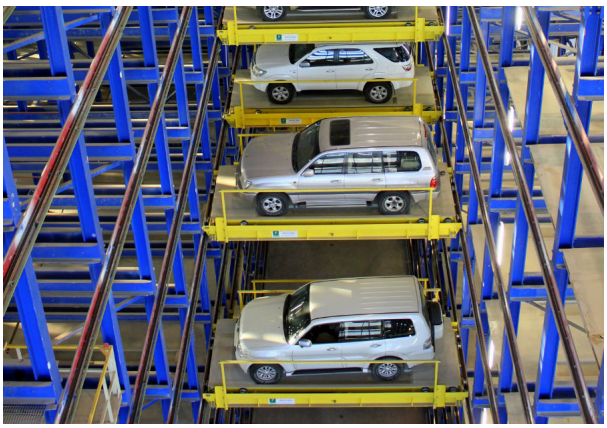

Figure 5.9: Al Jahra Court Automated Parking, Kuwait [65]

Lastly, as found in section 2.2, the dimensions of the modules should be chosen with care and are often limited by transportation regulations, rather than by hoisting (weight) limitations. In order to deal with this, a warning message has been programmed in the modular structure generator if the chosen module dimensions exceed the maximum allowable dimensions. The maximum dimensions differ locally and therefore can be changed.

5.3. 2D high-rise braced frame structure

First, the 2D high-rise braced frame structure from chapter 4 is considered. As it is a 2D model, the considered load cases are wind+vertical load from two directions as concluded in chapter 4. The parameters for this case and the 3D case considered in section 5.4 are listed in table 5.8. Additional results are presented in appendix A.4.1.

Input parameter	2D	3D
Dimension X [m]	3	3
Dimension Y [m]	3	3
Dimension Z [m]	3	3
Number of modules X-direction [-]	4	4
Number of modules in Y-direction [-]	N/A	4
Number of modules Z-direction [-]	40	40
Total building height [m]	120	120
Building dimension X-direction [m]	12	12
Building dimension Y-direction [m]	N/A	12
Corresponding wind load [kN/m^2]	1.85	1.85
Vertical load [kN/m^2]	10	10
N-parameter [-]	1	8

Table 5.8: Parameters for test cases

5.3.1. Results

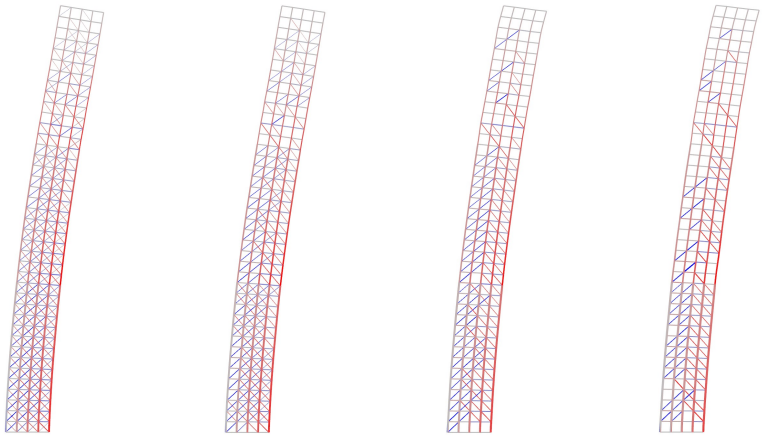

(a) (b) (c) (d)

Figure 5.10: Case study 2D high-rise braced frame at iteration 64, 128, 192 and 235 respectively (TR=0.8, 0.6, 0.4 and 0.27) for LC0

The results generally show an increase in structural weight as the number of diagonals decreases. The points where the structural weight jumps occur when the column dimension is changed. Due to standardization of column groups, all members are increased simultaneously. Due to this boundary condition, the placement of the diagonals is also somewhat influenced. It appears that around the transition from column groups at h/3 and 2h/3. more load is transferred to the underlying column groups through diagonals. This has to do with the fact that the underlying columns have larger dimensions and stiffness.

As columns and beams have considerable dimensions, part of the lateral load is also taken by rigid frame action as the columns are modelled as beam elements. Due to using the optimizer for multiple load cases, it is difficult to interprete the location of the diagonals. Generally it appears that the number of diagonals is higher in the lower segment of the building and decreases towards the top.

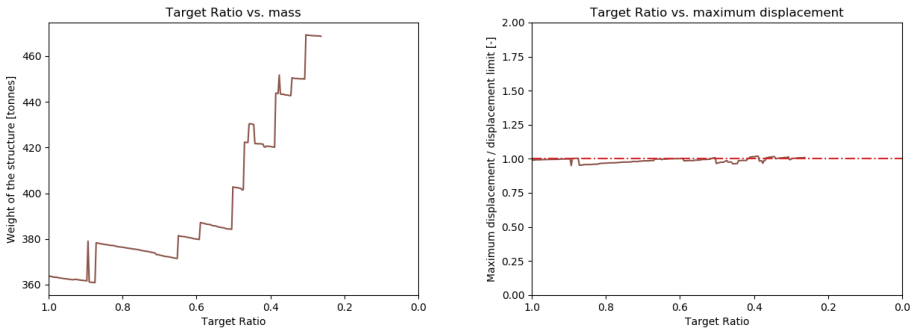

(a) (b)

Figure 5.11: Case study 2D high-rise braced frame, TR versus mass and displacement

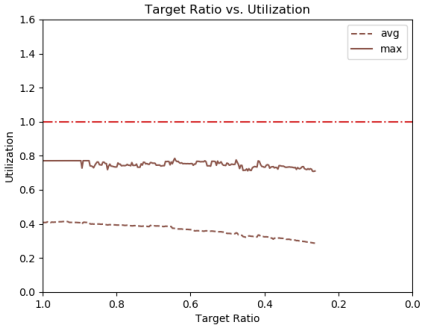

Figure 5.12: Case study 2D high-rise braced frame, TR versus utilization

5.3.2. Comparison with other structural systems

The result of the optimizer can be compared to conventional structural systems with the same number of diagonals. As shown in figure 2.3, typical structures for a 40-storey building are a framed-shear truss (core), belt-truss (outrigger) or truss-tubes (mega frame). These structures are considered and optimized with CS-optimization with similar boundary conditions (columns grouped, beams based on rules of thumb).

Core structure

	Coupled ESO<>CS (it. 160)	Core
col1	HD400x1202	HD400x1299
col2	HD400x509	HD400x1299
col3	HD260x225	HD400x1299
beams	HEA300	HEA300
Number of diagonals [-]	160	160
Total structural weight [tonnes]	402.8	937.0
Maximum displacement U.C.	0.97	2.16

Table 5.9: Coupled ESO<>CS versus core structure results

The coupled ESO<>CS method results in a structure which is more efficient than core structures. The core structure has a higher structural weight and the displacement condition is not met. Although the placement of diagonals seems somewhat arbitrary, the underlying principle of the method is clear and produces recognizable results for a single load case. With similar boundary conditions, the method provides a lighter structure and is therefore more efficient than the core structure, which has over double the weight. This mainly has to do with the internal lever arm which is very limited for a core structure.

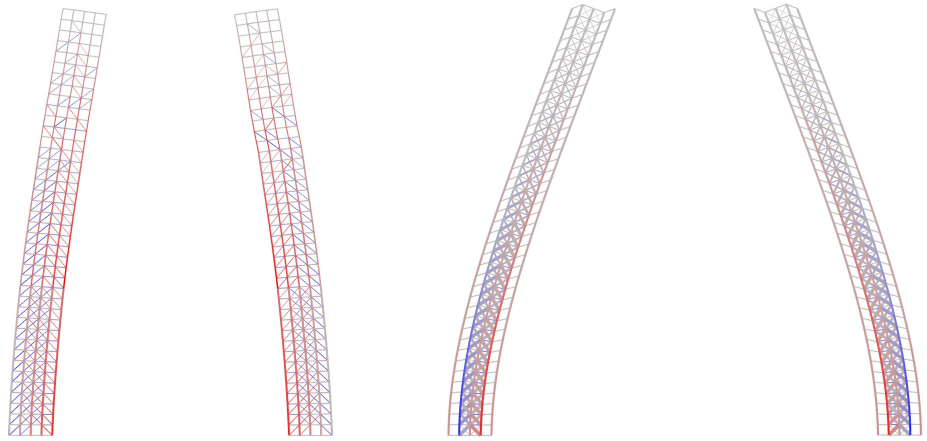

(a) (b) (c) (d)

Figure 5.13: Case study 2D high-rise braced frame at iteration 160 (TR=0.5, a,b) and core structure (c,d) for LC0 and LC1

Outrigger structure

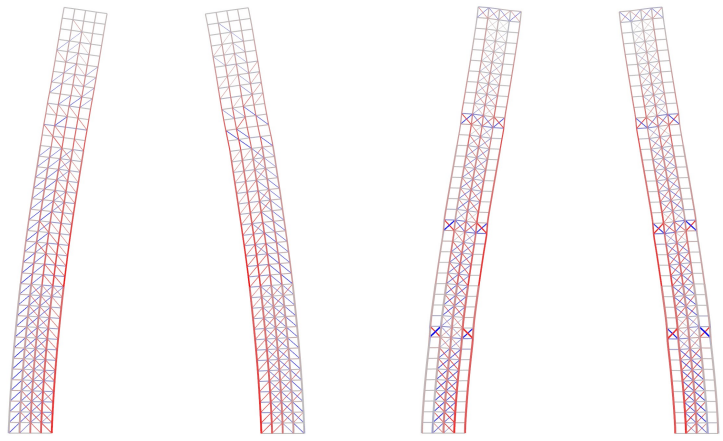

(a) (b) (c) (d)

Figure 5.14: Case study 2D high-rise braced frame at iteration 144 (TR=0.55, a,b) and outrigger structure (c,d) for LC0 and LC1

	Coupled ESO<>CS (it. 144)	Outrigger
col1	HD400x900	HD400x1202
col2	HD400x421	HD400x551
col3	HD260x225	HD260x299
beams	HEA300	HEA300
Number of diagonals [-]	176	176
Total structural weight [tonnes]	385.8	494.3
Maximum displacement U.C.	0.99	0.99

Table 5.10: Coupled ESO<>CS versus outrigger structure results

Adding outriggers to the core structure increases its efficiency. The outriggers increase the lever arm and therefore the structure is able to satisfy the boundary conditions for displacement (and utilization), while reducing the overall structural weight. However, with the same number of diagonals, the ESO<>CS optimized structure is still 22% lighter.

Mega frame structure

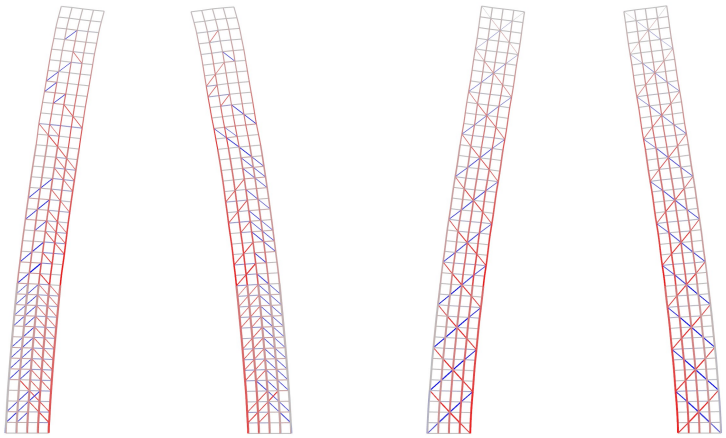

(a) (b) (c) (d)

Figure 5.15: Case study 2D high-rise braced frame at iteration 236 (TR=0.27, a,b) and mega frame structure (c,d) for LC0 and LC1

	Coupled ESO<>CS (it. 236)	Mega Frame
col1	HD400x1299	HD400x990
col2	HD400x463	HD400x509
col3	HD260x225	HD260x299
beams	HEA300	HEA300
Number of diagonals [-]	84	80
Total structural weight [tonnes]	468.8	431.6
Maximum displacement U.C.	1.01	0.96

Table 5.11: Coupled ESO<>CS versus mega frame structure results

Lastly, the ESO<>CS-optimized structure is compared with a mega frame. The ESO<>CS-optimization was terminated after 236 iterations which is the result that is compared to the mega frame, despite the slightly larger number of diagonals. The mega frame results in an 8% lower structural weight with 5% less diagonals, making it slightly more efficient than the ESO<>CS-optimized structure in terms of weight and number of diagonals.

5.4. 3D tower

In the 3D models, diaphragm action is added by including diagonals in the XY-plane which represent the floors. These diagonals initially do not participate in the ESO<>CS optimization and have similar dimensions to floor beams. The considered case has is a 12x12x120 rectangular box and its main parameters are listed in table 5.8. The case istherefore comparable with the 2D high-rise braced frame. Additional results for other load cases are presented in appendix A.4.2.

5.4.1. Results

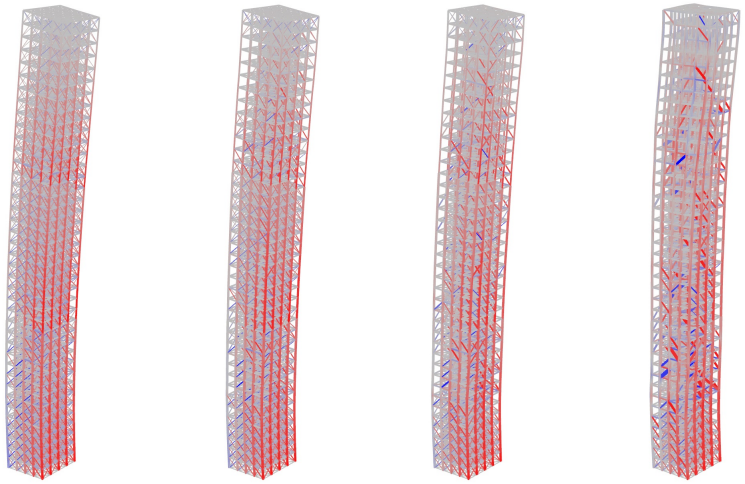

(a) (b) (c) (d)

Figure 5.16: Case study 3D tower at TR=0.8, 0.6, 0.4 and 0.19 for LC0

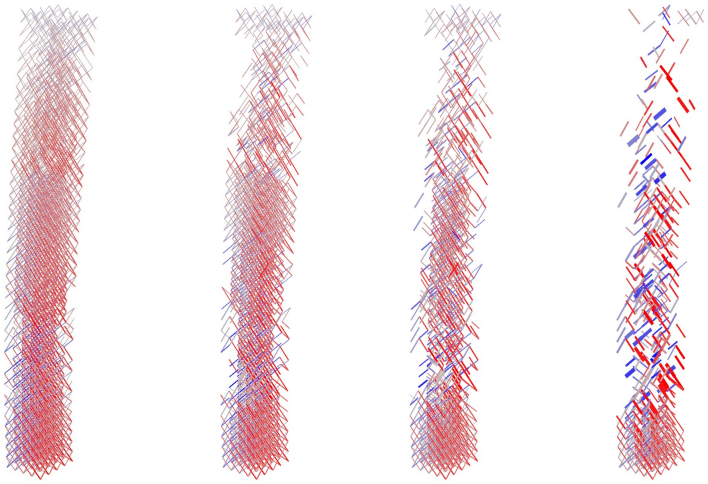

(a) (b) (c) (d)

Figure 5.17: Case study 3D tower at TR=0.8, 0.6, 0.4 and 0.19 for LC0 with diagonal view on

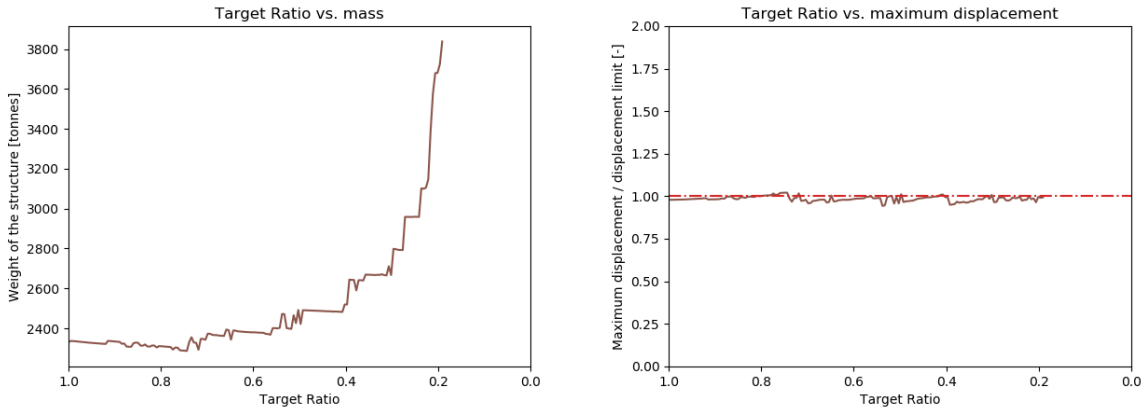

(a) (b)

Figure 5.18: Case study 3D tower, TR versus mass and displacement

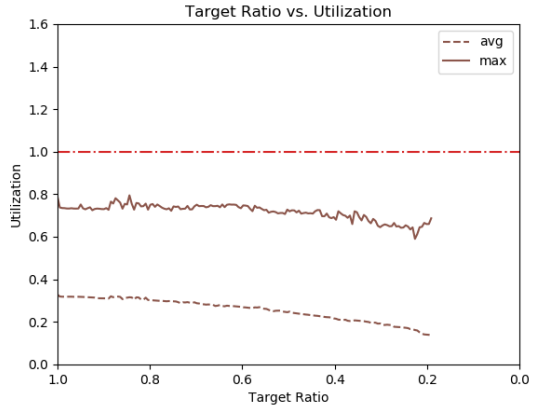

Figure 5.19: Case study 3D tower, TR versus utilization

It appears that again, the weight increases as TR decreases. There are less jumps in the graph than in the 2D case. The main reason for this is due to the fact that a change in the cross-section of a column group has less effect on the overall weight of the structure as there are relatively more diagonals and beams as displayed in table 5.12. Displacement is governing for all cases and the minimum structure weight is found at TR≈0.75, however differences in weight are small initially.

Element group	2D Braced Frame	3D Tower	Ratio 3D/2D
col1	70	350	5
col2	65	325	5
col3	65	325	5
diag	320	3200	10
beams	164	2952	18
total	684	7152	10.5

Table 5.12: Number of elements per group in 2D Braced Frame and 3D Tower at iteration 0

The results can be verified by checking the sum of the reaction forces at the support:

- The sum of vertical forces (Z-direction) should be equal to the number of storeys multiplied with the area and floor load: 40*(12*12)*10 = 5.76 * 10^4 kN.
- The sum of the horizontal forces in X- or Y-direction depending on load case should

be equal to the area multiplied with the wind pressure q_p which is (12*120)*1.85*1.5 = 4.005 * 10^4 kN.

- The force in the direction perpendicular to the wind direction considered in that load case must be zero.

	LC0	LC1	LC2	LC3
Sum forces X-direction [kN]	-7.61E-11	6.55E-11	-4.00E3	4.00E3
Sum forces Y-direction [kN]	-4.00E4	4.00E4	-1.38E-10	3.27E-11
Sum forces Z-direction [kN]	5.76E4	5.76E4	5.76E4	5.76E4

Table 5.13: Reaction forces at support 3D Tower

For all load cases, the sum of the reaction forces is approximately equal to the externally applied forces as listed in table 5.13. This validates that all modelled forces are transferred to the support.

5.4.2. Inclusion of floor diaphragms in CS-optimization

Generally there are more diagonals in the lower segment of the building. However it appears that the diagonals are placed on different axes or planes which is caused by the fact that diaphragm action is included. This way, the lateral force is free to transfer from one to another axis through the diagonals in the floor. This does not necessarily lead to the most efficient load path. In order to find a more efficient load path, it is opted to also include the floor diagonals in CS-optimization. This disallows a 'free' transfer of lateral force through different axes as floor diagonals must increase in size to accommodate the force transfer between axes. The floor diagonals cannot be removed and are only CS-optimized.

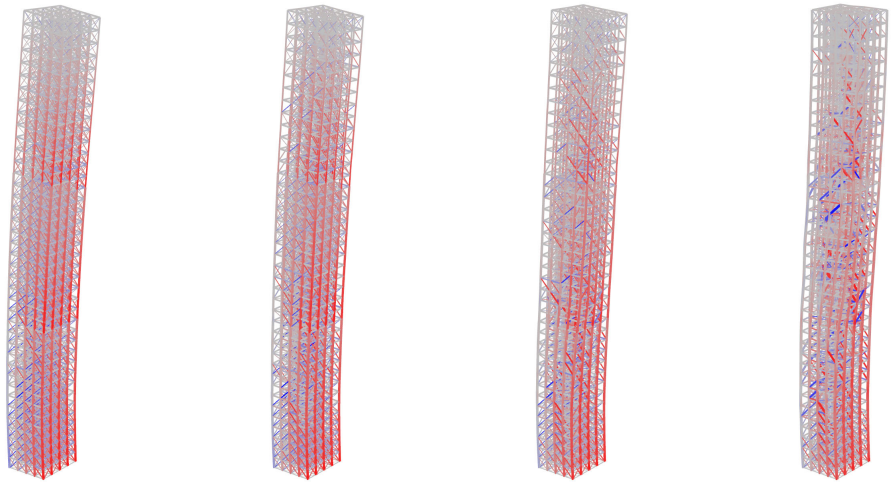

(a) (b) (c) (d)

Figure 5.20: Case study 3D tower with floors in CS-opt. at TR=0.8, 0.6, 0.4 and 0.2 for LC0

A similar exponential-like shape is observed in the TR/mass-graph. The curve seems to be a bit smoother which is caused by the fact that more elements are participating in CS-optimization and therefore a change of cross-section of an element group has a smaller impact. Again, displacement is governing. Including the floors diagonals in the CS-optimization results in a lower weight as the diagonals are now CS-optimized and no longer (over-)dimensioned by rules of thumb.

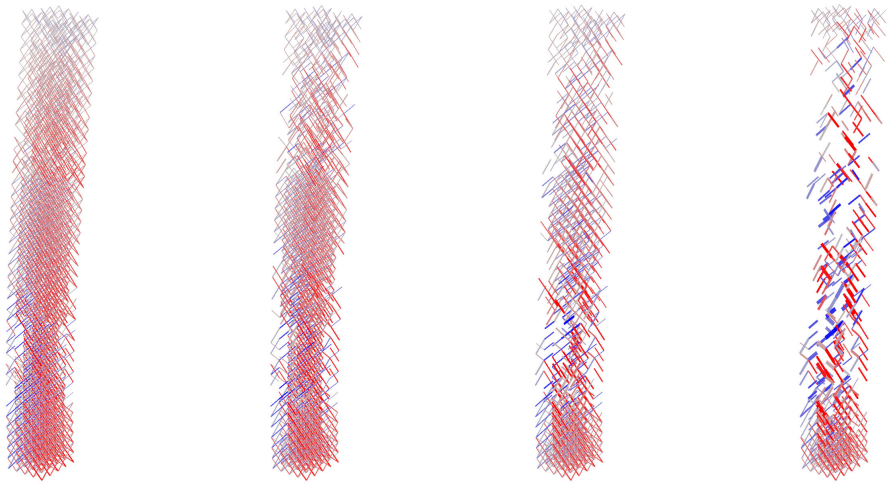

(a) (b) (c) (d)

Figure 5.21: Case study 3D tower with floors in CS-opt. at TR=0.8, 0.6, 0.4 and 0.2 for LC0 with diagonal view on

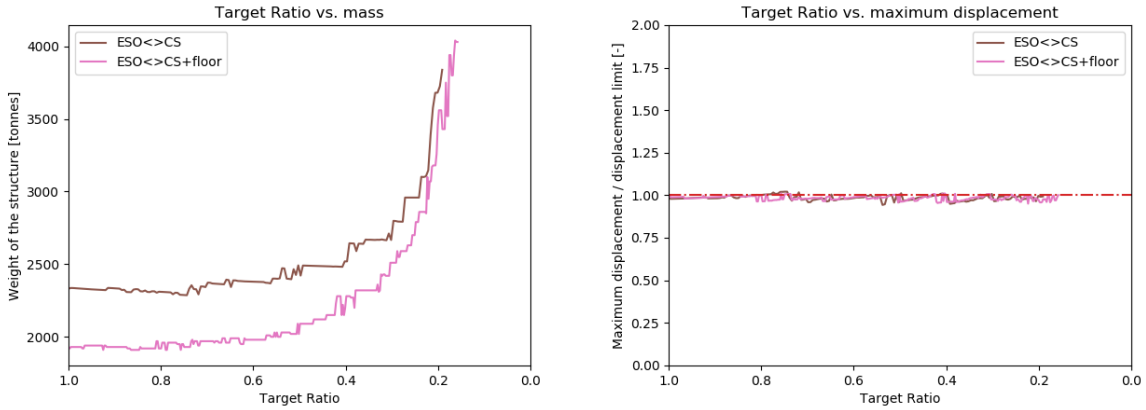

(a) (b)

Figure 5.22: Case study 3D tower with floors in CS-opt., TR versus mass and displacement

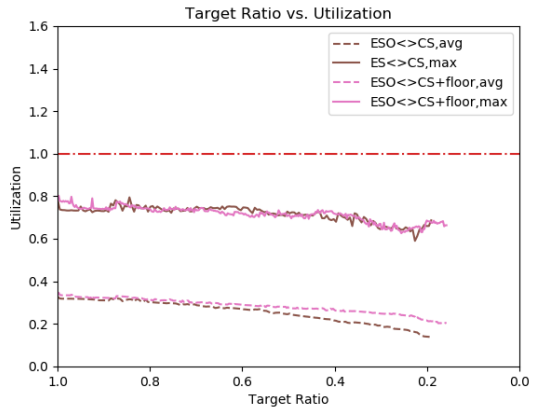

Figure 5.23: Case study 3D tower with floors in CS-opt., TR versus utilization

The placement of the diagonals seems a bit more logical as more diagonals are aligned. Lateral force is still able to move across different planes as there is still some diaphragm action. However, force moving from one plane to another now comes at the cost of increased material use in the floor diagonals. The reduction in structural weight is primarily due to the floor diagonals becoming smaller, however, as they cannot be removed, the floor diagonals will always allow some force transfer from one to another axis. The extent to which this happens is less than in the case with non-CS-optimized floor diagonals (which are generally larger in size) and therefore the lateral force tends to stay in the vertical bracing and columns (bending).

5.4.3. Comparison with other structural systems

Again, the structure is compared with conventional structural systems: core, outrigger and mega frame structures. Structures with same number of diagonals are considered in each comparison. The floor diagonals are included in the CS-optimization just as in subsection 5.4.2.

Core structure

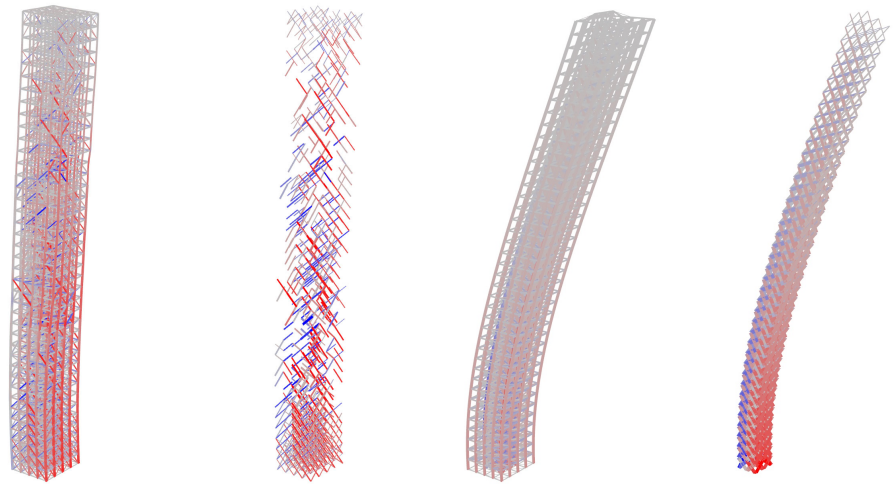

(a) (b) (c) (d)

Figure 5.24: Case study 3D tower (TR=0.3, a,b) and core structure (c,d) with diagonal view off and on for LC0

	Coupled ESO<>CS	Core
col1	HD400x900	HD400x1299
col2	HD400x551	HD400x1299
col3	HD260x299	HD400x1299
beams	HEA300	HEA300
Number of diagonals [-]	960	960
Total structural weight [tonnes]	2513.9	5452.2
Maximum displacement U.C.	0.97	2.73

Table 5.14: Coupled ESO<>CS versus core structure results (3D tower)

It is observed that the core structure does not satisfy the boundary condition for displacement and the cross-sections of the columns are increased to the largest available. The 3D tower however finds a solution with the same number of diagonals which is able to satisfy the boundary conditions with smaller cross-sections. This again likely has to do with the

lever arm which is limited for core structures. The core structure is therefore not a suitable structural system for this particular case.

Outrigger structure

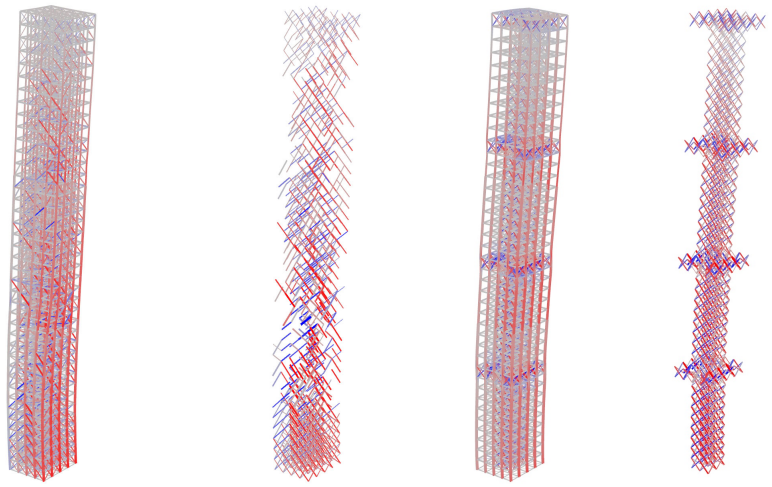

(a) (b) (c) (d)

Figure 5.25: Case study 3D tower (TR=0.37, a,b) and outrigger structure (c,d) with diagonal view off and on for LC0

	Coupled ESO<>CS	Outrigger
col1	HD400x818	HD400x1299
col2	HD400x509	HD400x634
col3	HD260x225	HD260x299
beams	HEA300	HEA300
Number of diagonals [-]	1184	1184
Total structural weight [tonnes]	2317.8	3012.5
Maximum displacement U.C.	0.97	0.99

Table 5.15: Coupled ESO<>CS versus outrigger structure results (3D tower)

The outrigger structure with four outriggers is able to satisfy the boundary condition for displacement and has a significantly lower weight than the core structure. Yet, the resulting structure from ESO<>CS-optimization with the same number of diagonals has a 23% lower weight and is therefore still more efficient. This result is very close to the 2D high-rise braced frame, in which this difference was 22%. The weight reduction is mainly due to the smaller column dimensions. Beams have the same dimensions in both cases and floor diaphragms and diagonals have relatively small contribution to the total structure weight compared to the columns.

Mega frame structure

Lastly, the mega frame structure is considered. Again, it is more efficient than the result of ESO<>CS-optimization. The optimization was terminated with 512 diagonals remaining as the CS-optimizer failed to meet its boundary conditions. This is more than the 230 diagonals of the megaframe structure, yet the mega frame structure results in a lower structural weight. The mega frame therefore is a much more efficient structure. This validates the principles of Halvorson and Warner [23] mentioned in chapter 2, as diagonals are loaded axially rather than by bending, while using the entire building width as lever arm. In the mega frame,

the diagonals are generally larger (mass of *diagonals* in mega frame is 20% higher) and are placed along the building perimeter which could make it visually more disturbing or increase connection complexity.

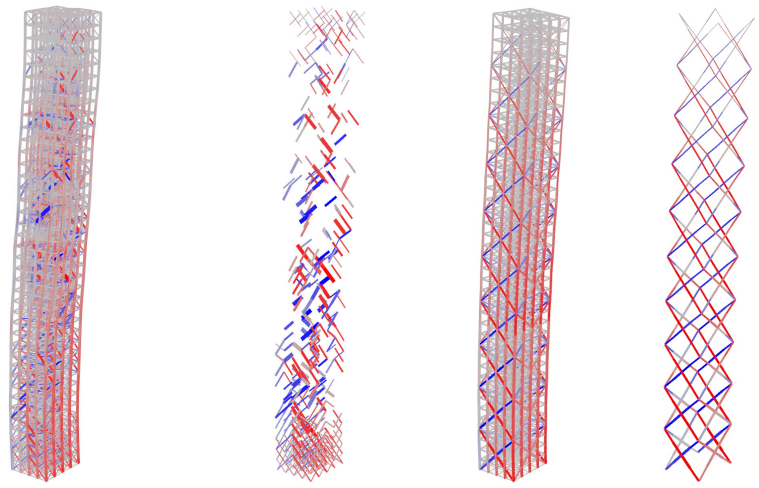

(a) (b) (c) (d)

Figure 5.26: Case study 3D tower (TR=0.16, a,b) and mega frame structure (c,d) with diagonal view off and on for LC0

	Coupled ESO<>CS	Mega frame
col1	HD400x1299	HD400x1086
col2	HD400x1299	HD400x509
col3	HD400x677	HD260x299
beams	HEA300	HEA300
Number of diagonals [-]	512	230
Total structural weight [tonnes]	4030.0	2597.8
Maximum displacement U.C.	1.00	0.97

Table 5.16: Coupled ESO<>CS versus mega frame structure results (3D tower)

If the ESO<>CS-result with more diagonals (e.g. same number as outrigger) is compared to the mega frame, the mega frame is about 12% heavier. Which structure is more optimal is again a trade-off between material and connection costs, but also placement of diagonals should be considered. In terms of absolute lowest mass, placing smaller diagonals almost everywhere (high TR) results in the lowest mass (27% lighter than mega frame) but a large number of connections. In cases with a lot of internal diagonals, internal separating walls could act as stabilizing elements and therefore be used more efficiently. These elements would then be less visible from the outside of the building.

5.5. Arbitrary shapes

For arbitrary shapes, the optimization principle works similar. Placement of diagonals in each module is not only effective for carrying lateral load, but also in structures with cantilevers. As desired, by using the script to generate a structural model and optimizing the structure using the coupled ESO<>CS method, any building geometry can quickly be translated to an optimized modular structural model. Naturally, the shape should resemble a (high-rise) building design and not be any arbitrary shape. The process from arbitrary shape to structural model is depicted in figure 5.27 and further elaborated in appendix B.2. The floor diagonals are also included in CS-optimization.

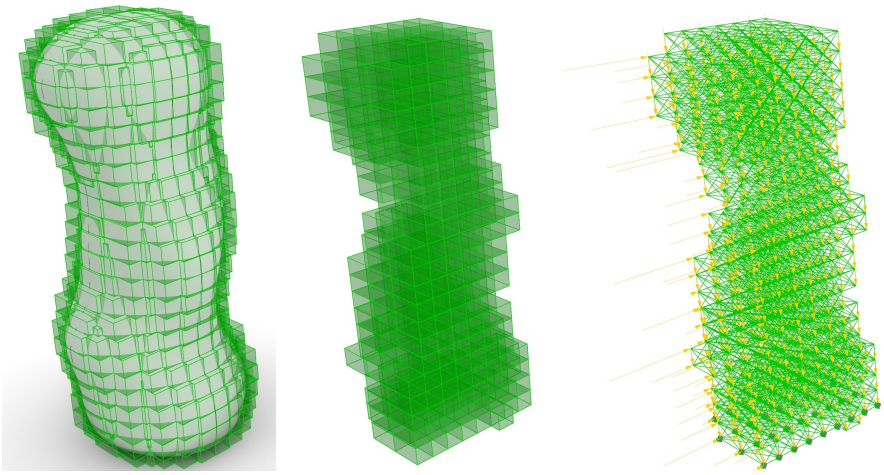

(a) (b) (c)

Figure 5.27: Procedure of geometry generation for arbitrary shape (one out of four load cases presented)

5.5.1. Results

The structural model is optimized for four load cases and the results for load case LC0 are presented below. Additional results are presented in appendix A.4.3, while the mass, displacement and utilization diagrams are for all load cases.

Input parameter	Value
Dimension X [m]	6
Dimension Y [m]	3
Dimension Z [m]	3
Total building height [m]	70.98
Corresponding wind load [kN/m^2]	1.61
Vertical load [kN/m^2]	10
N-parameter [-]	8

Table 5.17: Parameters for arbitrary shape

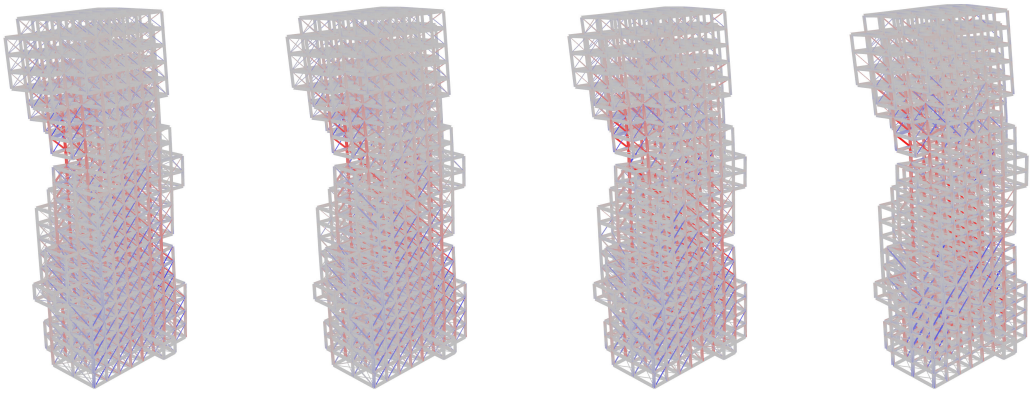

(a) (b) (c) (d)

Figure 5.28: Case study arbitrary shape at TR=0.8, 0.6, 0.4 and 0.17 for LC0

It appears that for this shape both utilization and displacement are close to the allowed limit for each TR. Initially, utilization is governing while at TR≈0.5, displacement becomes governing. Jumps in structural weight are again caused by changing cross-sections of a

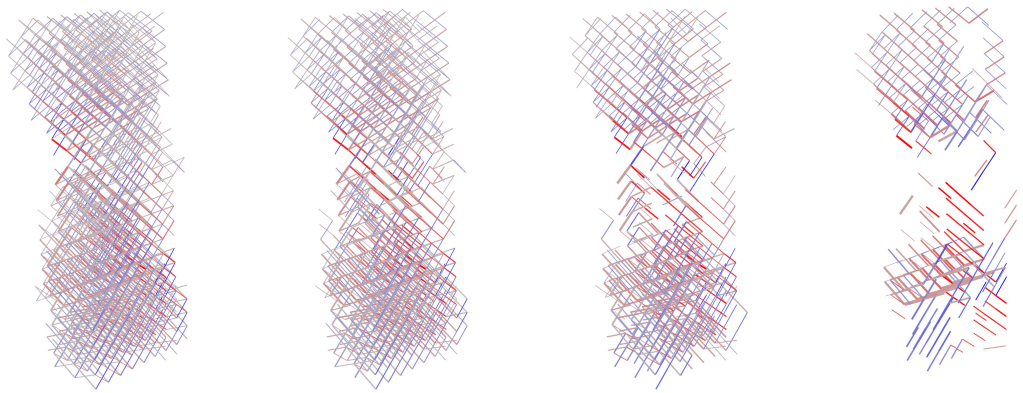

(a) (b) (c) (d)

Figure 5.29: Case study arbitrary shape at TR=0.8, 0.6, 0.4 and 0.17 for LC0 with diagonal view on

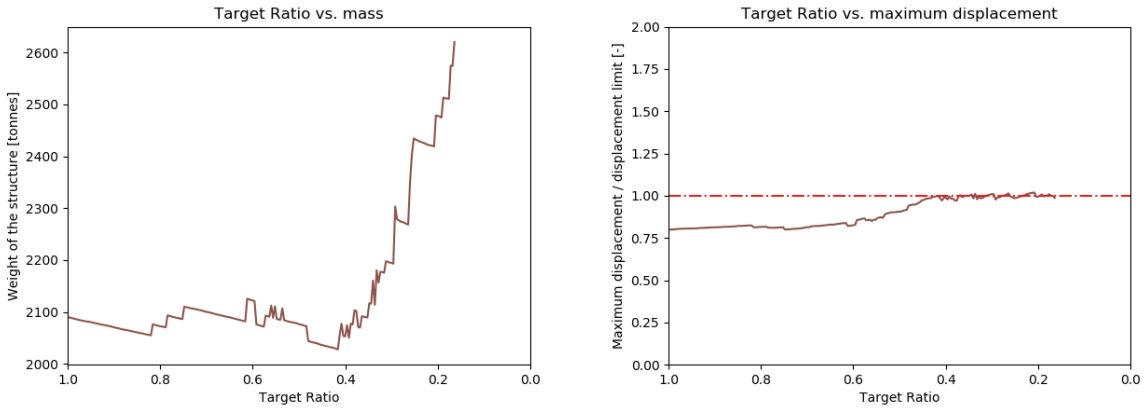

(a) (b)

Figure 5.30: Case study arbitrary shape, TR versus mass and displacement

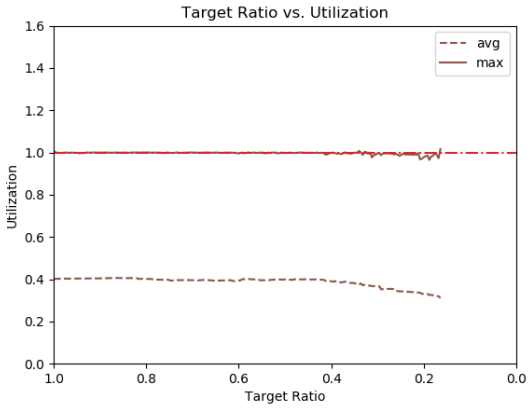

Figure 5.31: Case study arbitrary shape, TR versus utilization

column group. The structure with the minimum weight is found at a TR of 0.4. In arbitrary shapes the ESO<>CS-optimization method proves its worth as a structural design is generated with very little effort. In this case, it would be more time consuming to draw a conventional structure such as a core, outrigger or mega frame.

5.6. Discussion

Both in 2D and 3D, ESO<>CS-optimization with an initial design space with diagonals in each module results in a range of structural models in which the weight generally increases as number of diagonals (TR) decreases. The modular structure generator successfully transforms arbitrary shapes into a modular structure with the specified module dimensions, after which ESO<>CS-optimization can be carried out.

In the 2D high-rise frame structure, the ESO<>CS-optimized structure is more efficient than core and outrigger structures with the same number of diagonals, but less efficient than the mega frame structure.

Diaphragm action is included in the 3D models by including diagonals in the horizontal plane. Including these diagonals results in a force transfer from one axis to another. Therefore, these diagonals are taken into account in CS-optimization, resulting in a somewhat more logical load path with more diagonals on the same axis. However, part of the load is still able to transfer from one axis to another. A possible way to prevent this would be to include the floor diagonals in the ESO-part of the ESO<>CS-optimization as well. This would however greatly increase the number of iterations as there are much more diagonals to remove. At the same time, material saving in this part of the structure may be questionable as lateral force distribution in high-rise buildings usually happens through the floors which have a great lateral stiffness, while floor design often depends on other factors such as (sound) insulation and functional use.

A limitation of the optimization procedure is practicality due to the duration of the optimization. This strongly depends on the number of elements and iterations, however some of the optimizations took over 16 hours to complete using a modern workstation laptop, which is much longer than desired. Furthermore, the modular structure generator is limited to corner-supported steel modules built up from beam and truss elements. This is a design choice, but in order to increase applicability of the modular structure generator, considering four-sided (steel) modules and precast concrete modules would be desirable.

6

Conclusions and recommendations

6.1. Conclusions

The main question regarded in this research was:

> **How can the optimal structural design of any high-rise building with standardized corner-supported modules be generated and optimized?**

This question has been answered by creating a script which generates a structural model which is built up from corner-supported modules and includes diagonals in all vertical planes as design space for the lateral load-bearing system. Subsequently, the structural system is optimized using the coupled ESO<>CS method which removes unneccessary elements from the design space while optimizing the cross-sections of the remaining members, within given constraints. This eventually results in a range of solutions which differ in weight and number of elements, from which an optimum could be found by post-processing the solutions and putting weighing factors such as cost per connection and kilogram of material use. As the script works for any shape, it is a useful contribution to the early design stage of modular high-rise structures.

The most important conclusions are the following:

- Cross-section optimization and BESO for beams are both powerful tools for structural size and topology optimization. Applied separately, CS-optimization is more effective in saving weight in (high-rise) frame structures, however applying them successively (first BESO for beams, then CS-optimization) saves additional weight at some Target Ratios.
- The coupled ESO<>CS-method is especially more effective than the existing BESO>CS-method in stiffness problems, which is the case in most high-rise buildings. This is mainly caused by implicitly updating the cross-sections in each iteration which creates a positive feedback loop in which more force is taken by the heavily loaded members in each iteration. The removal of elements is based on lowest strain energy density, which is proportionate to the axial stress when truss elements are used.
- The number of elements removed per iteration (N-value) should be kept as low as possible. This leads to the most accurate results, but also to the greatest iteration time which is especially more inconvenient in larger structural models.
- By specifying boundary conditions such as standardized column and beam dimensions, practical solutions for modular construction are found. This does not necessarily lead to the structure with the lowest weight or least number of elements, but allows standardization of modules. Diagonals should be able to carry tension and compression as wind direction can change.

- Designing for multiple load cases simultaneously generally gives solutions in which the placement of the diagonals looks somewhat arbitrary and generally less diagonals can be removed while satisfying the verification criteria. This is also the case with existing topology optimization tools such as BESO2D [51] and BESO for beams. Also, all considered load cases are realistic design scenarios which should be considered and verified.

- The 2D cases and 3D cases considered show similar results, in which the structural weight generally increases as members are removed, however there are some local decreases in structural weight. The effect of an increase in cross-section of an element (column) group is larger in 2D cases as there are relatively more columns. This results in a more inconsistent graph.

- Including floor diagonals which provide diaphragm action in the CS-optimization results in more diagonals on the same axes as transfer of force to another axis comes at the cost of adding material in floor diagonals.

- For the rectangular towers considered in 2D and 3D, a core structure does not satisfy, while the ESO<>CS-optimization results in a 23% lighter structure than an outrigger structure with the same number of diagonals. A mega frame is even more efficient and has less diagonals than the structures found with ESO<>CS-optimization.

- ESO<>CS-optimization finds multiple results under which also results with lower structural weight than mega frames. This however comes at the cost of adding diagonals.

- Any shape which resembles a building can be translated into a modular volumetric structural model. Structures with cantilevers can also be analyzed as the diagonals in the vertical plane can transfer the vertical forces induced by cantilevers. Therefore ESO<>CS-optimization is especially relevant in cases where it is difficult and time consuming to draw 'conventional' structures.

6.2. Recommendations

Recommendations for further studies are:

- It is recommended to find a way to speed up the optimization procedure. Especially when the value for N is kept low, iteration time can take up to hours or even days.

- Assuming a different design space as input for the analysis. By intelligently choosing the design space, more efficient solutions might be found. An example could be to place diagonals only around the facade which creates the largest lever arm.

- Considering different building materials such as timber and concrete could lead to more sustainable structures but brings different challenges such as placement of reinforcement.

- Extending the method so that not only 1D (beam or truss) elements can be used, but also 2D elements which would represent walls, while varying the thickness of the walls. This way, a lateral bracing system with combined shear walls and lateral bracing can be designed.

- Using 2D elements to consider other modules than corner-supported modules with diagonal bracing. Examples are four-sided steel modules or precast concrete modules.

- In a more extreme case, experimenting with modules other than rectangular-shaped modules may lead to innovative designs. This would lead to optimization of individual modules rather than optimization of the structure as a whole, in which standardized modules are placed.

- As only the early design stage is considered, relatively strict boundary conditions are set. The model could be made more advanced and so that it will be able to produce not only early designs but also preliminary and more detailed designs, with corresponding boundary conditions.
- The method could be extended to an implicit BESO<>CS-optimization procedure, in which members can be added again. This could lead to additional material saving.
- By considering other boundary conditions, the coupled ESO<>CS-method is not only applicable for modular high-rise structures, but also in other optimization problems. More generally, combination of topology, size and shape optimization methods can lead to new methods which could lead to better optimization procedures for specific applications.
- The next step in producing a feasible modular construction concept would be to design the modules, including interior finishing and installations.

List of Figures

List of Tables

Bibliography

[1] United Nations. 68 percent of the world population projected to live in urban areas by 2050, says un | un desa department of economic and social affairs. URL https://www.un.org/development/desa/en/news/population/2018-revision-of-world-urbanization-prospects.html.

[2] Madeline Buijs and Casper Wolf. Bouwsector in rustiger vaarwater, May 2019. URL https://insights.abnamro.nl/2019/04/bouwsector-in-rustiger-vaarwater/.

[3] Andrei Girbacea. Assessment of demountable steel-concrete composite flooring systems. Master's thesis, Delft University of Technology, 2018. URL http://resolver.tudelft.nl/uuid:7ffa31ea-e903-46e4-87fb-a00c76a04799.

[4] JYR Liew, YS Chua, and Z Dai. Steel concrete composite systems for modular construction of high-rise buildings. In *Structures*. Elsevier, 2019.

[5] Hermes. Firms lauded for adopting new building methods, June 2017. URL https://www.straitstimes.com/singapore/firms-lauded-for-adopting-new-building-methods.

[6] Lloyd Alter. What went wrong: The story behind the Atlantic Yards prefab tower. URL https://www.treehugger.com/modular-design/what-went-wrong-story-behind-atlantic-yards-prefab-tower.html.

[7] Elena M Generalova, Viktor P Generalov, and Anna A Kuznetsova. Modular buildings in modern construction. *Procedia engineering*, 153:167–172, 2016.

[8] Geoff Craighead. High-rise building definition, development, and use. *High-Rise Security and Fire Life Safety*, page 1–26, 2009. doi: 10.1016/b978-1-85617-555-5.00001-8.

[9] Designing Buildings Wiki. High-rise building - designing buildings wiki. URL https://www.designingbuildings.co.uk/wiki/High-rise_building.

[10] Dan Cortese. What is a skyscraper. URL https://www.theb1m.com/video/what-is-a-skyscraper.

[11] CTBUH. CTBUH Height Criteria | Council on Tall Buildings and Urban Habitat. URL https://www.ctbuh.org/criteria/.

[12] by. Development History of High-rise Buildings, January 2017. URL http://www.civilengineeringforum.me/development-high-rise-buildings/.

[13] Eric Jaffe. New York and Chicago's Century-Old Skyscraper Contest. URL http://www.theatlanticcities.com/jobs-and-economy/2013/08/new-york-and-chicagos-century-old-skyscraper-contest/6391/.

[14] New World Encyclopedia. Skyscraper - New World Encyclopedia. URL https://www.newworldencyclopedia.org/entry/Skyscraper.

[15] Wim Langejan. Ontwikkelaar: 'Hoger bouwen dan de Dom is 'een dingetje', maar op deze plek kan het', December 2018. URL https://www.ad.nl/utrecht/ontwikkelaar-hoger-bouwen-dan-de-dom-is-een-dingetje-maar-op-deze-plek/-kan-het~a6a7eb5f/.

[16] SS Bhavikatti. *Basic Civil Engineering, New Age, 2010: Basic Civil Engineering*, volume 1. Bukupedia, 2010.

[17] F.A.M. Soons, B.P.M. van Raaij, Wagemans L.A.G., S. Pasterkamp, and S.H.J. van Es. *Quick Reference*. Section Structural and Building Engineering Delft, 2014.

[18] Lilly Cao. Could Tall Wood Construction Be the Future of High-Rise Buildings?, September 2019. URL https://www.archdaily.com/924341/could-tall-wood-construction-be-the-future-of-high-rise-buildings.

[19] TU Delft. High-rise timber buildings, . URL https://www.tudelft.nl/citg/over-faculteit/afdelingen/engineering-structures/sections-labs/biobased-structures-and-materials/research/high-rise-timber-buildings/.

[20] India Block. World's tallest modular tower is now Clement Canopy in Singapore, July 2019. URL https://www.dezeen.com/2019/07/02/clement-canopy-worlds-tallest-modular-tower-bouygues/.

[21] Mir M. Ali and Kyoung Sun Moon. Advances in Structural Systems for Tall Buildings: Emerging Developments for Contemporary Urban Giants. *Buildings*, 8(8):104, August 2018. doi: 10.3390/buildings8080104. URL https://www.mdpi.com/2075-5309/8/8/104.

[22] Jack Sommer and Katie Warren. The 22 tallest buildings in the world right now, ranked, April 2019. URL https://www.businessinsider.com/the-tallest-buildings-in-the-world-2015-12.

[23] Robert Halvorson and Carrie Warner. Structural design innovation: russia tower. *The Structural Design of Tall and Special Buildings*, 16(4):377–399, 2007.

[24] R. Abspoel. *Building Structures 2 CIE4281 Steel Part*. 04 2013.

[25] P.H. Ham and year = 2017-month = 04 pages = title = Structural calculations of High Rise Structures Terwel, K.C.|.

[26] The Skyscraper Center. The Skyscraper Center. URL http://www.skyscrapercenter.com/.

[27] Sander van Eerden. Hoogtepunt voor binnenstedelijke woningbouw, 2019. URL https://www.cementonline.nl/hoogtepunt_voor_binnenstedelijke_woningbouw?file=1510235369.2239.pdf.

[28] TU Delft. *Concrete Building Structures reader CIE3340/CIE4281*. 11 2016.

[29] Andrew William Lacey, Wensu Chen, Hong Hao, and Kaiming Bi. Structural response of modular buildings–an overview. *Journal of Building Engineering*, 16:45–56, 2018.

[30] Mark Lawson, Ray Ogden, and Chris Goodier. *Design in modular construction*. CRC Press, 2014.

[31] Doyoon Kim. *Preliminary Life Cycle Analysis of Modular and Conventional Housing in Benton Harbor, MI*. PhD thesis, 2008.

[32] Mohammad Kamali and Kasun Hewage. Life cycle performance of modular buildings: A critical review. *Renewable and sustainable energy reviews*, 62:1171–1183, 2016.

[33] Khaled M Amtered El-Abidi and Farid Ezanee Mohamed Ghazali. Motivations and limitations of prefabricated building: An overview. In *Applied Mechanics and Materials*, volume 802, pages 668–675. Trans Tech Publ, 2015.

[34] Martens Transport. Vergunningen en ontheffingen | Martens Transport Oosterhout b.v. URL https://martenstransport.nl/exceptioneel_transport/vergunningen.

[35] Evofenedex. Eén ontheffing voor exceptioneel vervoer. URL https://www.evofenedex.nl/kennis/actualiteiten/een-ontheffing-voor-exceptioneel-vervoer.

[36] Gemeente Rotterdam. Exceptioneel transport in rotterdam. URL https://www.rotterdam.nl/loket/documentenkcc/infobladExceptioneelTransport.pdf.

[37] Liebherr. LTM mobile cranes - Liebherr. URL https://www.liebherr.com/en/int/products/mobile-and-crawler-cranes/mobile-cranes/ltm-mobile-cranes/ltm-mobile-cranes.html?page=3.

[38] R Mark Lawson, Ray G Ogden, and Rory Bergin. Application of modular construction in high-rise buildings. *Journal of architectural engineering*, 18(2):148–154, 2011.

[39] Marco Villares. Farewell spaceboxes. URL https://www.delta.tudelft.nl/article/farewell-spaceboxes.

[40] River Beech Tower, Supertall Elevator Maintenance, Talking Tall, Modular High-Rise, In Numbers, and Tall Timber-A Global Audit. Ctbuh journal.

[41] HTA. HTA Design - 101 George Street. URL https://www.hta.co.uk/project/101-george-street.

[42] BCA. Prefabricated Prefinished Volumetric Construction (PPVC). URL https://www.bca.gov.sg/BuildableDesign/ppvc.html.

[43] "Clement Canopy is the first structure on the isl and to use an all-concrete version of the Prefabricated Prefinished Volumetric Construction system.". Two 40-Story Towers Completed in Singapore | Council on Tall Buildings and Urban Habitat. URL https://www.ctbuh.org/news/two-40-story-towers-completed-in-singapore/.

[44] Nikkei Asian. Singapore's prefab condo tower is the next big thing. URL https://asia.nikkei.com/Business/Singapore-s-prefab-condo-tower-is-the-next-big-thing.

[45] Yie Sue Chua, Jat Yuen Richard Liew, and Sze Dai Pang. Robustness of prefabricated prefinished volumetric construction (ppvc) high-rise building. In *Proceedings of the 12th International Conference on Advances in Steel-Concrete Composite Structures. ASCCS 2018*, pages 913–919. Editorial Universitat Politècnica de València, 2018.

[46] Raphael T Haftka and Zafer Gürdal. *Elements of structural optimization*, volume 11. Springer Science & Business Media, 2012.

[47] Matteo Bruggi and Alberto Taliercio. Topology optimization for the development of eco-efficient masonry units. In *Eco-Efficient Masonry Bricks and Blocks*, pages 425–445. Elsevier, 2015.

[48] RYAN Johan, MICHAEL CHERNYAVSKY, ALESSANDRA FABBRI, NICOLE GARDNER, M HANK HAEUSLER, and YANNIS ZAVOLEAS. Building intelligence through generative design.

[49] Juan Pablo Leiva. Structural optimization methods and techniques to design efficient car bodies. *Vanderplaats Research and Development, Inc*, 2011.

[50] Prashant Kumar Srivastava, Simant, and Sanjay Shukla. Structural optimization methods: A general review. *International Journal of Innovative Research in Science, Engineering and Technology*, 6, 2017.

[51] Mike Xie and Xiaodong Huang. *Evolutionary topology optimization of continuum structures: methods and applications*. John Wiley & Sons, 2010.

[52] Lennert van der Linden. Parametric design and engineering: Introduction, 2019.

[53] Chara Ch Mitropoulou, Yiannis Fourkiotis, Nikos D Lagaros, and Matthew G Karlaftis. 4 evolution strategies-based metaheuristics in structural design optimization. In *Metaheuristic Applications in Structures and Infrastructures*, pages 79–102. Elsevier, 2013.

[54] Simulia. Topology and shape optimization with abaqus. October 2011.

[55] F Cucinotta, E Guglielmino, G Longo, G Risitano, D Santonocito, and F Sfravara. Topology optimization additive manufacturing-oriented for a biomedical application. In *Advances on Mechanics, Design Engineering and Manufacturing II*, pages 184–193. Springer, 2019.

[56] Pasi Tanskanen. The evolutionary structural optimization method: theoretical aspects. *Computer methods in applied mechanics and engineering*, 191(47-48):5485–5498, 2002.

[57] Virginia Young, Osvaldo M Querin, GP Steven, and YM Xie. 3d and multiple load case bi-directional evolutionary structural optimization (beso). *Structural optimization*, 18(2-3): 183–192, 1999.

[58] A Aremu, I Ashcroft, R Hague, R Wildman, and C Tuck. Suitability of simp and beso topology optimization algorithms for additive manufacture. In *21st Annual International Solid Freeform Fabrication Symposium (SFF)–An Additive Manufacturing Conference*, pages 679–692, 2010.

[59] C Preisinger. Karamba user manual for version 1.3.2, 2019.

[60] Arash Radman. Bi-directional evolutionary structural optimization (beso) for topology optimization of material's microstructure. 2013.

[61] TU Delft. Vuistregels voor het ontwerpen van een draagconstructie, 2013. URL `http://wiki.bk.tudelft.nl/mw_bk-wiki/images/1/12/Vuistregels.pdf`.

[62] PRSRT STD. Metals in construction. 2010.

[63] Bracing systems. URL `https://www.steelconstruction.info/Bracing_systems`.

[64] T Vrouwenvelder and H Steenbergen. Implementation of eurocodes: Handbook 3—actions effects for buildings-chapter 3: Wind actions. *Leonardo Da Vinci Pilot Project*, 2005.

[65] 2020. URL `http://leedsliving.co.uk/city-living/who-in-the-world-has-the-coolest-car-park/attachment/al-jahra-court-robotic-parking-system/`.

[66] Shiro Yoshida. Michell truss: Shape optimization vs. analytical solution.

[67] Graham Knapp. dancergraham/eurocode. URL `https://github.com/dancergraham/eurocode/blob/master/ec1.py`.

[68] Arie Willem De Jongh. Brep plane split component. URL `https://www.grasshopper3d.com/forum/topics/brep-plane-split-component`.

A

Optimization study results

A.1. BESO for beams (cantilever beam)

A handy plugin which is used for topology optimization of beam elements is BESO for beams. As mentioned in chapter 3, the component removes least strained elements from the model until a TR is reached. Below is an example of the BESO for beams component for a cantilever beam loaded by a point load at the edge. Truss elements have been used.

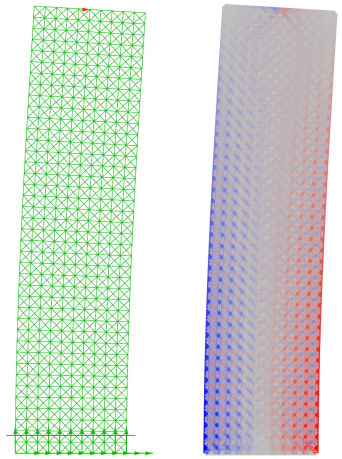

(a) (b)

Figure A.1: Cantilever beam model (a) and initial analysis (b)

Dimension X [m]	2.5
Dimension Z [m]	10
Number of segments X-direction [-]	10
Number of segments Z-direction [-]	40
Load [kN]	50
Cross-section	HEA100

Table A.1: Initial parameters test cases mid-rise and high-rise

This result can be compared to a Michell truss such as presented in figure A.3. It appears that BESO for beams results in a different shape, however there are some similarities. In both cases, there is more material at the supports, which decreases towards the top. Also, similar tension and compression lines are observed (colours for tension and compression are reversed in figure A.3).

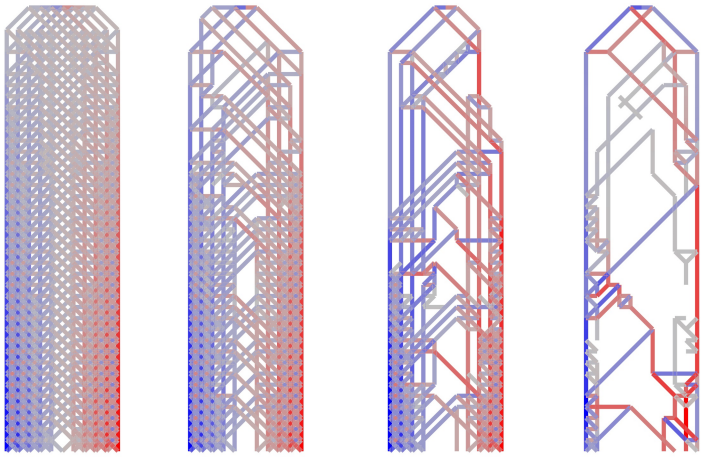

(a) (b) (c) (d)

Figure A.2: Cantilever beam after BESO for beams at TR=0.8, 0.6, 0.4 and 0.2 (deformation scale off)

This suggests that BESO for beams may not lead to the optimal solution as defined by Michell. A further study on optimization techniques has been performed in chapter 3 and 4 using various methods including BESO for beams, CS-, BESO>CS- and two-way coupled ESO<>CS-optimization.

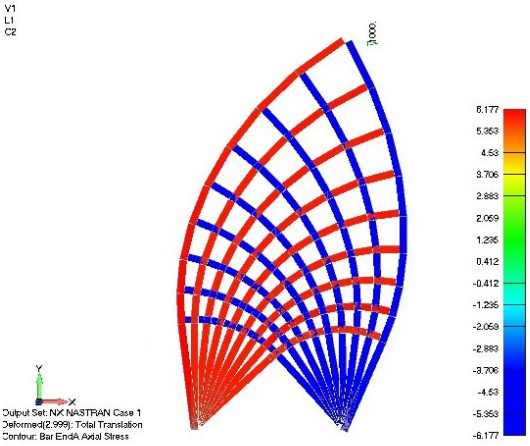

Figure A.3: Michell truss [66]

A.2. List of cross-sections

The list of cross-sections the cross-section optimizer can choose from is shown below. Only cross-sections with the same family attribute as the initial cross-section can be chosen.

IPE	HEAA	HEA	HEB	HEM	HL	HD	HP	I
80	100	100	100	100	920x344	260x54.1	200x43	80
100	120	120	120	120	920x368	260x68.2	200x53	100
120	140	140	140	140	920x390	260x93.0	220x57	120
140	160	160	160	160	920x420	260x114	260x75	140
160	180	180	180	180	920x449	260x142	260x87	160
180	200	200	200	200	920x491	260x172	305x79	180
200	220	220	220	220	920x537	320x74.2	305x88	200
220	240	240	240	240	920x588	260x225	320x88	220
240	260	260	260	260	1000AA	320x97.6	305x95	240
270	280	280	280	280	920x656	320x127	320x103	260
300	300	300	300	300	1000A	320x158	305x110	280
330	320	320	320	320	920x725	260x299	320x117	300
360	340	340	340	340	1000B	320x198	305x126	320
400	360	360	360	360	1000M	360x134	305x149	340
450	400	400	400	400	920x787	320x245	320x147	360
500	450	450	450	450	1000x443	360x147	305x180	380
550	500	500	500	500	1000x483	360x162	305x186	400
600	550	550	550	550	1000x539	360x179	320x184	425
	600	600	600	600	1000x554	400x187	305x223	450
	650	650	650	650	1000x591	360x196	360x109	475
	700	700	700	700	920x970	400x216	400x122	500
	800	800	800	800	1000x642	320x300	360x133	550
	900	900	900	900	920x1077	400x237	400x140	600
	1000	1000	1000	1000	1000x748	400x262	400x158	
					920x1194	400x287	360x152	
					1100A	400x314	400x176	
					1000x883	400x347	360x174	
					920x1269	400x382	360x180	
					920x1377	400x421	400x194	
					1100B	400x463	400x213	
					1100M	400x509	400x231	
					1000x976	400x551		
					1100R	400x592		
						400x634		
						400x677		
						400x744		
						400x818		
						400x900		
						400x990		
						400x1086		
						400x1202		
						400x1299		

Table A.2: Cross-section list in cross-section optimizer

A.3. BESO>CS-optimization results

This section includes additional results from the cases considered in chapter 3. The cases considered are similar however the initially chosen cross-sections differ.

A.3.1. Braced frame structure (wind load)

Cross-section 2

This case includes the same structure with the same loads as considered in chapter 3, but only with different initial cross-sections to check the influence of the starting point of each optimization method and thus the stability of the solutions.

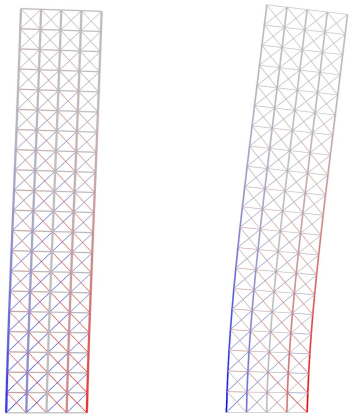

(a) (b)

Figure A.4: Braced frame under wind load, before (a) and after (b) CS-optimization

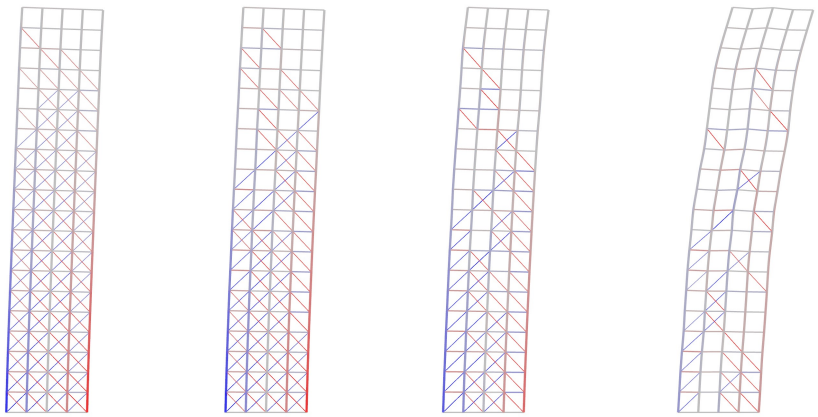

(a) (b) (c) (d)

Figure A.5: Braced frame under wind load after BESO, TR=0.8, 0.6, 0.4 and 0.2 respectively

The plots of TR versus the mass and displacement give more or less similar results. It seems that BESO results in lower weight of the structure, which is logic as the initial starting weight is also lower. For BESO>CS, more or less the same curve is obtained for both the mass and displacement, with a minimum structure weight at a target ratio of approximately 0.4. At low TR, the displacement for BESO exceeds the limit excessively.

The utilization graph shows approximately similar results, with the average and maximum utilization decreasing for BESO>CS and increasing for BESO only. Similarly to the maximum

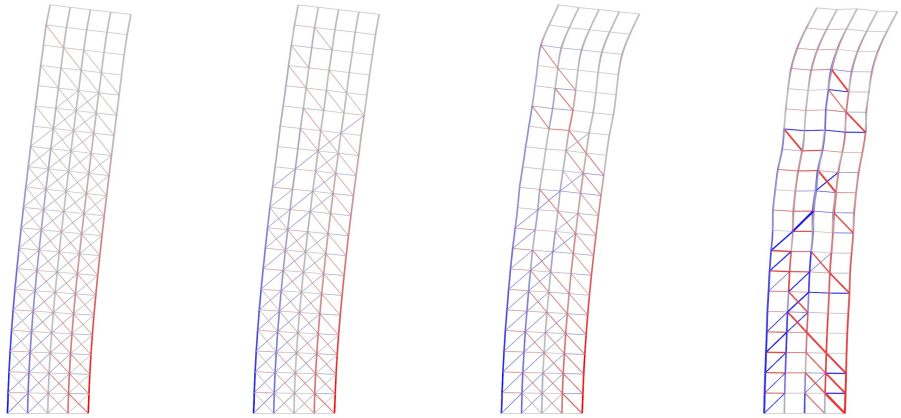

(a) (b) (c) (d)

Figure A.6: Braced frame under wind load after BESO>CS, TR=0.8, 0.6, 0.4 and 0.2 respectively

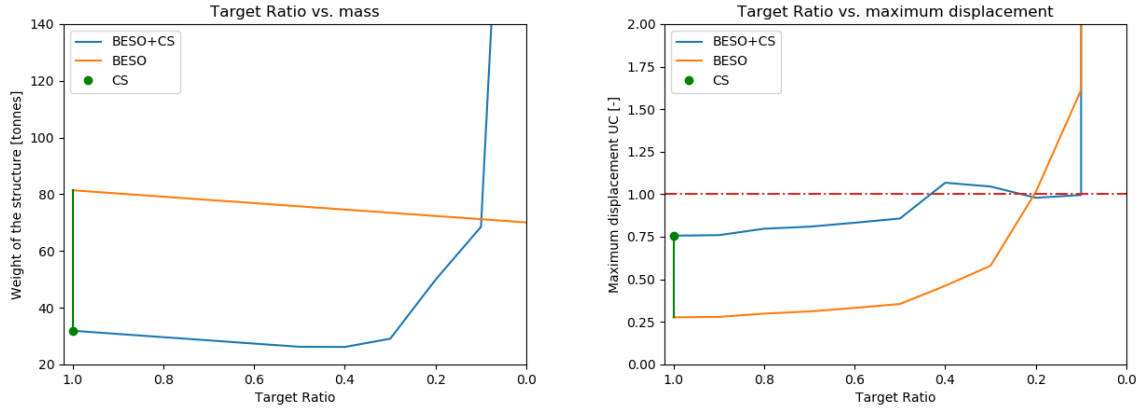

(a) (b)

Figure A.7: Braced frame structure under wind load, TR versus mass and displacement

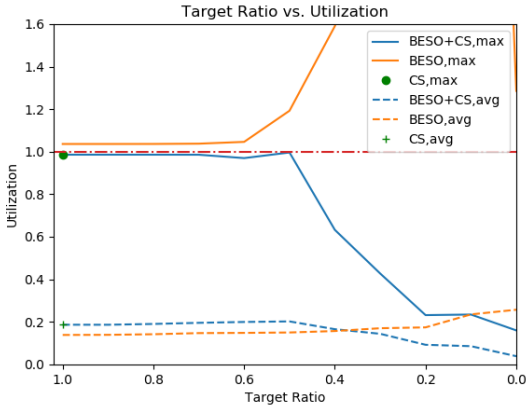

Figure A.8: Braced frame structure under wind load, TR versus utilization

displacement at small TR, the maximum utilization also increases above the limit as this limit is not a boundary condition for BESO but only for CS-optimization.

A.3.2. Braced frame structure (wind+vertical load)

Cross-section 2

This case considers wind+vertical load with cross-section (2) from table 3.5.

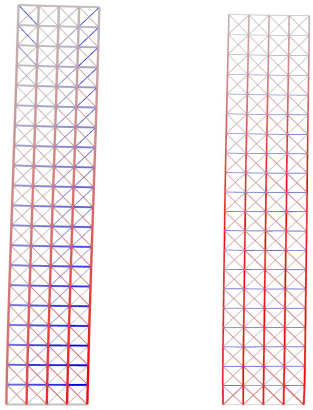

(a) (b)

Figure A.9: Braced frame under wind+vertical load, before (a) and after (b) CS-optimization

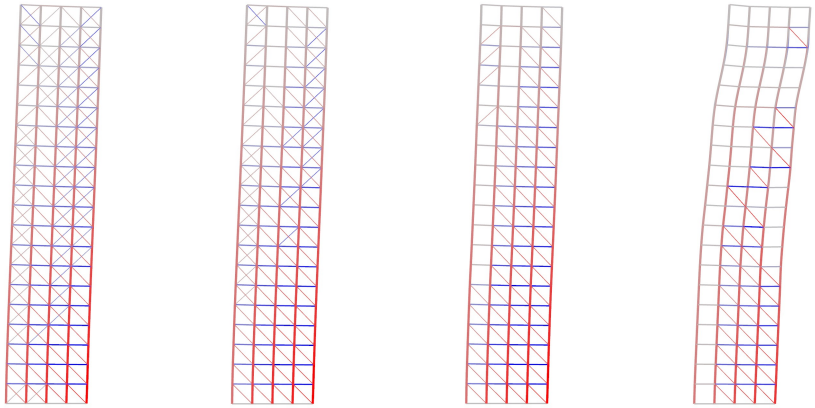

(a) (b) (c) (d)

Figure A.10: Braced frame under wind+vertical load after BESO, TR=0.8, 0.6, 0.4 and 0.2 respectively

Again, for BESO>CS a similar curve is found. For BESO, generally the curve shape stays the same however displacement and utilization exceed above their limits at TR≈0.3. The peak in the maximum utilization curve at TR≈0.6 for BESO is noteworthy. It appears however that this peak utilization value only occurs in one member. A characteristic of BESO however is that elements can also be added (within a design space), which is likely what would happen in the next iteration as the maximum utilization value decreases.

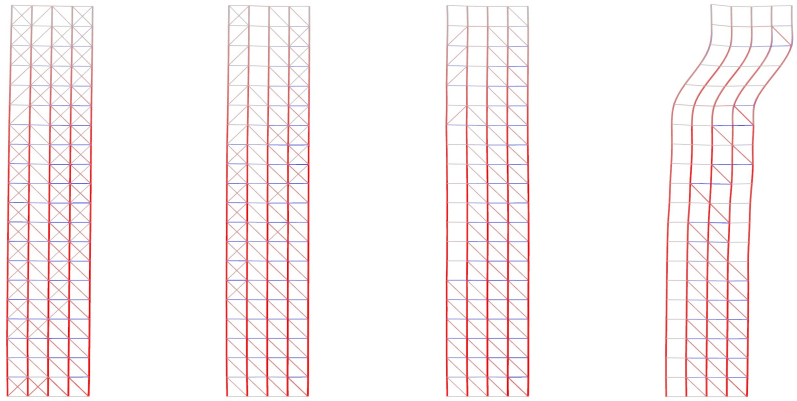

(a) (b) (c) (d)

Figure A.11: Braced frame under wind+vertical load after BESO>CS, TR=0.8, 0.6, 0.4 and 0.2 respectively

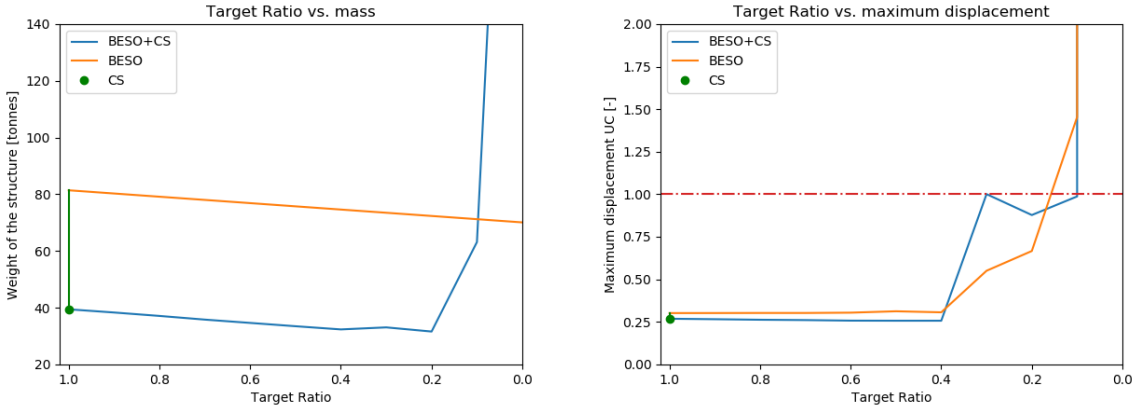

(a) (b)

Figure A.12: Braced frame structure under wind+vertical load, TR versus mass and displacement

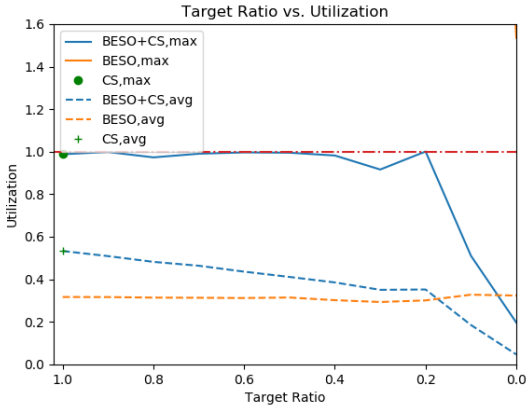

Figure A.13: Braced frame structure under wind+vertical load, TR versus utilization

A.3.3. Core structure (wind load)

Cross-section 2

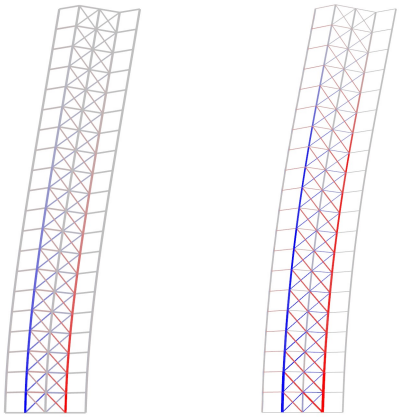

(a) (b)

Figure A.14: Core structure under wind load, before (a) and after (b) CS-optimization

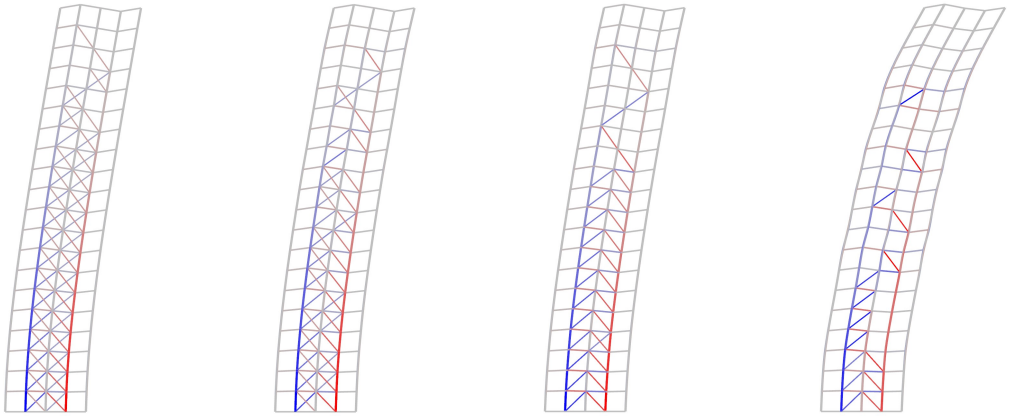

(a) (b) (c) (d)

Figure A.15: Core structure under wind load after BESO, TR=0.8, 0.6, 0.4 and 0.2 respectively

Also for the core structure, the starting point of the analysis has limited influence for BESO>CS and CS-optimization. For BESO, there are some differences, however less extreme than in the braced frame structure. This could be because of the fact that the initial mass of the core structure for cross-section 1 and 2 is closer than in the braced frame structure (109.1 and 89.0 tonnes versus 109.2 and 81.4 tonnes respectively).

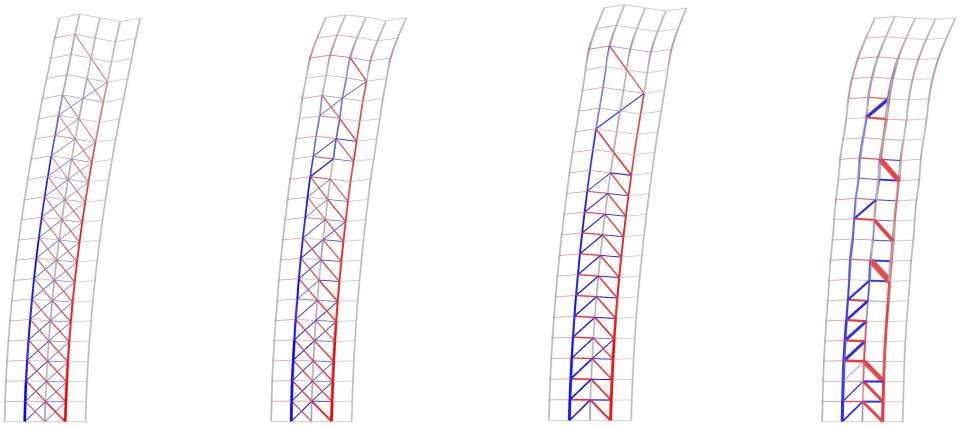

(a) (b) (c) (d)

Figure A.16: Core structure under wind load after BESO>CS, TR=0.8, 0.6, 0.4 and 0.2 respectively

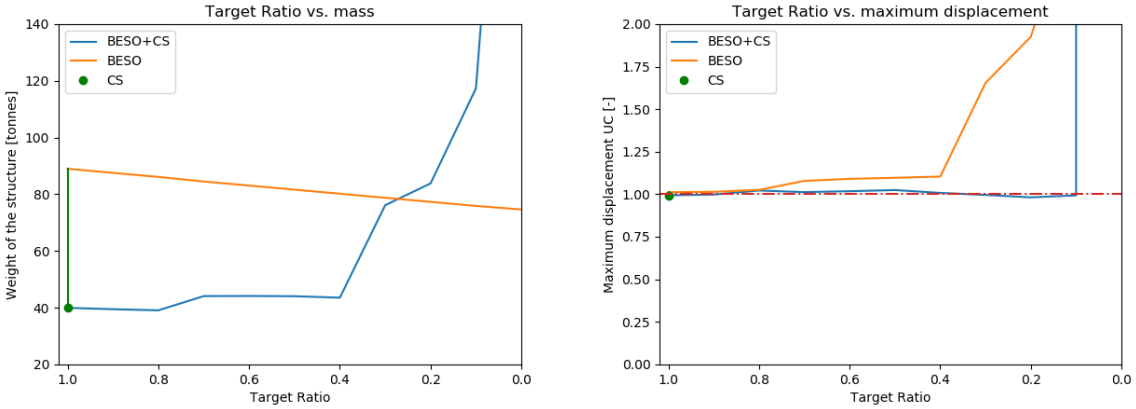

(a) (b)

Figure A.17: Core structure under wind load, TR versus mass and displacement

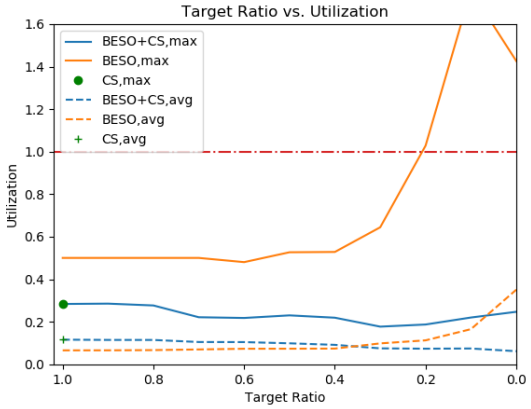

Figure A.18: Core structure under wind load, TR versus utilization

A.3.4. Core structure (wind+vertical load)

Cross-section 2

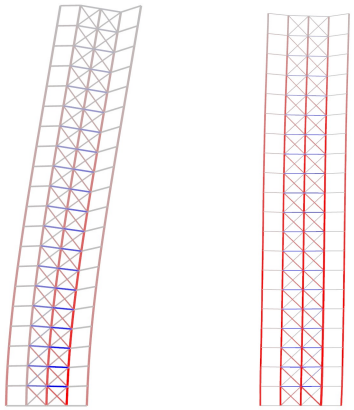

(a) (b)

Figure A.19: Core structure under wind+vertical load, before (a) and after (b) CS-optimization

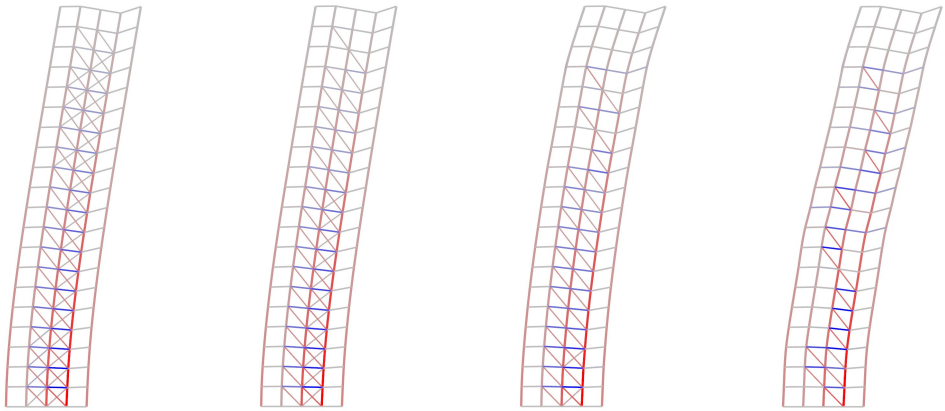

(a) (b) (c) (d)

Figure A.20: Core structure under wind+vertical load after BESO, TR=0.8, 0.6, 0.4 and 0.2 respectively

With smaller cross-sections initially, the results do not differ greatly from the case with heavier initial cross-sections. Similarly to earlier findings, BESO>CS and CS-optimization is rather insensitive to the initial input while BESO seems more sensitive to the initial cross-sections. This is mainly visible in the Target Ratio at which the structure fails to satisfy the safety criteria. For cross-section 1, this was at approximately 0.1, whereas for cross-section 2, the maximum utilization limit is exceeded at a TR≈0.2.

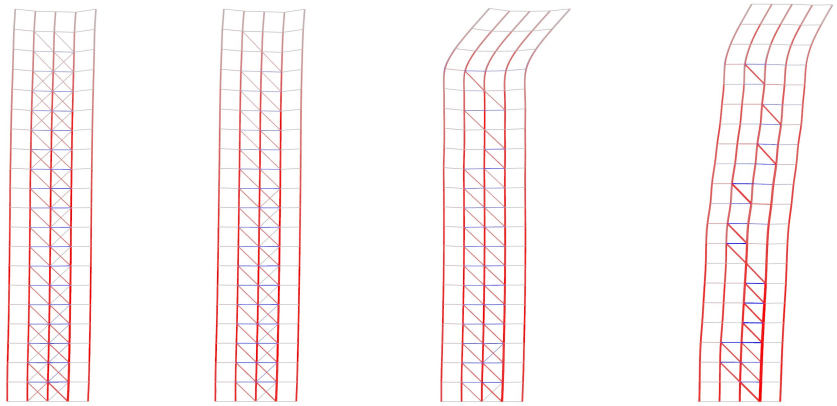

(a) (b) (c) (d)

Figure A.21: Core structure under wind+vertical load after BESO>CS, TR=0.8, 0.6, 0.4 and 0.2 respectively

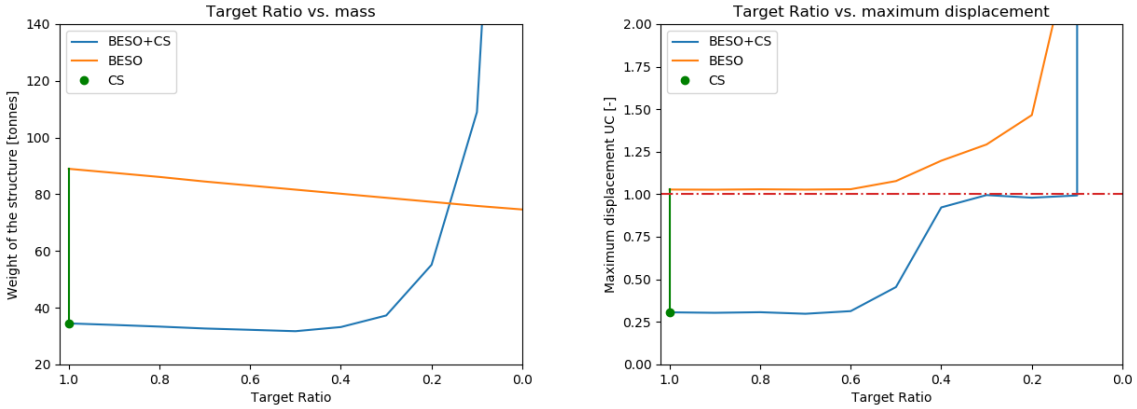

(a) (b)

Figure A.22: Core structure under wind load, TR versus mass and displacement

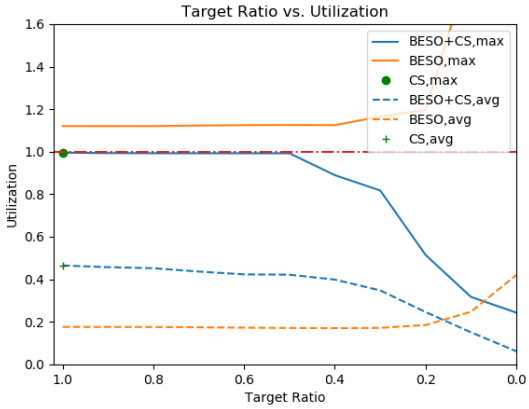

Figure A.23: Core structure under wind load, TR versus utilization

A.4. Case study results

The results shown below are for the case studies considered in chapter 5. These include the results for load cases LC1, LC2 and LC3.

A.4.1. 2D high-rise braced frame structure

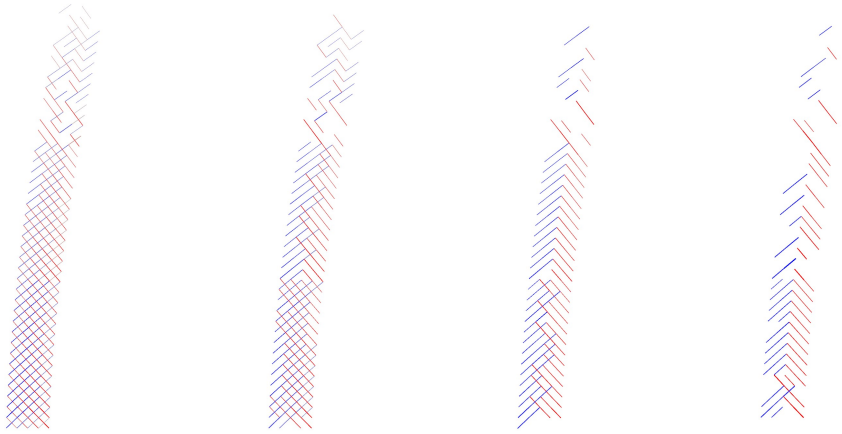

(a) (b) (c) (d)

Figure A.24: Case study 2D high-rise braced frame at iteration 64, 128, 192 and 235 respectively (TR=0.8, 0.6, 0.4 and 0.27) for LC0 with diagonal view on

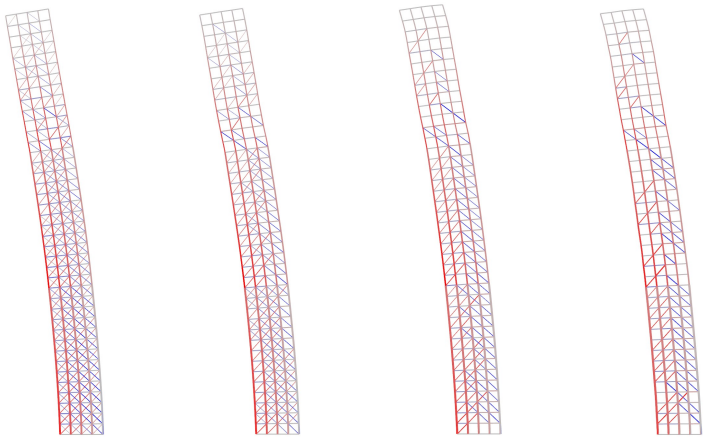

(a) (b) (c) (d)

Figure A.25: Case study 2D high-rise braced frame at iteration 64, 128, 192 and 235 respectively (TR=0.8, 0.6, 0.4 and 0.27) for LC1

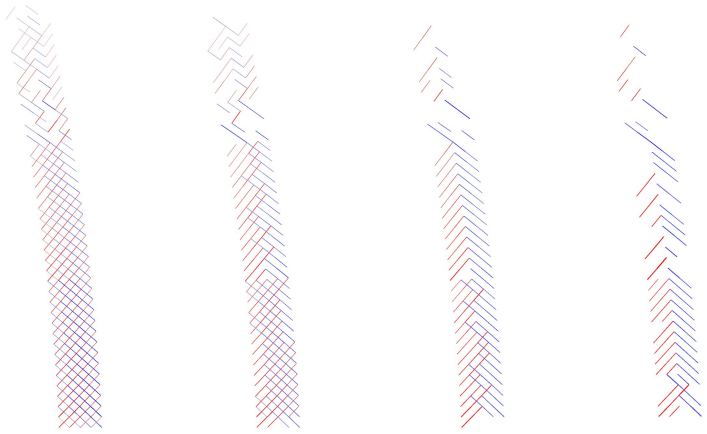

(a) (b) (c) (d)

Figure A.26: Case study 2D high-rise braced frame at iteration 64, 128, 192 and 235 respectively (TR=0.8, 0.6, 0.4 and 0.27) for LC1 with diagonal view on

A.4.2. 3D tower

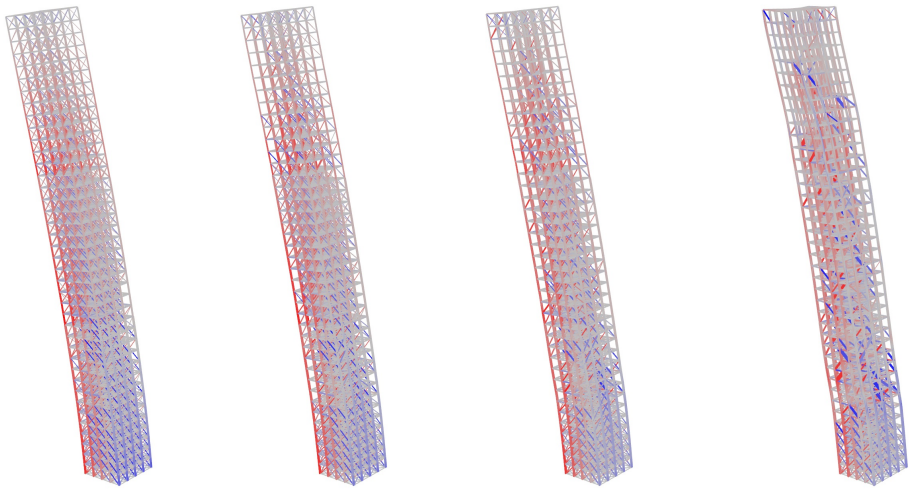

(a) (b) (c) (d)

Figure A.27: Case study 3D tower at TR=0.8, 0.6, 0.4 and 0.19 for LC1

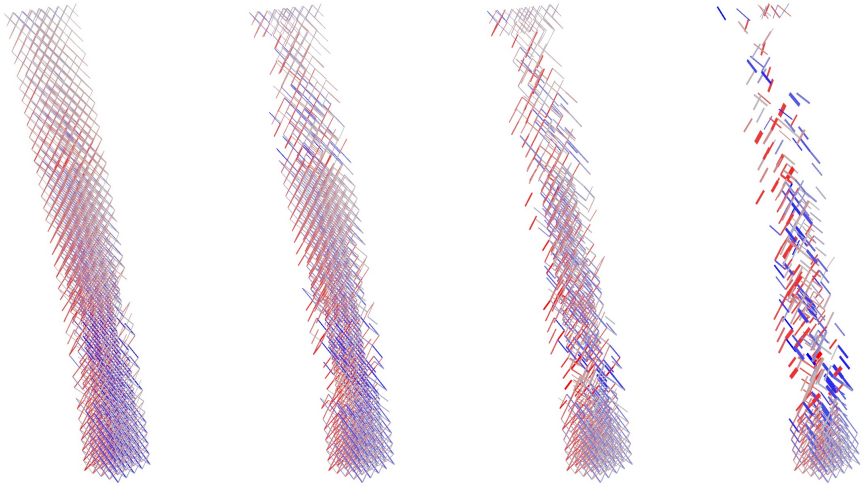

(a) (b) (c) (d)

Figure A.28: Case study 3D tower at TR=0.8, 0.6, 0.4 and 0.19 for LC1 with diagonal view on

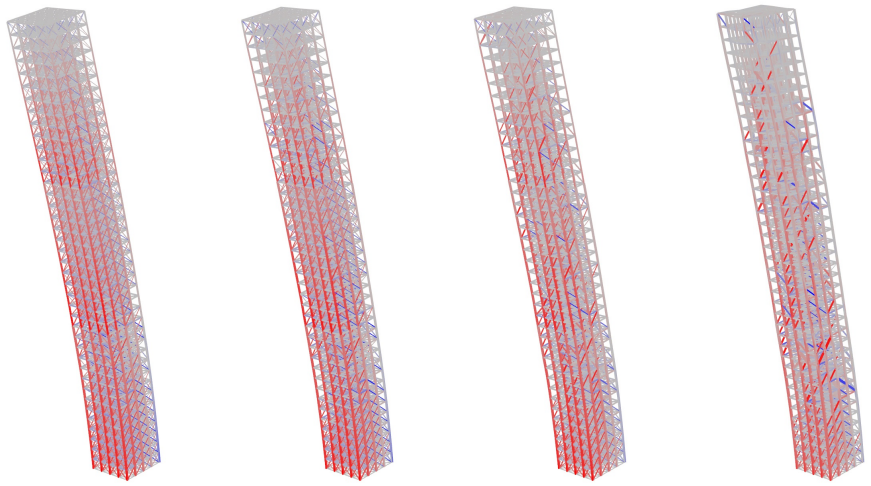

(a) (b) (c) (d)

Figure A.29: Case study 3D tower at TR=0.8, 0.6, 0.4 and 0.19 for LC2

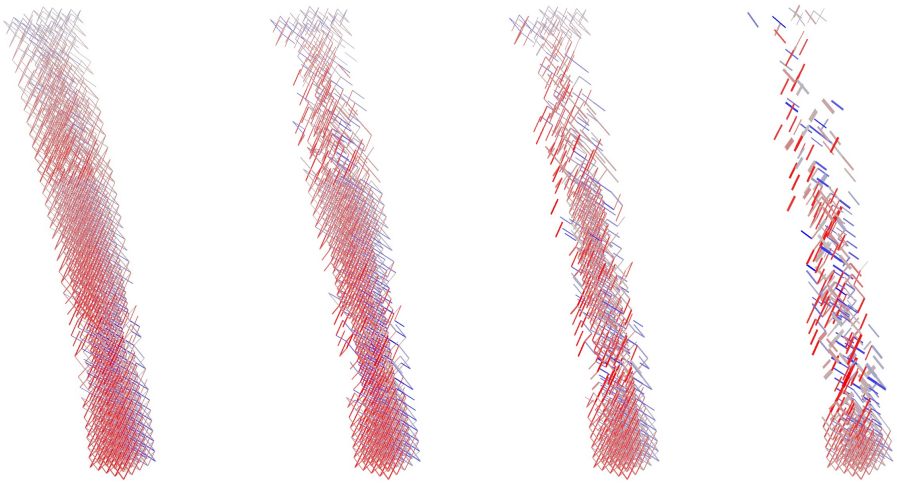

(a) (b) (c) (d)

Figure A.30: Case study 3D tower at TR=0.8, 0.6, 0.4 and 0.19 for LC2 with diagonal view on

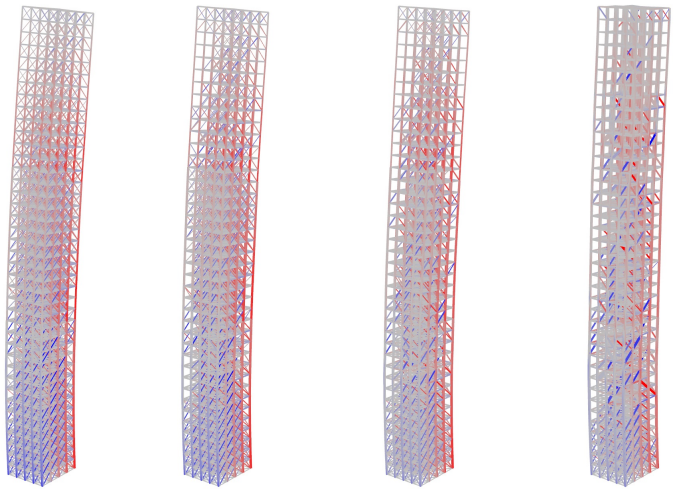

(a) (b) (c) (d)

Figure A.31: Case study 3D tower at TR=0.8, 0.6, 0.4 and 0.19 for LC3

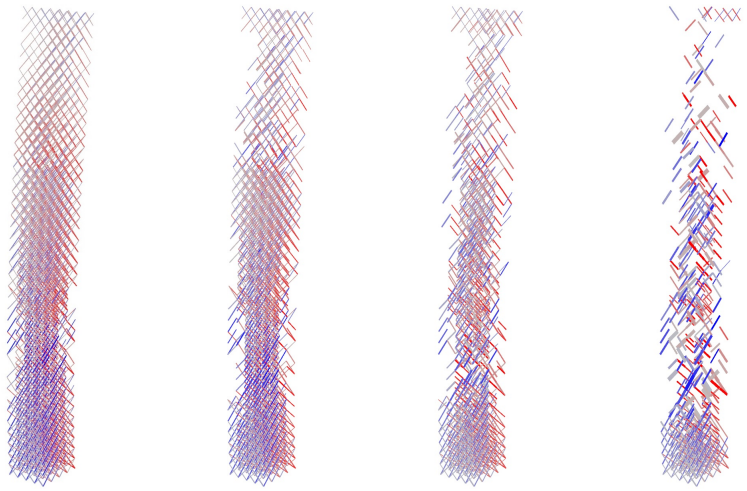

(a) (b) (c) (d)

Figure A.32: Case study 3D tower at TR=0.8, 0.6, 0.4 and 0.19 for LC3 with diagonal view on

Inclusion of floor diaphragms in CS-optimization

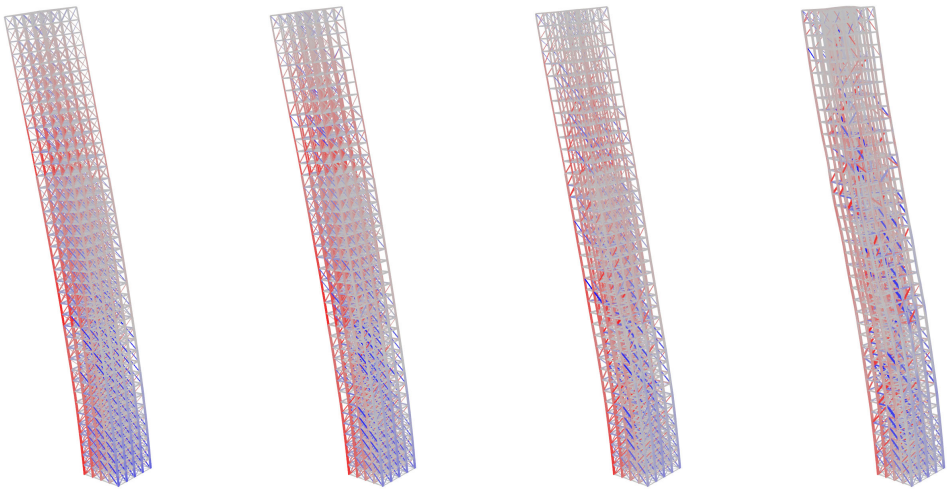

(a) (b) (c) (d)

Figure A.33: Case study 3D tower with floors in CS-opt. at TR=0.8, 0.6, 0.4 and 0.2 for LC1

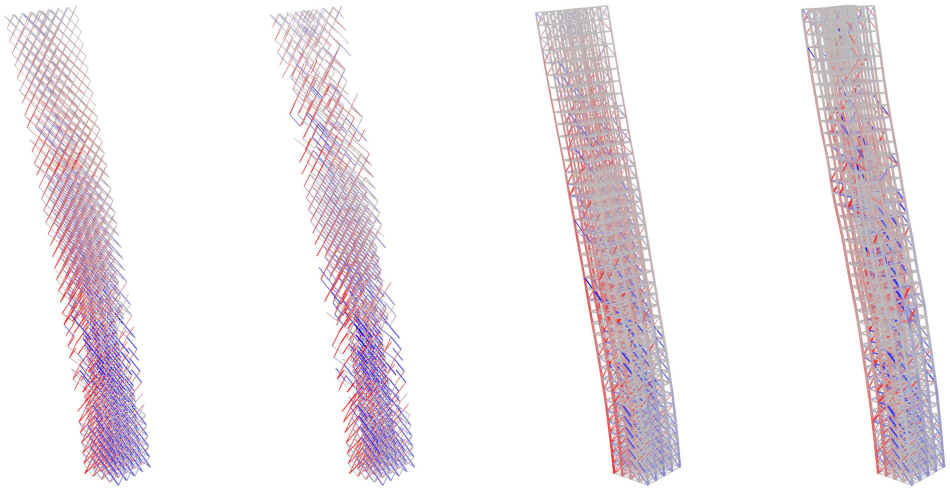

(a) (b) (c) (d)

Figure A.34: Case study 3D tower with floors in CS-opt. at TR=0.8, 0.6, 0.4 and 0.2 for LC1 with diagonal view on

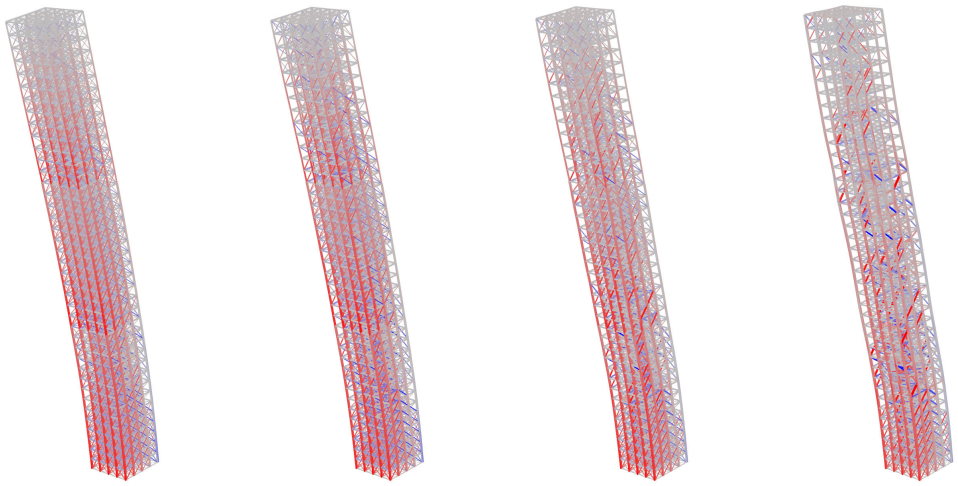

(a) (b) (c) (d)

Figure A.35: Case study 3D tower with floors in CS-opt. at TR=0.8, 0.6, 0.4 and 0.2 for LC2

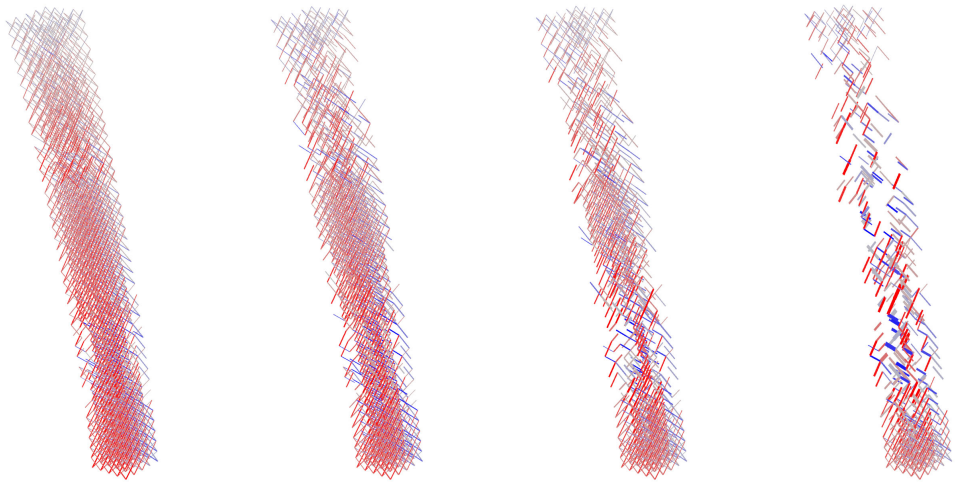

(a) (b) (c) (d)

Figure A.36: Case study 3D tower with floors in CS-opt. at TR=0.8, 0.6, 0.4 and 0.2 for LC2 with diagonal view on

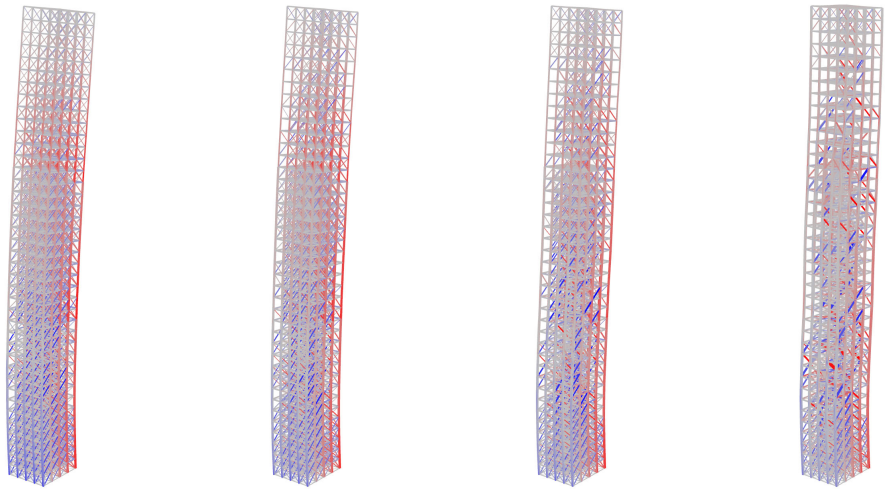

(a) (b) (c) (d)

Figure A.37: Case study 3D tower with floors in CS-opt. at TR=0.8, 0.6, 0.4 and 0.2 for LC3

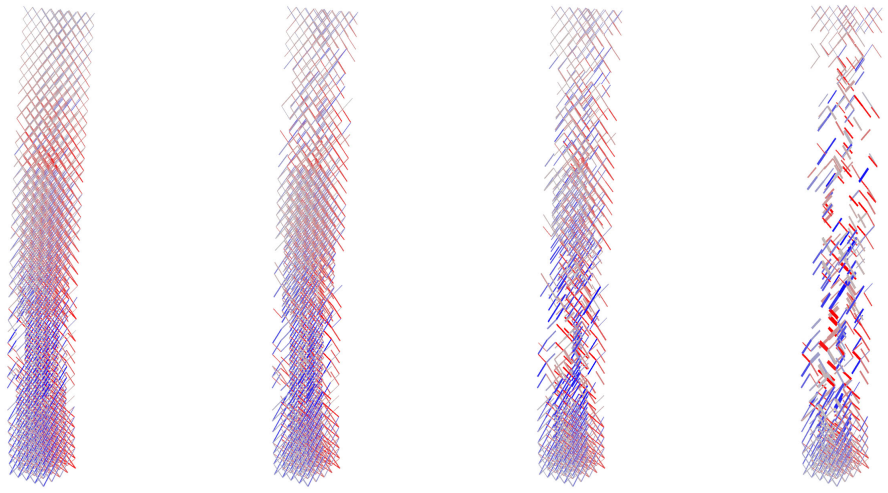

(a) (b) (c) (d)

Figure A.38: Case study 3D tower with floors in CS-opt. at TR=0.8, 0.6, 0.4 and 0.2 for LC3 with diagonal view on

Comparison with other structural systems

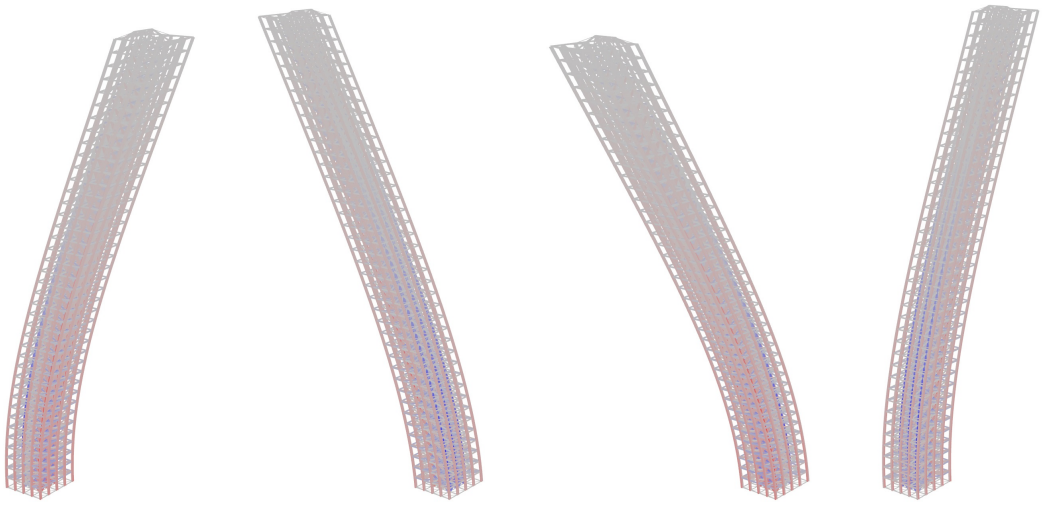

(a) (b) (c) (d)

Figure A.39: Case study reference core structure for LC0, LC1, LC2 and LC3

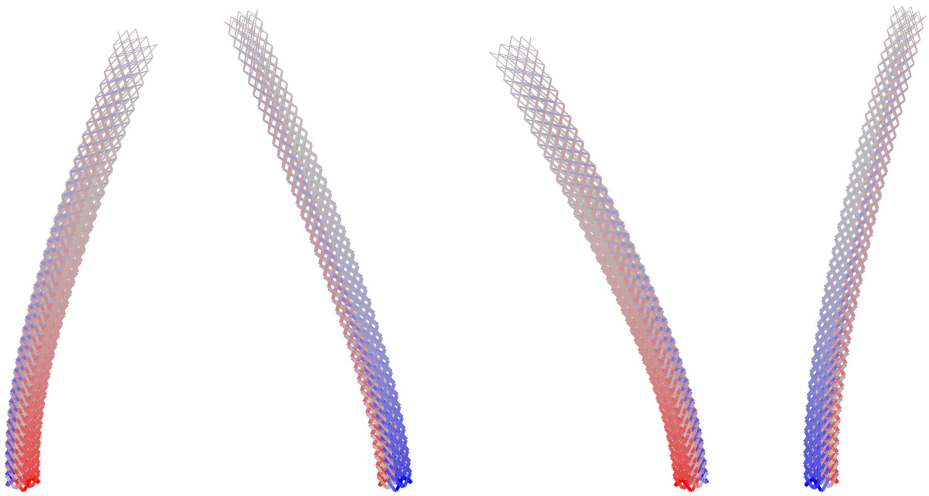

(a) (b) (c) (d)

Figure A.40: Case study reference core structure for LC0, LC1, LC2 and LC3 with diagonal view on

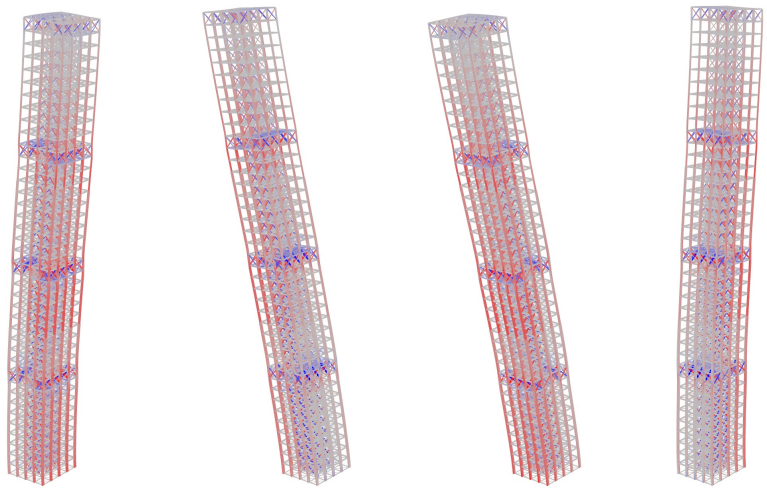

(a) (b) (c) (d)

Figure A.41: Case study reference outrigger structure for LC0, LC1, LC2 and LC3

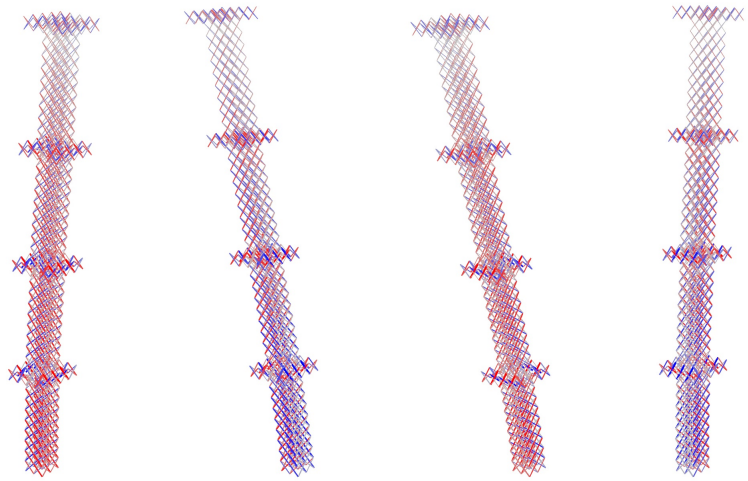

(a) (b) (c) (d)

Figure A.42: Case study reference outrigger structure for LC0, LC1, LC2 and LC3 with diagonal view on

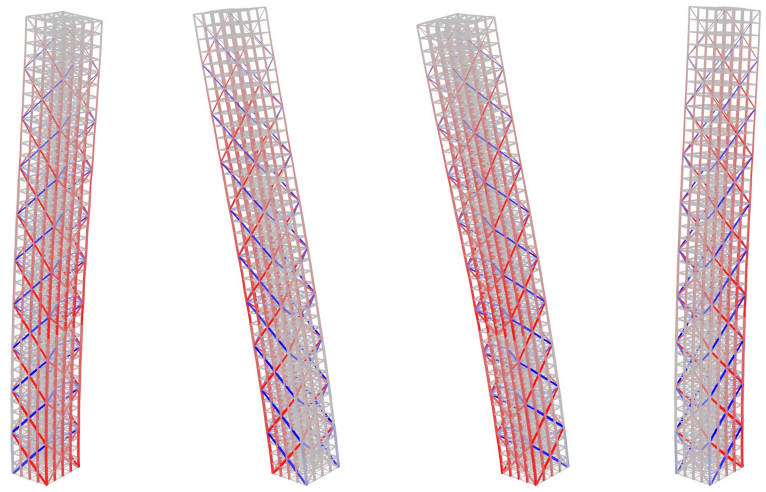

(a) (b) (c) (d)

Figure A.43: Case study reference mega frame structure for LC0, LC1, LC2 and LC3

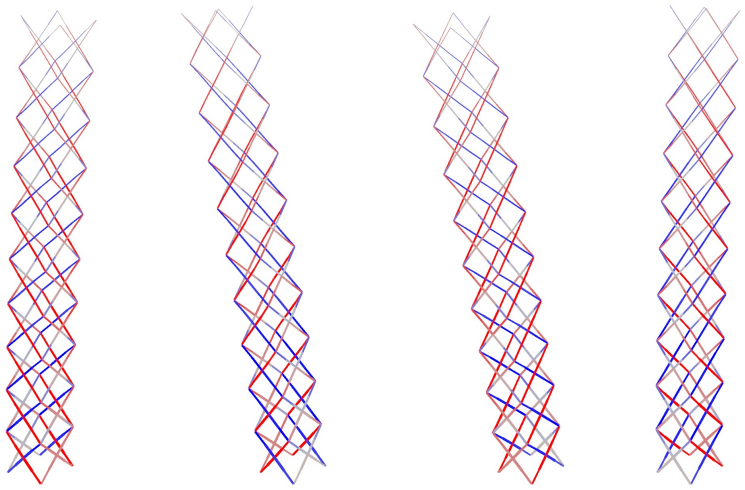

(a) (b) (c) (d)

Figure A.44: Case study reference mega frame structure for LC0, LC1, LC2 and LC3 with diagonal view on

A.4.3. Arbitrary shape

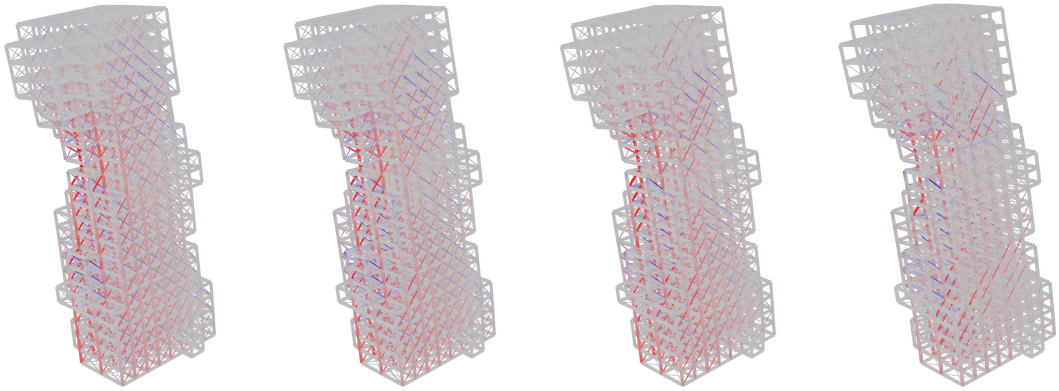

(a) (b) (c) (d)

Figure A.45: Case study arbitrary shape at TR=0.8, 0.6, 0.4 and 0.17 for LC1

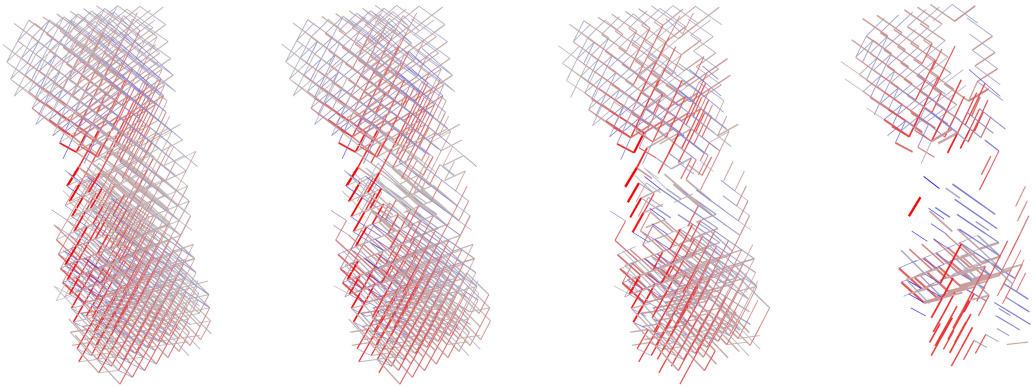

(a) (b) (c) (d)

Figure A.46: Case study arbitrary shape at TR=0.8, 0.6, 0.4 and 0.17 for LC1 with diagonal view on

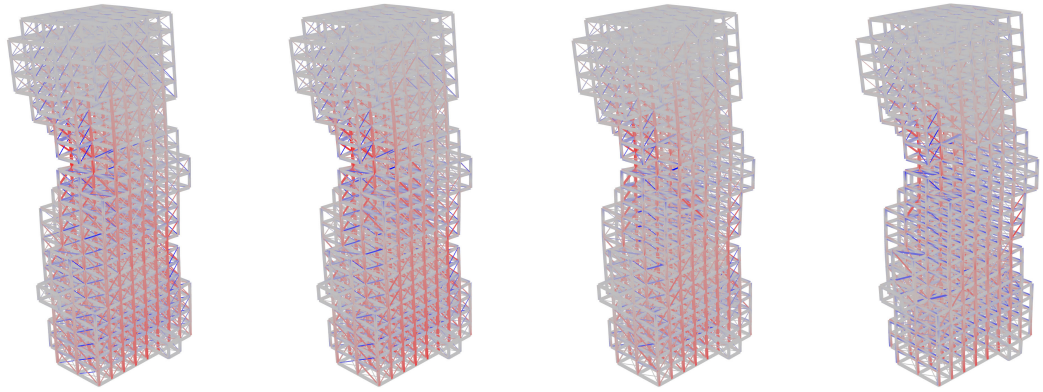

(a) (b) (c) (d)

Figure A.47: Case study arbitrary shape at TR=0.8, 0.6, 0.4 and 0.17 for LC2

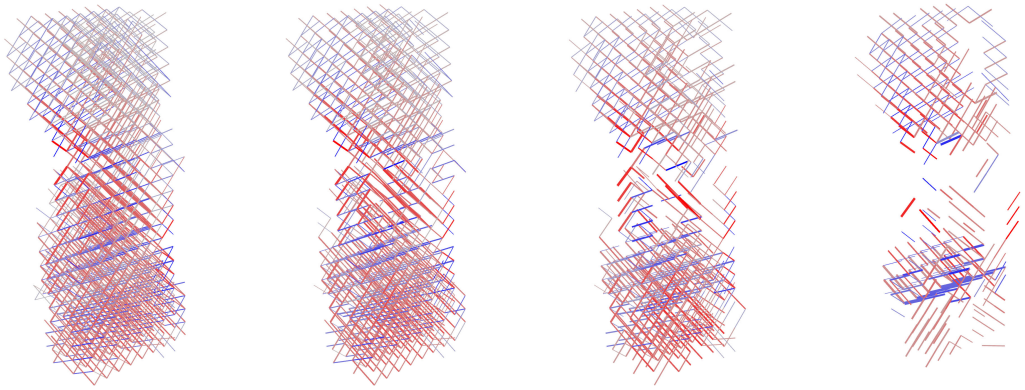

(a) (b) (c) (d)

Figure A.48: Case study arbitrary shape at TR=0.8, 0.6, 0.4 and 0.17 for LC2 with diagonal view on

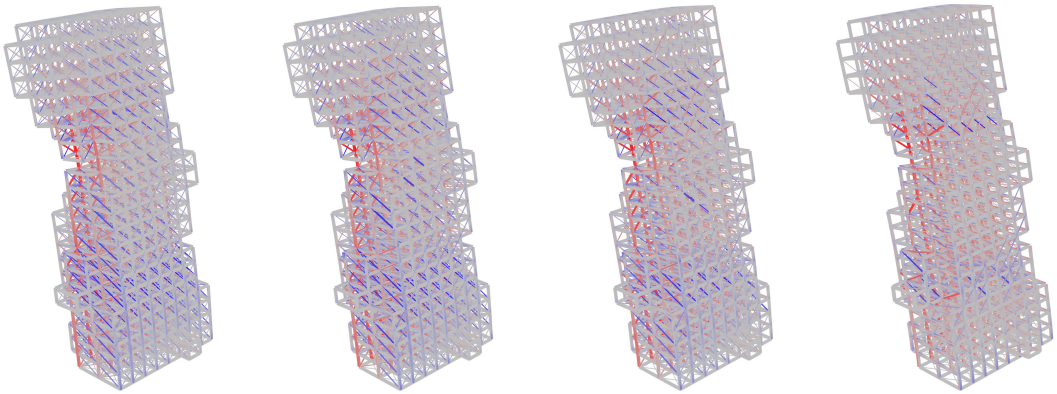

(a) (b) (c) (d)

Figure A.49: Case study arbitrary shape at TR=0.8, 0.6, 0.4 and 0.17 for LC3

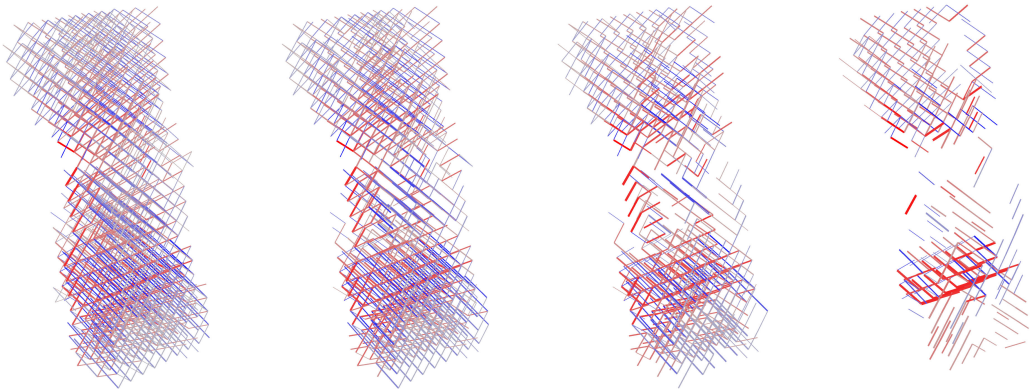

(a) (b) (c) (d)

Figure A.50: Case study arbitrary shape at TR=0.8, 0.6, 0.4 and 0.17 for LC3 with diagonal view on

B

Scripts and implementations

B.1. Wind pressure calculation

The peak wind pressure as described in NEN-EN1991-1-4 and in section 5.2.1 has been programmed in a Python script in order to integrate this in the parametric model. A code from Knapp [67] has been used as a template and modified to be applicable in the Grasshopper script. This way, the peak wind pressure and therefore the acting horizontal load ogn the building can be calculated automatically by making use of the predefined geometry.

Firstly, the input parameters have to be set up. It is assumed that the building is in the Netherlands and therefore the Dutch National Annex NEN-EN 1991-1-4+A1+C2/NB is used to calculate the peak wind pressure $q_p(z)$. The main input parameters are the wind area, terrain category and building height. The building height z follow from the bounding box of the geometry input in the script.

```
"""Provides a scripting component.
    Inputs:
        windarea: The wind area
        terain: The terrain category
        z: Building height [m]
    Output:
        wind pressure [kN/m2]: The wind pressure qp according to Eurocode
        EN 1991-1-4 in [kN/m2]"""

__author__ = "tonyt"
__version__ = "2019.12.02"

import rhinoscriptsyntax as rs# import numpy as np
from math import log

"""
Structural wind loading according to Eurocode EN 1991-1-4:2005.
Initial proof of concept of an OOP approach using Python.
By Graham Knapp
"""

rho = 1.25  # density [kg/m3] from base Eurocode
_document = 'EN 1991-1-4:2005 +A1:2010'


class Site():
    """
    represents a site with a given terrain roughness and basic wind speed.
    test from https://eurocodes.jrc.ec.europa.eu/doc/WS2008/SX016a-EN-EU.pdf
    Values are taken from Dutch National Annex NEN-EN 1991-1-4+A1+C2/NB.
    """
    z0_by_terrain = {'O': 0.005, 'II': 0.2, 'III': 0.5}

    zmin_by_terrain = {'O': 1., 'II': 4., 'III': 7.}

```

```
    vb0_by_windarea = {'I': 29.5, 'II': 27., 'III': 24.5}

    def __init__(self, windarea, terrain, co=1.0):
        self._windarea = windarea                    # wind area
        self._vb0 = self.vb0_by_windarea[windarea]  # fundamental value of the
                                                     # basic wind velocity [m/s]
        self._terrain = terrain                      # terrain category
        self._z0 = self.z0_by_terrain[terrain]       # roughness length [m]
        self._zmin = self.zmin_by_terrain[terrain]  # minimum height [m]
        self._co = co                                # orography factor

    def iu(self, z):
        """Calclate turbulence intensity at a given height z
        """
        z = max(z, self._zmin)
        return 1 / (self._co * log(z / self._z0))

    def cr(self, z):
        """Calculate mean wind speed ratio at a given height z
        """
        z = max(z, self._zmin)
        return (0.19 * (self._z0 / 0.05) ** 0.07) * log(z / self._z0)

    def qp(self, z):
        """Calculate peak wind velocity pressure [Pa] at a given height
        """
        u = self.cr(z) * self._vb0
        _qp = 0.5 * rho * (u ** 2.) * (1 + 7 * self.iu(z))
        return _qp

print Site(windarea,terrain).qp(float(z)) * 1e-3
```

B.2. Geometry generation

The script defines a bounding box around the input volume (BRep), such that cantilevers or extraordinary shapes are also divided into modules. The module dimension can be specified in X-, Y- and Z-direction after which the script defines split points and creates planes to split the BRep with. A GHPython script component by De Jongh [68] which is presented below has been used which cuts the BRep with the planes in three directions.

Subsequently, the structural geometry has been drawn in a single module (figure 5.6) and copied across all modules using the Box Mapping component. Duplicate beam elements are then removed. Specifying material, cross-sectional properties, supports and loads makes the model ready for the analysis in Karamba. The main differences here are the fact that the model is in 3D and therefore there are different constraints at the support (all degrees of freedom restrained). Also, the load is applied as a mesh load (load per area) rather than line load (load per length). The mesh load is automatically converted to line loads applied on the columns, as well as point loads on the nodes. It is also important to consider wind from four directions in the three-dimensional model.

```
import rhinoscriptsyntax as rs
import Rhino as rh
import System as sys
import scriptcontext as sc

""" S
Split Brep plane 2012,
by Arie-Willem de Jongh

Inputs:
        brp: BRep to be split
        pln: Planes where BRrep must be split
Output:
        pieces: Individual pieces of Brep
"""


arrBrep =[]
arrBrep.append(brp)

if brp and pln:

    bb = rh.Geometry.Brep.GetBoundingBox(brp,rh.Geometry.Plane.WorldXY)

    for i in pln:
        bool,extU,extV = rh.Geometry.Plane.ExtendThroughBox(i,bb)
        extU.T0 = extU.T0 - 1
        extU.T1 = extU.T1 + 1
        extV.T0 = extV.T0 - 1
        extV.T1 = extV.T1 + 1

        planeSrf = rh.Geometry.PlaneSurface(i,extU,extV)
        splitter = planeSrf.ToBrep()
        arrBrepC = arrBrep[:]
        for j in arrBrepC:
            brep = rs.coercebrep(j)
            tbrep = brep.Split(splitter,0.001)
            if tbrep:
                arrBrep.remove(j)
                for k in tbrep:
                    h=k.CapPlanarHoles(0.001)
                    if h:
                        arrBrep.append(h)
                    else:
                        arrBrep.append(k)

pieces = arrBrep
```

B.3. Coupled ESO<>CS-optimization method

The implementation of the method makes use of the following software tools:

- Grasshopper
  - Karamba
  - Anemone
  - GHPython

Karamba is used for parametric structural analysis, Anemone is used for creating the loop while GHPython and basic Grasshopper components to connect the structural analysis data to the optimization.

The first component in the script is the 'Loop Start' component which is an Anemone component which starts the loop. The component requires the number of repeats, the data to be repeated and a trigger to start the loop. In this case, the number of repeats is depends on the total number of elements and the number of elements removed per iteration. The data to loop 'D0' is the structural model from Karamba, whereas 'D1' and 'D2' represent the maximum displacement and mass of the structure after each iteration. The 'Loop Start' component is connected to 'Loop End' to enclose the loop.

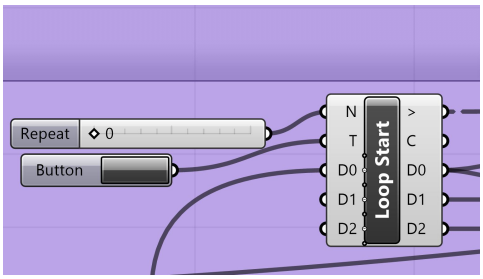

Figure B.1: ESO script (1)

Within the loop, first the strain energy are derived from the 'DO'-output, which is the structural model. Deformation energies are retrieved from Karamba3D and summed for axial force and bending to obtain the total strain energy of each member. The model output 'D0' is simultaneously disassembled to retrieve the element data. From the element data, the area, length and element-identifier of each element is needed to calculate the strain energy density.

Next, a GHPython component is used to calculate the strain energy density of each element in the current model. A list is created with the index number of each element, after which the elements which are not diagonal elements are removed from the list. The list is sorted from low to high strain energy density. This is the list of element indices which may be removed. The Python script is presented below.

```
"""Provides a scripting component.
    Inputs:
        Area: The cross-sectional area of each member
        Length: The length of each member
        StrainEnergy: The strain energy of each member
        ElemID: The element identifier of each member (diagonals are indicated
        with 'diag')
    Output:
        sorted_index: The indices of the diagonals, sorted by low to high
        strain energy density"""

__author__ = "tonyt"
__version__ = "2020.01.13"

Volume = [a*b for a,b in zip(Area,Length)]
indices = range(len(ElemID))
```

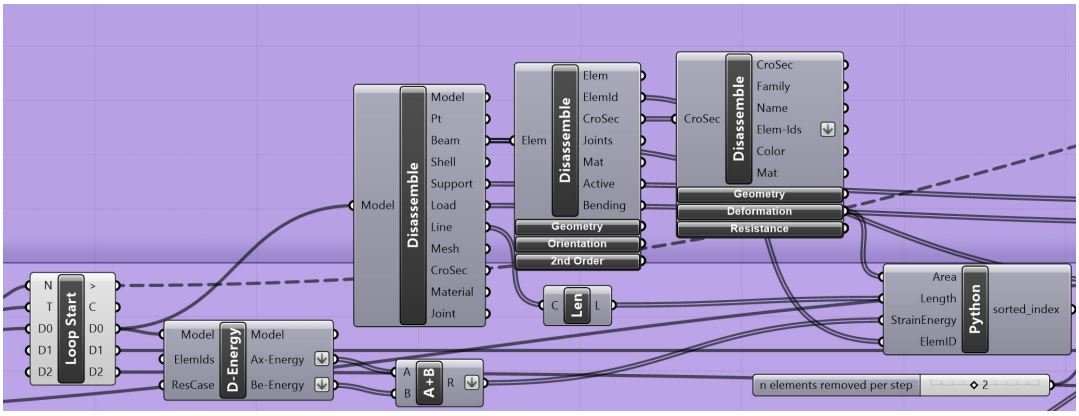

Figure B.2: ESO script (2)

```
strain_energy_density = [(a*1.0)/b for a, b in zip(StrainEnergy,Volume)]
for i in range(len(ElemID)):
    if ElemID[i] != "diag":
        indices.remove(i)
strain_energy_density_index = sorted(indices, key=lambda k: strain_energy_density[k])
sorted_index = strain_energy_density_index
```

By using split list and cull index components, elements from the list are removed. The number of elements removed per iteration step can be specified here. The elements are removed starting from the top of the list, thus the elements with the lowest strain energy density are removed first.

Then, the model is reassembled without the removed elements. Analysis using the Karamba3D Analyze component and Cross-Section optimization takes place using the OptiCroSec component. After CS-optimization, the mass and displacement are outputted and stored in an array which is then inputted into the 'Loop End' 'D1' and 'D2' input. This way, the maximum displacement and mass will be stored for each iteration. The 'Loop End' component has a toggle to exit the loop before the number of iterations runs out if requested.

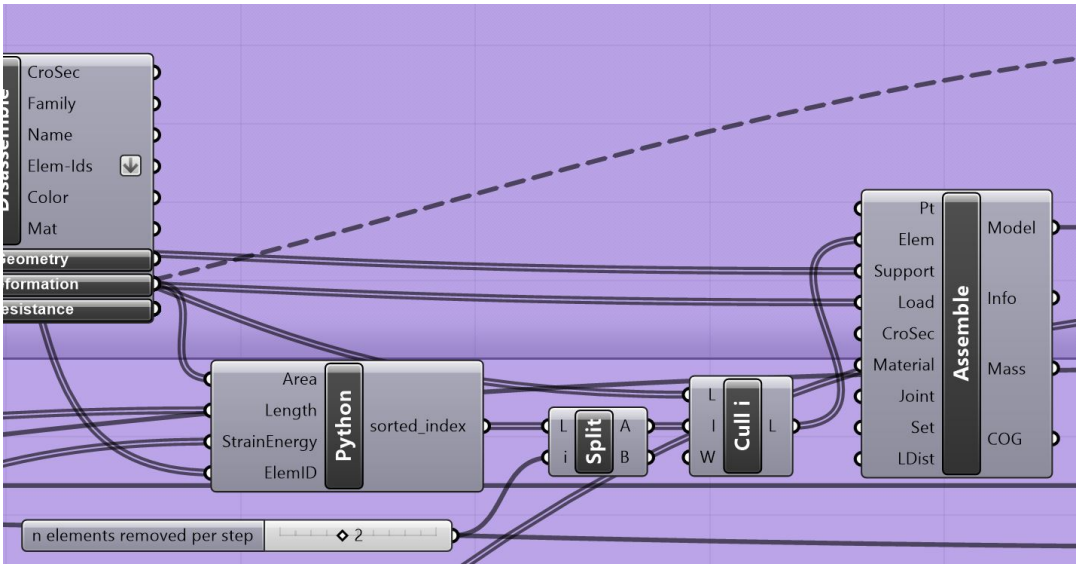

Figure B.3: ESO script (3)

The 'Loop End' component then transfers the data from 'D0', 'D1' and 'D2' back to the 'Loop Start' component for the next iteration. Thus, essentially what the script does is remove the elements with the lowest strain energy density in each iteration, perform a CS-optimization with the updated model and repeats this until the desired number of iterations is completed.

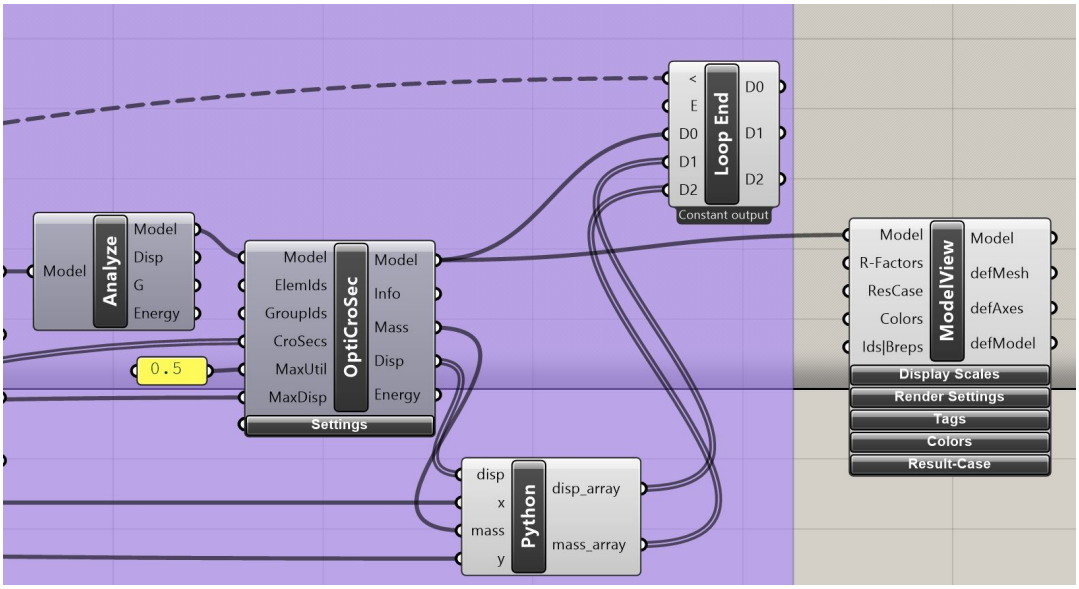

Figure B.4: ESO script (4)

By turning on the 'Model View', the updated model can be seen in each iteration.

B.4. User Interface

The user interface has been set up using the Human UI plugin for Grasshopper. The user interface includes three tabs:

- Geometry generation
- Analysis and optimization
- Results

The first window includes the parameters for the module dimension in X-, Y- and Z-direction. If a BRep is specified, the geometry is generated by hitting the toggle and the structural model is created.

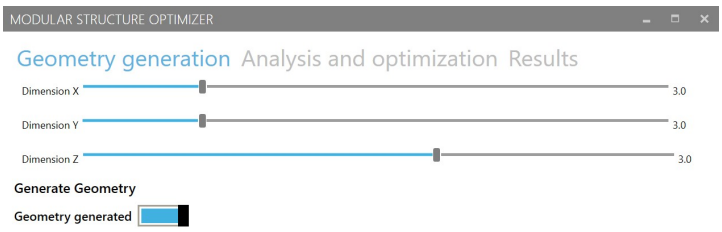

Figure B.5: User Interface for modular structure optimizer (Geometry Generation)

Next, the loads and elements removed per iteration can be changed in the 'analysis and optimization'-tab. Vertical load can be switched on and off and the value can be changed. Wind area and terrain category can be chosen after which the wind pressure is calculated given the building height derived from the BRep. The number of elements removed per step can be changed, which affects total (maximum) number of iterations, but also accuracy of the results. Before running the optimization, it is important to check all parameters and clear previous optimization output. Once the optimization is started, the number of iterations is counted and displayed. The iteration stops when the structure fails to meet the verification criteria, which at an iteration number of lower than or equal to the maximum number of iterations.

When the analysis is completed, the results can be explored in the 'results'-tab. The iteration number can be manually selected and all considered load cases can be viewed in the Rhino viewport. The mass, maximum displacement, average and maximum utilization (for all LCs combined) are displayed. Optionally, the view can be changed to diagonals only.

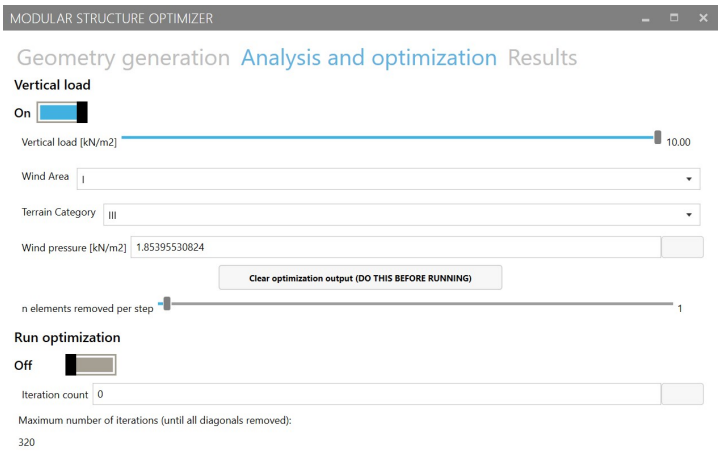

Figure B.6: User Interface for modular structure optimizer (Analysis and Optimization)

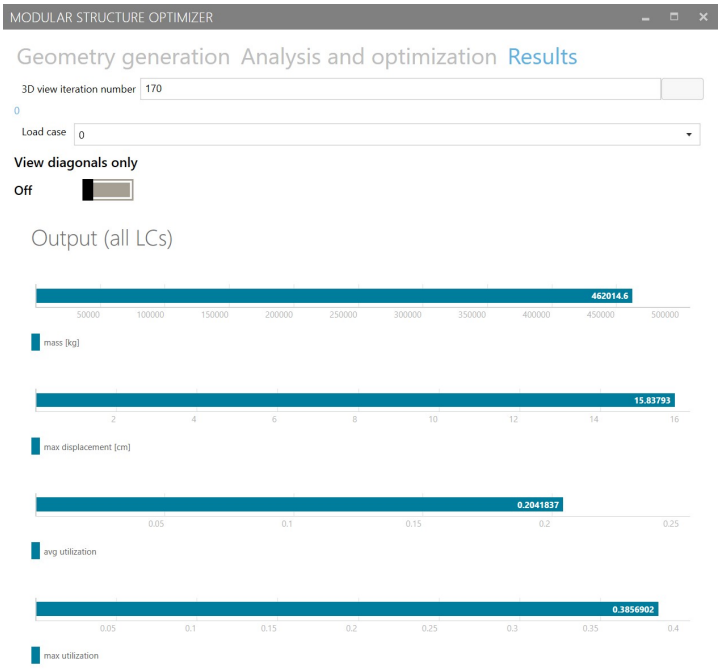

Figure B.7: User Interface for modular structure optimizer (Results)